Light-Induced pH Cycle

- a non-invasive method to control biochemical reactions -

Heike Kagel

Dissertation
To achieve the academic degree of
doctor rerum naturalium
(Dr. rer. nat.)
In the scientific discipline biochemistry

Submitted to
Mathematical Science Faculty
- Institute for Biology and Biochemistry -
University Potsdam

Submitted: P̄otsdam- Golm, 25.03.2019

Board of examiners:

1. Prof. Dr. Katja Arndt (Chair)
2. Prof. Dr. Frank F. Bier (1. Reviewer, msain supervisor)
3. Prof. Dr. Ilko Bald (2. Reviewer)
4. Prof. Dr. Michel Köhler (3. Reviewer)
5. Prof. Dr. Uta Wollenberger
6. Prof. Dr. Silke Leimkühler
Mentor: Prof. Dr. Marcus Frohme

Published online at the
Institutional Repository of the University of Potsdam:
https://doi.org/10.25932/publishup-43435
https://nbn-resolving.org/urn:nbn:de:kobv:517-opus4-434353

Acknowledgements

This work was done as a cooperation project of the University of Applied Sciences and with the University Potsdam. I would like to thank all my fantastic colleges and people I met on my way for their great support and the pleasant working atmosphere. Special thanks go to Philip Franke and Jens Fischbach for their professional and to Karolin Keil and Anna Grebinyk for their moral support.

First of all, I would like to thank Prof. Dr. Marcus Frohme (University of Applied Sciences) and Prof. Dr. Schrader (University of Applied Sciences) for creating the opportunity to work in a scientific environment, for the warm welcome in their groups *Molecular Biology and Functional Genomics* and *Photonic*. Marcus always had time and gave a helping hand when needed. Also a very warm thank you to my friend Rainer who acquainted me with "Vanni", which initiated my work at the University of Applied Sciences.

Furthermore I would like to thank my mentor Dr. Jörn Glökler, who had the idea for this project and who supported me throughout the whole project with constructive criticism and plenty of good ideas.

Special thanks goes to my supervisor Prof. Dr. Bier (University Potsdam) for his interest and support for my work.

Last but not least I would like to send a sparkly thanks to my wonderful Hasipupsimausischnuffel (no translation possible!), my loving family and faithful friends for their great support, for enduring my whining (which was alternately weak to very strong) and for never stopping to believe in me that I could do this work - even when I did. Thank you.

Abstract

Background Many biochemical reactions depend on the pH of their environment and some are strongly accelerated in an acidic surrounding. A classical approach to control biochemical reactions non-invasivly is by changing the temperature. However, if the pH could be controlled by optical means using photo-active chemicals, this would mean to be able to accelerate suitable biochemical reactions. Optically switching the pH can be achieved by using photoacids. A photoacid is a molecule with a functional group that releases a proton upon irradiation with the suitable wavelength, acidifying the environmental aqueous surrounding. A major goal of this work was to establish a non-invasive method of optically controlling the pH in aqueous solutions, offering the opportunity to enhance the known chemical reactions portfolio. To demonstrate the photo-switchable pH cycling we chose an enzymatic assay using acid phosphatase, which is an enzyme with a strong pH dependent activity.

Results In this work we could demonstrate a light-induced, reversible control of the enzymatic activity of acid phosphatase non-invasivly. To successfully conduct those experiments a high power LED array was designed and built, suitable for a 96 well standard microtiter plate, not being commercially available. Heat management and a lateral ventilation system to avoid heat accumulation were established and a stable light intensity achieved. Different photoacids were characterised and their pH dependent absorption spectra recorded. By using the reversible photoacid G-acid as a proton donor, the pH can be changed reversibly using high power UV 365 nm LEDs. To demonstrate the pH cycling, acid phosphatase with hydrolytic activity under acidic conditions was chosen. An assay using the photoacid together with the enzyme was established, also providing that G-acid does not inhibit acid phosphatase. The feasibility of reversibly regulating the enzyme's pH dependent activity by optical means was demonstrated, by controlling the enzymatic activity with light. It was demonstrated that the enzyme activity depends on the light exposure time only. When samples are not illuminated and left in the dark, no enzymatic activity was recorded. The process can be rapidly controlled by simply switching the light on and off and should be applicable to a wide range of enzymes and biochemical reactions.

Conclusions Reversible photoacids offer a light-dependent regulation of pH, making them extremely attractive for miniaturizable, non-invasive and time-resolved control of biochemical reactions. Many enzymes have a sharp pH dependent activity, thus the established setup in this thesis could be used for a versatile enzyme portfolio. Even though the demonstrated photo-switchable strategy could also be used for non-enzymatic assays, greatly facilitating the assay establishment. Photoacids have the potential for high throughput methods and automation. We demonstrated that it is possible to control photoacids using commonly available LEDs, making their use in highly integrated devices and instruments more attractive. The successfully designed 96 well high power UV LED array presents an opportunity for general combinatorial analysis in e.g. photochemistry, where a high light intensity is needed for the investigation of various reactions.

Publications

Journal Contributions

1 **H. Kagel**, , F.F.Bier, M. Frohme, J. Glökler *"Reversibly Controlling Enzymatic Activity Using a Photoacid"*, Manuscript submitted to **ACS Omega, assigned to editor**

2 **H. Kagel**, Hannes Jacobs, J. Glökler, M. Frohme, F. F. Bier (2019)*"A Novel Microtiter Plate Format High Power Open Source LED Array"*, **Photonics**, vol. 6, 17; [doi:10.3390/photonics6010017]

3 **H. Kagel**, M. Frohme, J. Glökler (2019) *"Photoacids in Biochemical Applications"*, **Cellular Biotechnology**, vol. 4, no. 1-2, pp. 23-30, 2018, [doi: 10.3233/JCB-189004]

4 **H. Kagel**, Julia Honselmann Genannt Humme, Edvaldo Antonio Ribeiro Rosa, Rozane de Fátima Turchiello, Arandi Ginane Bezerra Junior (2015) *"Plasmonic enhancement in the photoinactivation of Escherichia Coli using rose bengal and gold nanoparticles "*, **Biophotonics South America**, vol. 9531, 953138 [doi: 10.1117/12.2180947]

Conference Contributions

1 **H. Kagel**, M. Frohme, J. Glökler *"Reversibly controlling enzymatic activity using a photoacid"*, Presentation at **Chemistry for Advances in Diagnosis and Therapy** Seminar in Elgersburg, Germany 2019

2 **H. Kagel**, M. Frohme, J. Glökler *"Liph Cycle - a non- invasive method to control biochemical reactions"*, Presentation at **Trends in Biomedical Sciences**, in Wildau, Germany 2019

3 **H. Kagel**, M. Frohme, J. Glökler *"Liph Cycle - a non- invasive method to control biochemical reactions"*, Presentation at **DNA Mitteldeutschland Symposium** in Potsdam-Golm, Germany 2018

4 **H. Kagel**, M. Frohme *"Controlling Enzyme Activity with Light using Photo Acids "*, Presentation at the **PhD Symposium on Bioanysis** in Luckenwalde, Germany 2017

Contents

1 Acronyms

6CN2 6-Cyano-2-Naphthol

AP Acid phosphatase

AB Acetate Buffer

BCG Bromcresol Green

CF-MUP 6-chloro-8-fluoro-4-methylumbelliferone phosphate

CF-MU 6-chloro-8-fluoro-4-methylumbelliferone

DMSO Dimethyl sulfoxide

DNA Deoxyribonucleic acid

DLP Digital light processing

dsDNA double stranded DNA

ESPT Excited state proton transfer

G- Acid 2-Naphthol-6,8-disulfonic acid

HPTS 8-hydroxy-1,3,6-pyrenetrisulfonate

HPLC High pressure liquid chromatography

HP High Power

IR Infra-red

LED Light Emitting Diode

MP Medium power

mPAH metastable photoacid

pNPP para-Nitrophenylphosphate

PAG photoacid generators

PAH reversible photoacids

PCR polymerase chain reaction

R- Acid 2-Naphthol-3,6-Disulfonic Acid

RB Reaction buffer

ssDNA Single stranded DNA

TB Thermopol Buffer

UVA Ultraviolet A

2 Preamble

Controlling enzymatic activity with light is a desirable achievement in a multitude of applications and of high research interest [1, 2]. Many enzymes have a sharp pH profile, being active only when the pH value is higher or lower than a certain limit. Hence, if the pH value could be controlled optically, it would be possible to regulate a vast variety of enzymatic reactions in a non-invasive manner. Optical control of pH can be achieved by using reversible photoacids [3, 4, 5] to photo-induce a reversible pH jump. A photoacid is an aromatic alcohol that transforms into a strong acid upon irradiation [6] and undergoes excited state proton transfer (ESPT) in this process [7, 8, 9]. The acidity enhancement after excitation is typically on a scale of a factor of $10^6 - 10^8$ thus decreasing the pK_a by $6 - 8$ units [10]. Generally, photoacids are subdivided into two main classes: Photoacid generators (PAGs) and reversible photoacids (PAs). PAGs dissociate upon irradiation and irreversibly form strong acids while undergoing a photo destructive process. This unique property to acidify the surrounding upon irradiation has often been used in photo-polymerization. In a seminal experiment, Kohse et al. succeeded in optically starting the activity of the enzyme acid phosphatase by a laser–induced pH jump [1] using a PAG. Although, this reaction is irreversible, it demonstrated the feasibility of a non-invasive initiation of an enzyme other than thermal control. In contrast to a PAG, a reversible photoacid is not structurally disintegrated upon illumination, but re-associates with it's proton after returning to the ground state. Very common families of photoacids include phenol, naphthol and pyrene derivatives. Characteristic is the functional group for all reversible photoacids, which donates the proton in the ESPT process [5] and is able to interact with the surrounding. Depending on various factors the photo-released proton can diffuse and escape the zone of influence of the parent ion, enabling it to react with the surrounding environment. It is also possible that it is recaptured by the parent ion after it has returned back to the ground state. The dissociation can be induced by a laser pulse, converting a weak acid into a strong acid [11, 12, 13]. This process takes place on the scale of pico- to nanoseconds. Reversible photoacids have been extensively used to study ESPT. However, their applications in biochemistry and biology are still scarce and are reviewed in our recent publication [14]. This work is focussed on developing and establishing a pH dependent biochemical assay, which can be conducted in a cycled, reversible fashion by a photo-switchable strategy using a photoacid.

3 Theoretical Background and State of the Art

3.1 Photoacids

A photoacid is an aromatic alcohol, that transforms into a strong acid upon irradiation [6] and undergoes excited state proton transfer (ESPT) in this process. The acidity enhancement after excitation is typically on a scale of a factor of $10^6 - 10^8$, thus decreasing the pK_a by $6 - 8$ units [10]. Photoacidity was first investigated by Weber, Förster and Weller, more than half a century ago [15]. The majority of research focussed on the dynamical studies of acid base reactions by using the unique properties of photoacids [3, 8, 16] Generally photoacids are subdivided into two main classes: **photoacid generators** (PAGs) and **photoacids** (PAH). While PAGs irreversibly undergo proton photo dissociation, PAHs reversibly recombine thermally after the photo induced dissociation. Photoacidity is most often described by the Förster cycle diagram, see figure 3.1.

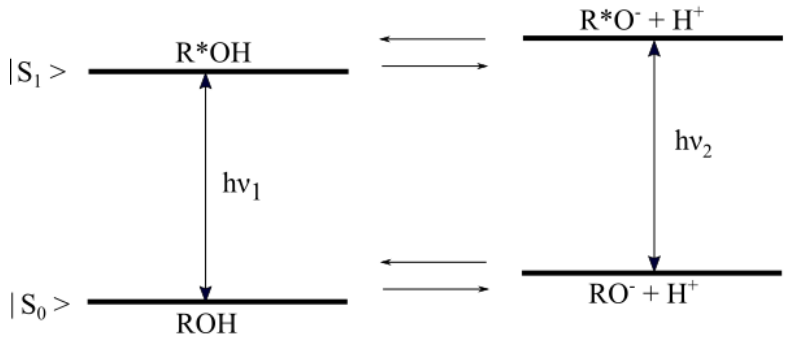

Figure 3.1: Schematic representation of a photoacid's energy level, excited by light with the frequency $h\,\nu_1$ where RO*H is the excited photoacid with its conjugate base R*O⁻. $|S_1>$ represents the first singlet excited state and $|S_0>$ the ground state

Following Förster, photoacidity is defined in terms of K_a^*, the excited state equilibrium constant for the dissociation reaction of the photoacid [17].

$$\Delta pK_a = pK_{a0} - pK_a^* = \frac{Nh\Delta\nu}{ln(10)RT} \tag{3.1}$$

Where N is the Avogadro constant, h is the Planck constant and $\Delta\nu = \nu_1 - \nu_2$. ν_1 being the 0-0 transition of the acid and ν_2 the 0-0 transition of the anion. K_a being defined as the equilibrium constant, as it is valid for proton transfer reactions in water:

$$HA + H_2O \Longleftrightarrow H_3O^+ + A^- \tag{3.2}$$

HA being the Bronsted Acid, which donates a proton H^+ to the solvent, e.g. water. In this process an anion A^- is produced. Thus a photoacid can also be defined as a molecule, where the ground state acidity is lower than its acidity in the exited state: $pK_a^* < pK_{a0}$; pK_{a0} being the equilibrium constant for the proton dissociation reaction in the ground state and pK_a^* being the equilibrium constant for the proton dissociation reaction in the excited state. After excitation, the liberated proton of the ion pair can follow two options: It either recombines with the excited, deprotonated state photoacid, RO^{*-} to finally return to the ROH^* state, which is known as the germinate recombination process, or it diffuses to the bulk solvent, $RO^{*-} + H^+$ [5].

The fluorescence intensity (from S1 to S0) is a function of the pH in solution, which can be monitored by titrating the photoacid while in the excited state. This has been shown by Weller [17]. Gradually adding a strong acid (e.g. HCl) to a photoacid solution shifts the acid-base-equilibrium towards the acid form (when starting in alkaline or neutral conditions). Thus, by continuously recording absorption spectra, while titrating a strong acid, will result in similar informations about the acid- base equilibrium, as monitoring the fluorescence. Using this method the pK_a^* can be experimentally estimated. Much more precise, however also increasingly complicated, is the direct kinetic measurement of the ESPT [18] to determine the pK_a^*.

3.1.1 Irreversible Photoacids - PAGs

Photo Acids Generators (PAGs) diossociate upon irradiation and form strong, irreversible, acids while undergoing a photo- destructive process. Their unique properties have often been used in photo-polymerization to enhance polymer properties or adding a post processing step for novel material formation [19, 20, 21]. PAGs were not only used for polymerization, but also for starting an enzymatic reaction - Kohse et al. succeeded in optically controlling the activity of acid phosphatase by a laser–induced pH jump [1]. This allowed the development of a non-invasive initiation of a biochemical reaction. A wide range of enzymes have pH dependent activities, thus offering a condition by which enzyme activity can be optically controlled by a light pulse, using a PAG. In a fundamental experiment acid phosphatase was combined with a PAG (2 nitrobenzaldehyde) in an aqueous solution [1]. The enzyme is active at a pH below 8 and has its optimum activity at a pH of 5. The hydrolytic activity of acid phosphatase was controlled by switching the conditions from an alkaline pH of 8 to an acidic pH of 6. To yield a pH-jump of nearly two units, a short laser pulse was used, inducing the proton release of the PAG. Typical sample irradiation times were 250 ms, lowering the pH sufficiently to activate the enzyme. In order to monitor the altered activity 6-chloro-8-fluoro-4-methylumbelliferone phosphate (CF-MUP) was used as a substrate. CF-MUP significantly changes absorption at 360 nm after hydrolysis from CF-MUP to 6-chloro-8-fluoro-4-methylumbelliferone (CF-MU) [1]. CF-MUP was also used by Yang et al. to track the activity of acid phosphatase [22]. Kohse et al. arrived at an experimental setup without any loss of enzyme activity. Thus, it is possible to locally change the pH rapidly in a very small volume, even controlling enzymatic activities in an optical, non-invasive manner without loss of activity. Other promising enzymes with a significant pH-profile concerning activity are suggested in their work. Those could possibly be activated in a similar manner, offering a wide range

of applications. Examples are: laccase, catalase, polyphenol oxidase, β-glucosidase and L-arginine decarboxylase [1]. Acid phosphatase will be considered in more detail in section 3.2.2. However, as a PAG was used the enzyme activity could be triggered once only and the process was irreversible.

3.1.2 Reversible Photoacids -PAHs

In contrast to a PAG, a reversible photoacid does not dissociate upon illumination, but thermally re-associates with a proton after returning back to the ground state. Very common families of photoacids can be seen in figure 3.2. Those include phenol, naphthol and pyrene derivates. Characteristic is the functional group for all reversible photoacids, which donates the proton in the ESPT process. Dependent on various factors, the photo-induced liberated proton can either diffuse away from the parent ion and escape the zone of influence of the parent ion, which makes it possible to react with the surrounding. Or is recaptured by the parent ion after this has returned back to the ground state [23]. Generally all ESPT examinations, as well as ultra short pH jumps experiments are conducted with a short laser pulse in the range of nano- or picoseconds, e.g. using ultrafast laser spectroscopy [11].

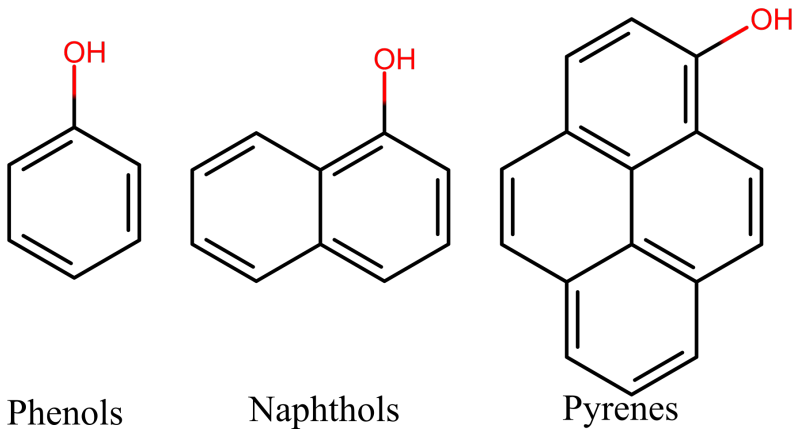

Figure 3.2: Common families of known reversible photoacids. Mandatory to function as a photoacid is the functional OH group

As phenols and their derivatives are toxic [24, 25] and absorb in the UVB region [26] they were not chosen for this work. LED illumination sources in the UVB spectra are less powerful and are very expensive. Furthermore UVB irradiation often damages biological compounds, such as DNA and enzymes [27, 28].

Reversible photoacids are highly acidic in the excited state (low pK^*) and usually display a weak acidity in ground state (pK_0 close to neutral pH). Figure 3.3 schematically shows the deprotonation process of a pyrene derivative.

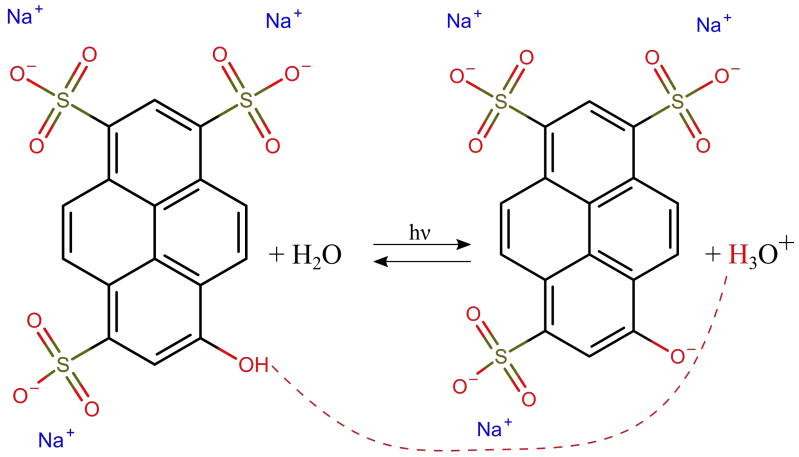

Figure 3.3: Schematic chemical reaction when a reversible photoacid is illuminated with the appropriate wavelength *hv*: Upon irradiation an ESPT takes place and the liberated proton can interact with the aqueous surrounding. The process is reversible

Photoacids used in this work are:

- 8-Hydroxypyrene-1,3,6-Trisulfonic Acid (HPTS)
- 2-Naphthol-6,8-disulfonic acid (G-acid)
- 2-Naphthol-3,6-Disulfonic Acid (R-acid)
- 6-Cyano-2-Naphthol
- 3-Amino-2-Naphthol
- 3-Bromo-2-Naphthol
- mPAH1 (metastable)

HPTS

The pyrene derivative HPTS, by appearance a light yellow liquid when in an acidic environment and a bright yellow when present in neutral or alkaline conditions. The pyrene derivative is probably the most prominent and best studied photoacid. It is characterized by an acid dissociation constant ($pK^* = 0.5$), which is much lower than that of the ground state (pK_0=7.7) [11, 3, 4]. Not only has HPTS been extensively used for ESPT studies [5], but also for biological applications to monitor the pH as per fluorescence in cells in near neutral pH [29] or to develop a sterilizeable HPTS- based sensor, which can be used for online pH monitoring of an E. coli fermentation [30].

As for all photoacids, the pK_{a0} value of HPTS varies with the nature and ionic strength of the solution. At a physiological pH, the pK_{a0} will be around 7.7, with a fluorescence quantum yield of almost 100 % in both, alkaline and acidic solution, when excited with

light of a larger wavelength then 400 nm [29]. The chemical structure of HPTS can be seen in figure 3.4. HPTS is a water-soluble compound, which makes it a great potential photoacid for biological applications, as many photoacids are not soluble in water, e.g. 1-Napthol. Gutman et. al demonstrated in their work [11, 13] that aqueous solutions could be acidified on a microsecond scale by exiting the photoacid HPTS, using a short laser pulse of 50 ns. Also Hynes et al. demonstrated the photochemical proton transfer in aqueous solution using HPTS, phenol and substituted phenols [31]. PH indicators, such as bromcresol green, were used for a second-order diffusion controlled reaction: The photoinduced proton ejected from the photoacid changed the formation of the pH indicator and made a spectroscopic determination of pH change possible. Also using HPTS, Haghighat et al. could measure an increase in proton conductivity upon irradiation by doping materials with the photoacid [23]. Thus demonstrating, that the released proton is indeed liberated and can interact with its surrounding.

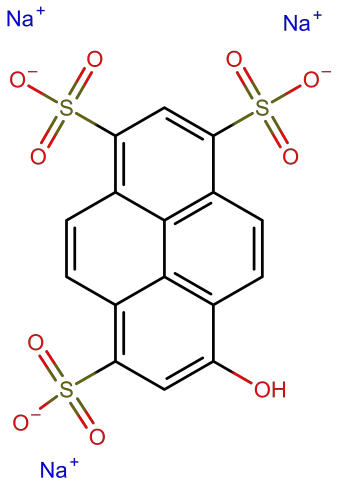

Figure 3.4: Molecular structure of HPTS

An example for a bioelectrical, miniaturizable device using a photoacid is given by Peretz-Soroka et al. [32]. They developed a prototype with which they could control and monitor the pH using a nanowire-based FET device. Silicon nanowires were chemically modified by photoactive HPTS derivatives and by biomolecules, e.g. enzymes. All of the involved compounds were immobilized to the surface. Effected by the surface-anchored photoacid molecules, a photo-induced pH jump could be detected resulting in a proton transfer to the solvent. This was achieved by measuring the change in surface potential alteration which modulates the current flow. HPTS exhibits a pH-dependent adsorption shift and therefore additionally allowed the pH determination by ratiometric fluorescence measurements in parallel: Two excitation wavelengths at 405 nm and 450 nm have been used. At a pH below 7 the absorbance at 450 nm rapidly decreases and thus the fluorescence [33]. Using this characteristic of HPTS, both as a photoacid and as a fluorescence pH indicator Peretz-Soroka et al. performed the experiment using HPTS and trypsin modified silicon nanowires. Trypsin acidifies the solution while hydrolyzing its specific substrate N $-\alpha$-Benzoyl-L-arginine ethyl ester (BAEE), thus resulting a long-term change in conductivity and pH. The enzyme activity was monitored using the described device and method above [32]. As a next step a HPTS-pepsinogen complex was anchored to the silicon nanowires. The inactive proenzyme pepsinogen is actived at an acidic pH of about 2-4 by self-processing resulting in the active protease pepsin. In addition, the reaction leads to further acidification of its surrounding by the hydrolysis reaction [34]. By steady HPTS

illumination using a wavelength of 400 nm a pH jump was caused. The generation of the active pepsin was controlled and monitored with a single multifunctional device. Therefore, local modulation and monitoring of surface pH by the use of a reversible photoacid was successfully achieved, offering the development of multifunctional bio-FETs [35].

G-acid

2-naphthol-6,8-disulfonate (G-acid) is transparent when in solution, both in acidic and alkaline environment and belongs to the family of naphthols. Just as HPTS, due to the sulfonate groups, it is a negatively charged molecule (figure 3.5). G-acid also has a low toxicity and is well soluble in water.

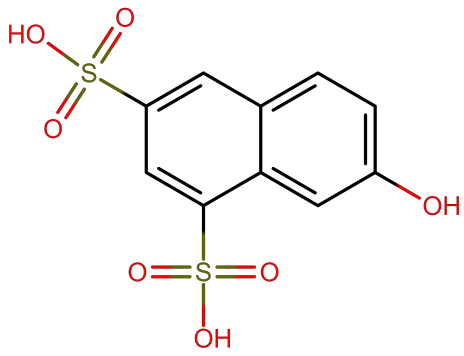

Figure 3.5: Molecular structure of G-acid

G-acid has an even more significant ΔpK_a when irradiated: The pK_{a0} in it's ground state is $pK_{a0} = 8,99$, which is significantly lowered to and excited $pK_a^* = 0.7$ [17]. This is more than 8 units difference and thus G-acid is an even stronger photoacid than HPTS. Considering the price, which is dramatically lower than that of HPTS, it offers an attractive alternative. However, as it is a naphthol derivative, it does not absorb in the visible spectrum, but in the UV-Spectra. This strongly limits the possibilities of cost- effective and easily available irradiation sources. Kaufmann et al demonstrated the possibility of ultra fast pH jumps, using 2-naphthol-6,8-disulfonate. They determined the life time of the excited state to be 14 ns, the reverse process is diffusion dependent and takes up to microseconds [36].

Photoacids cannot only induce pH jumps, but are also suitable to analyse biomaterials, their proton transfer rates, as well was their binding characteristics. Amdursky et al. used surface-bound photoacids to study excited-state proton transfer and binding sites on insulin amyloid fibril surfaces [37, 5]. G-acid was one of the naphthol derivatives used in this study. Diseases, such as Alzheimer or Parkinson are related to the formation of amyloid fibrils [38, 39]. During the fibrillogenesis process, the soluble amyloid proteins aggregate into an insoluble structure. It is important to fully understand the structure of amyloid fibrils to be able to design molecular inhibitors to fibrillogenesis [40, 41]. This can be achieved by studying and understanding the surface structure of amyloid fibrils and their interaction with aqueous surrounding. Amdursky et al. analyzed the surface and binding sites of amyloid fibrils, using different photoacids: Aim of this study was to explore various binding sites of insulin amyloid fibril. The use of photoacids of

different strength allowed the group to analyse the propagation of protons along the fibril surface. Also, using this strategy photoacids can be used as a marker for amyloid fibrils, employing their fluorescence upon excitation. The group used photoacids of different strength: The naphthol- based photoacids strongly differed in their pK_a^*, thus releasing a significantly different proton concentration upon irradiation. Also the selected naphthol derivatives differed in their sulfonic groups and thus in their binding capacity. Followed by extensive molecular dynamics simulations, the binding modes and mechanisms of the surface-bound photoacids were analysed, resulting in a detailed characterization of different binding modes to the surface of amyloid fibrils. The results of Amdursky et al. could contribute to the design of future fibrillogenesis inhibitors. Hence, photoacids can also be applied as fluorescent markers to understand the binding mechanism of small molecules, such as photoacids, to amyloid fibrils.

R-acid

2-naphthol-3,6-disulfonic acid or R-acid also belongs to the family of 2-naphthols. When present as salt, R-salt, it is an important dye intermediate. It is produced from naphthalene by a combination of the unit processes of sulfonation, nitration, reduction, and hydrolysis. When present as salt, R-salt is used in the manufacture of a large number of azo dyes and pigments [42]. It's molecular structure is very similar to G-acid (figure 3.6).

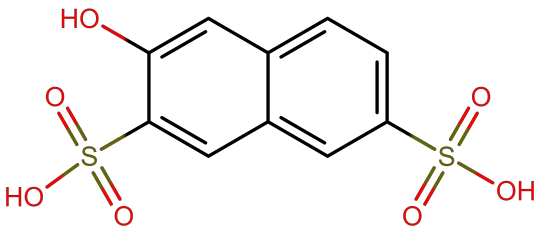

Figure 3.6: Molecular structure of R-acid

R-salt has been used to study the saturated adsorption capacity of chitosan-β -cyclodextrin [43] and has been used to functionalize polystyrene divinyl benzene (8%) copolymer in order to do elemental analysis of polystyrene divinyl benzene and kinetic studies of chromium [44]. It has also been used to study the acid-base equilibrium reactions within the trimethyl ammonium-modified mesoporous silica vs. the reaction equilibrium in bulk water [45]. Furthermore R-acid was found to have adsorption and corrosion inhibitive properties on iron electrode in sulfuric acid [46]. R-acid is listed as a photoacid in "Chemistry of Phenols" [17], however the pK_a and pK_a^* is not calculated and thus unknown.

6-Cyano-2-Naphthol

White to tan in appearance is this naphthol derivative. 6-cyano-2-naphthol (6CN2) has more hazardous statements and exhibits a greater toxicity. It is acutely toxic when swallowed and causes skin irritation [47]. 6-cyano-2-naphthol has a $pK_{a0} = 8.4$ when in the ground state. This lowers to $pK_a^* = 0.2$ [48] . Due to the magnitude of the large pH jump it is also referred to as "Super Photoacid" and has been used for ESPT experiments [49]. The

molecular structure of 6-cyano-2-naphthol is sketched in figure 3.7. The proton-transfer kinetics and photophysical behaviour of 6CN2 have been investigated by Nakayama et al. [50].

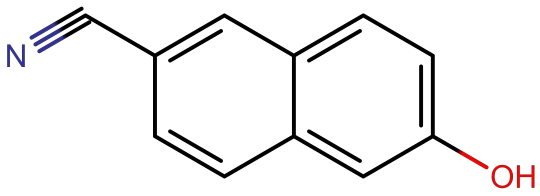

Figure 3.7: Molecular structure of 6-cyano-2-naphthol

Also, its derivative 5-cyano-2-naphthol has been analysed and also belongs to the group of "Super Photoacids". Gopich et al. demonstrated the the ESPT of 5-cyano-2-naphthol is reversible and happens in a few nanoseconds [51]. Apart from that steady-state and time-resolved fluorescence of 5-cyano-2-naphthol in various pure solvents, such as ethanol and dimethyl sulfoxide (DMSO) have been studied [52].

3-Amino-2-Naphthol

This photoacid is a naphthol derivative (figure 3.8), which is acutely toxic when swallowed and causes skin irritation [53]. The ESPT for the very similar compounds 8-amino-2-naphthol and 5-amino-2-naphthol was analysed and the pK_a was found to be $pK_a = 9.5$ for the ground state $pK_a^* = 1.1$ for the excited state for both derivatives [54]. However, 3-Amino-2-Naphthol hasn't been studied yet. In a patent, 3-Amino-2-Naphthol is also listed as a part of a photo-curable composition [55].

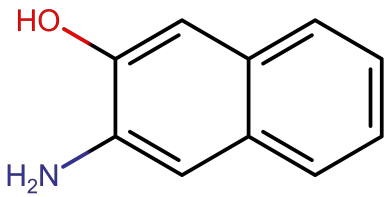

Figure 3.8: Molecular structure of 3-amino-2-naphthol

Also, this photoacid seems to be a promising candidate for releasing protons to aid in photosynthesis and will be analysed soon [56]. However this photoacid is generally not well studied yet.

3-Bromo-2-Naphthol

Also part of the naphthol family is 3-bromo-2-naphthol. It's molecular structure can be seen in figure 3.9. It is toxic and causes skin irritation [57]. It's very similar derivatives 6-bromo-2-naphthol and 1-bromo-2-naphthol have been used to study the ESPT. For 6-bromo-2-naphthol the $pK_a = 7.8$ in the ground state and $pK_a^* = 1.4$ in the excited state.

For 1-bromo-2-naphthol the $pK_a = 9.2$ in the ground state and $pK_a^* = 3.1$ in the excited state [58].

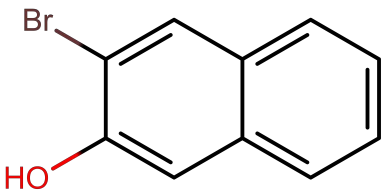

Figure 3.9: Molecular structure of 3-bromo-2-naphthol

Generally speaking, reversible photoacids introduced in this section are mostly used to demonstrate either ESPT or to induce very short lived pH jumps using a short laser pulse as an optical trigger. However, PAHs have scarcely been illuminated continuously and have never been excited using simple light emitting diodes (LEDS) as illumination sources in free solution.

3.1.3 Metastable Photoacids - mPAHs

The recently discovered metastable photoacids (mPAH) present a new opportunity regarding photoinduced pH jumps: While the irradiation of a PAH results in a very short lived pH jumps (microseconds until recombination process has taken place), metastable photoacids can change the pH for minutes to hours [59]. Figure 3.10 shows two different metastable photoacids. mPAH2 has been used in this thesis and is referred to as mPAH.

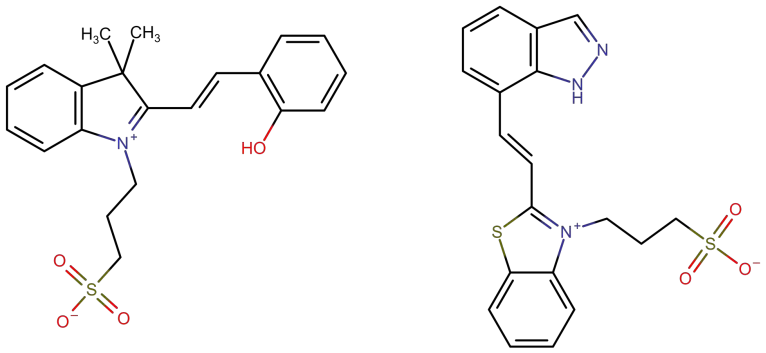

mPAH 1 mPAH 2

Figure 3.10: Two examples of metastable photoacids, mPAH1 and mPAH2

The long pH jump is correlated to the different approach in designing the mPAHs: They are generally designed by linking an electron- accepting moiety and a weakly acidic nucleophilic moiety with a double bond, which enables an absorption of visible light [6]. As both, the forward and backward, reactions are multi-stepped the half live is extended from seconds to hours [6]. A schematic sketch of the proposed mechanism is displayed in figure 3.11.

Moreover the pK_{a0} of mPAH is usually below 8, thus exhibiting an initial pH of 5.5 or similar when being dissolved in aqueous solution [60]. If they can be dissolved in aqueous

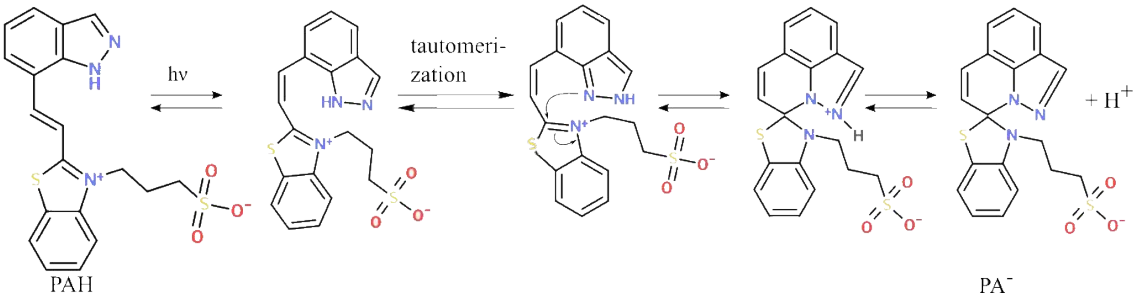

Figure 3.11: Proposed mechanism of Liao et al. for the photo induced excited photoacid state. The photoacid first forms a tautomer, thus shifing electron density charges and finally the proton is liberated and can interact with the aqueous surrounding.

solutions at all, as some of them are only soluble in methanol [19].

Metastable photoacids have been used to switch pH indicators in solution [60] and cause a colour change in pH indicator doped polymer and PCL films , [61]. A huge drawback is the often very slow recombination rate of mPAH, which can take longer than 24 hours. Some even have a half-life as high as 128 h [62], thus making it unsuitable for biological applications. Nevertheless Luo et al conducted an experiment with multidrug-resistant bacteria in which they used a mPAH to enhance the bacteria killing by a photo-induced pH drop [2]. The starting pH here was 5.8, which is not applicable for most biological reactions, usually requiring a physiological pH of about 7. Driven by the desire to open up opportunities for mPAH in the biological field yet another metastable photoacid was developed, which is able to keep it's proton in PBS buffer with a pH of 7.4 [63]. This is also the photoacid tested in this thesis . After irradiation with visible light the mPAH reached it's original pH after being kept in the dark for 48 h.

Apart from metastable photoacids, there are also metastable photobases, which principally function similar to metastable photoacids: They donate an OH– and thus increase the pH value of a solution. They have been used to change the structure of a single stranded DNA from a random coil to the stable i-motif form by increasing the pH value upon illumination [64, 65]. However, as demonstrated by Liu et. al, they have the same current drawback as mPAHs: Their recombination rate is very slow and they are destructed with each applied photo-induced pH cycle.

Overall mPAHs and photobases propose promising options for biological applications when being further developed. Also they are usually not commercially available for buying, but have to be synthesised independently.

An overview of characteristics of photoacid used in this thesis is given in table 3.1.

Table 3.1: Overview of photoacids used and their pK in ground state (pK_{a0}) and excited state(pK_a^*), as well as the dfference between the two (Δ pH)

Photoacid	pK_{a0}	pK_a^*	**Δ** pH
HPTS	7.7	0.5	7.2
G-acid	8.99	0.7	8.29
R-acid	n.a.	n.a.	n.a.
6-Cyano-2-Naphthol	8.4	0.2	8.2
3-Amino-2-Naphthol	n.a.	n.a.	n.a.
3-Bromo-2-Naphthol	n.a.	n.a.	n.a.
mPAH	10.1	1.25	8.85

3.2 Biochemical reactions

Control of biochemical components or reactants is often achieved by changing temperature. A prominent example are smart polymeric materials that respond to a change in temperature [66]. However, those materials, as well as many other biochemical processes, also respond to environmental stimuli such as pH. Examples for pH dependent components are versatile: polymeric materials [66], pH dependent enzymes, amino acids [67] and electrophoresis [68]. Generally hydrolytic activity is either accelerated by enzymes or an acidic pH value [69].

3.2.1 Using UV light in Biochemical Reactions

To use a photoacid in a wide range of biochemical applications it must fulfil certain requirements: It should be soluble in water, have a low toxicity and be excitable with commonly available, cheap illumination sources, such as LEDs. LEDs have several advantages compared to more conventional illumination sources: They are more efficient, have a long life time, a compact size, and high reliability [70]. Furthermore they can be easily obtained and the mounting is significantly less complex than that of laser systems. Modern LEDs allow long-term generation of irradiation with a wide range of wavelengths available [71]. Recent advances in LED technology provide efficient light sources in the UV and blue wavelength spectrum [72, 73, 74]. A high power 365 nm LED array was developed in this thesis. Thus examples for the need to use high power LEDs in biochemistry will be presented for this wavelength. An example for using high power LEDs in research is exemplified by Hölz et al. [75] who replaced a commonly used high-pressure mercury arc lamp by an ultra-high power 365 nm LED for use in photolithography, offering economic and ecological advantages, as well as lower hardware costs and a very long lifetime.

Moreover, 365 nm LEDs light can be used to degrade organic pollutants, such as malachite green dye or diazinon, in water [76]. Also, UV radiation seems to play a role in forming DNA- protein crosslinkings that may significantly influence bacteria inactivation in correlation with light intensity used [77]. Some applications require the use of high power illumination sources. For example to fabricate oligonucleotide microarrays (1,000 W Hg

arc lamp was used in [78]), to extend investigations of photochemical reactions which involve free radicals using higher light intensities or selective removal of photolabile protecting groups [79, 80], e.g. LEDs with 3 W or higher. Furthermore, determination of hydroxyl radical reaction rate constants can be facilitated using high power UV LEDs [81]. Due to their small size high power UV LEDs are used to design new photoreactors to improve photocatalytic processes [82]. The previously presented examples demonstrate that LEDs are versatile in their applications [83] and high power LEDs can be used in many different biochemical areas.

Complex biochemical assays and their reactions are preferably run and analysed in parallel to conduct experiments in the same environmental conditions. Combinatorial assays, especially for chemical or biochemical applications, demand arrays that allow individual control with high throughput possibilities and the option for automation. A standard format is the 96 well microtiter plate [78]. Various applications, e.g. microfluidic environments, demand illumination with a specific spectrum and a certain intensity, such as 365 nm UV- light. Also, irradiation often requires to be strictly limited to a precise position.

When working with light-dependent biochemical assays, it is desirable to use an LED array which is suitable for microtiter plates. There are some companies, that specialized in the fabrication of such arrays, demonstrating the need and interest in them. Currently a variety of low or medium power LED arrays in microtiter format are available with different wavelengths [84, 85, 86, 87, 88]. Those are mainly used for cell or bacteria cultivation. When high power UV illumination is demanded a solution of using a single ultra high power LED to illuminate one microtiter plate homogeneously is available [89]. This does allow irradiation experiments using high power UV light, but does not offer spatial illumination control. Thermal management and maintaining stable illumination becomes more challenging the higher the intensities of the LEDs are. Nevertheless, the previously listed commercial illumination devises further demonstrate the increased usage of LEDs in a microtiter plate format in biochemistry, beyond classical illumination purposes, such as street lights. The challenge in designing a large high power LED array is mainly the heat management, as overheating will decrease the intensity output and high temperatures may be opposed to the illumination task, which is e.g. a temperature limited reaction [90]. So far, a high power LED array using UV light in microtiter plate format is not commercially available yet.

To maintain a stable illumination heat development and LED cooling is mandatory. To estimate the LED heat dissipation, the casing temperature T_C can be measured directly from an IR image. The T_J, which is the significant parameter for LED heat and stability management is calculated as follows and have to be taken into account when designing an LED array:

$$T_J = \Theta_{JC} * P_D + T_C \tag{3.3}$$

where T_J is the operating junction temperature in °C, Θ_{JC} is the junction-to-case thermal resistance in °C/W, P_D the Power dissipation in W and T_C the case temperature in °C [91]. The LEDs used in this thesis have a stable output intensity to a maximum junction temperature of 65 °C, a maximum power dissipation of 2660 mW and a junction-to-case thermal resistance of 15 °C/W (datasheet). The power dissipation and junction-to-case thermal resistance are constant throughout the experiment. Due to this fact it is sufficient to consider the casing temperature only.

3.2.2 Enyzmes

Many enzymes are specialised to work in an acidic environment and are inactive at a neutral or alkaline pH. One example for an enzyme that is active in an acidic environment (optimum pH 4) is pepsin. It is a very potent enzyme, which breaks down large protein molecules into small peptides and converting almost all of the structural proteins into soluble small molecular weight substances [92]. However, once activated by an acidic pH the enzyme's activity is irreversible and it irreversibly denatures at a pH of 8 [93]. For this work robust enzymes are needed that can undergo a number of pH cycles and have a reversible, pH dependent activity. Acid phosphatase from potato and S1 nuclease fulfil this conditions and are used in this work. A short overview of their characteristics will be given in the following section.

S1 Nuclease

S1 nuclease is non-specific endonuclease which is mainly active on single stranded DNA and RNA [94]. It catalyses the degradation of single stranded nucleic acids into oligonucleotides and 5′ mononucleotide, depending on the enzyme concentration.

A unit is defined as the amount S1 nuclease required to hydrolyse 1 µg of denatured DNA in 1 minute at 37°C. It's used to cut overhangs of dsDNA or to hydrolyse ssDNA. When used in high concentrations it can also hydrolyse dsDNA or RNA as well as cut dsDNA when a nick in one strand is present, $ZnSO_4$ is essential for the enzyme's activity. The schematic functionality is shown in figure 3.12. The enzyme is stable and active up to 65°C [94]. It has an optimum activity at a pH of ca 4.8 and is nearly inactive at a pH of 7 and higher [95, 96].

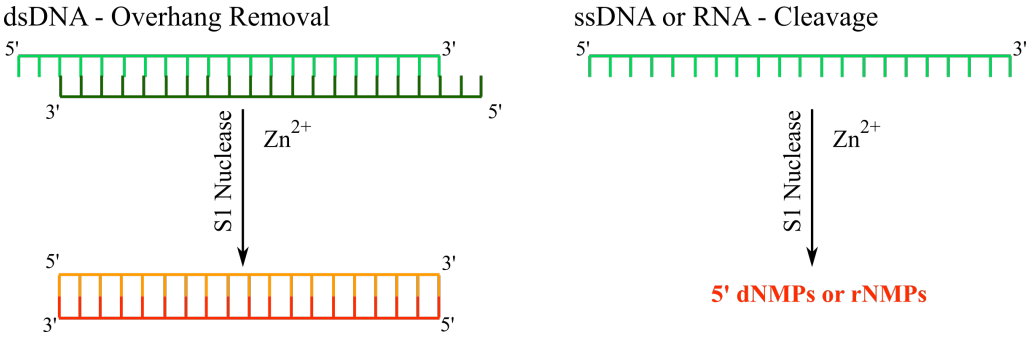

Figure 3.12: Schematic functionality of S1 nuclease. The enzyme need zinc ions for its reaction. The S1 nuclease removes overhangs from dsDNA and fully cleaves single stranded DNA.

Acid Phosphatase

Acid phosphatases are enzymes of the group phosphatases. The activity optimum of them is at an acidic pH of 4.5 - 5.5 [97]. Acid phosphatases non-specifically catalyse the hydrolysis of e.g. monoesters to produce inorganic phosphate under acidic conditions [98].

The used enzyme, acid phosphatase (AP) from potato (EC 3.1.3.2) is a non-specific phosphomonoesterase, which can appear in multiple molecular forms of similar molecular mass. The enzyme's activity strongly depends on the pH. Acid phosphatase from potato is active between pH 4-7 [99], with an activity optimum at a pH of 5 – 5.3 [97, 100]. Whereas, at a pH of 8 the activity is several orders of magnitude lower, about 3% [1]. 50% enzymatic activity of AP can be lost after 30 minutes at 60°C and 100% of its activity after two hours at 70°C [101].

A standard assay to determine AP's activity is the p-nitrophenyl phosphate (pNPP) assay [102]. The pNPP assay is a colorimetric assay. The substrate pNPP is hydrolysed by acid phosphatase into the product p-nitrophenol (pNP) + Pi in purified HPLC grade water:

$$pNPP \xrightarrow{\text{Acid Phosphatase}} pNP + P_i \tag{3.4}$$

The chromogenic reaction product, pNP turns yellow (λ_{max} = 405 nm) at a pH of 12 and can be detected using an microtiter plate reader [103].

4 Thesis Outline

Main goal of this PhD thesis is the establishment of a new method to remotely control biochemical applications in a non invasive manner using the pH value as a regulatory parameter. Photoacids shall be used to achieve a photo-induced pH control. The newly developed approach shall be faster and more economic than classical approaches, enabling the user to control pH dependent processes optically. The thesis consists of three main parts (I) Finding and characterizing suitable photoacids, also in respect to biochemical compatibility (II) Development of a high power LED array (III) Combination of established methods and establishing an assay to control an enzyme's activity by optical pH cycling.

First part of the thesis shall be about analysing and finding a suitable photoacid. An ideal photoacid should full fill the following conditions:

- Water soluble
- Low toxicity
- Absorption in the visible spectra at physiological pH
- High $pK_a (\geq 7)$
- Low $pK_a^* (\leq 2)$
- Moderately priced

A suitable light source to excite the photoacids shall and thus an optimal excitation source shall be found. Furthermore, the magnitude of the light-induced pH jump shall be determined.

Second part of the thesis consists in the development of a high power LED array suitable for a standard 96 well microtiter plate format in order to allow combinatorial assays. This is necessary to achieve a high reproducibility of the experiments, which is facilitated by running samples in parallel. Also a reliable setup has to be established. Different constructions and the influence of light intensities, illumination stability, as well as finding optimum LED mounting methods shall be analysed and determined.

The last part of the thesis shall combine all three preceding parts and methods by establishing a cyclic method to control the pH value and thus enzymatic activity. Suitable, robust enzymes with a strong, pH dependent activity shall be identified and assays established. The enzymes have to be specific in their reaction and have to tolerate strong light and have to display a certain robustness to repeatedly pH changes. The detection method for the enzymatic activity must not interfere with the photoacid's spectra. Furthermore, the enzymatic activity should not be inhibited by the photoacid. The cyclic, photo-induced, process is sketched in figure 4.1 and is a two step procedure. First, all components are in the dark, the enzyme is inactive at a neutral or alkaline pH value. Light is switched on, the photoacid is excited and the liberated proton can interact with the surrounding, acidifying it. Hence, in the second step, the enzyme gets active while the light is switched on and the pH is lowered. When light is switched off again., the pH value returns to neutral or alkaline and the enzyme is inactive again. The described cycle shall be repeated several

times, reversibly switching the pH value.

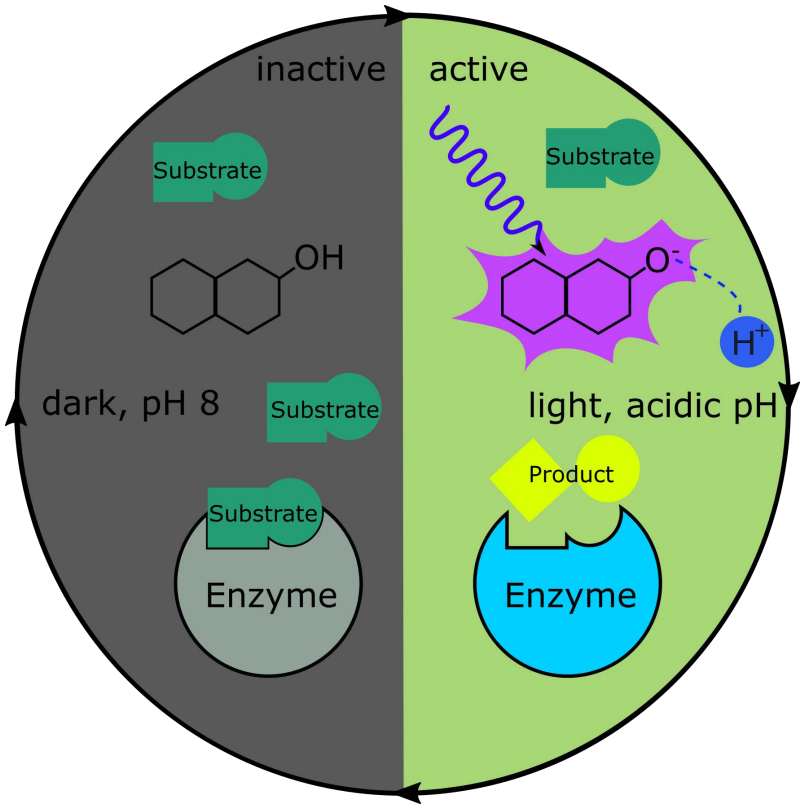

Figure 4.1: Schematic mechanism of controlling biochemical applications with light. As an example an enzyme with a pH dependent activity is chosen. This hydrolyses a substrate in an acidic environment. In darkness the pH is 8 and the enzyme is inactive. Upon illumination a two- stepped procedure is trigged: The photoacid is excited and a proton is liberated that can interact with the aqueous surrounding, acidifying it. The enzyme is then activated and hydrolyses the substrate. Adapted from [104]

The whole process shall take place in solution without immobilising any of the components to a surface.

5 Materials and Methods

5.1 Materials

5.1.1 Photoacids

If not indicated differently all photoacids were purchased from Sigma Aldrich (Hamburg, Germany) purity $\geq$ 98% (HPCE).
The following photoacids were used:

- 8-hydroxypyrene-1,3,6-trisulfonic acid (HPTS), CAS 6358-69-6
- 2-naphthol-6,8-disulfonic Acid (G-acid) from Carbosynth Ltd, Compton, UK CAS 118-32-1
- 2-naphthol-3,6-disulfonic Acid, CAS 148-75-4
- 6-cyano-2-naphthol, CAS 52927-22-7
- 3-amino-2-naphthol, CAS 5417-63-0
- 3-bromo-2-naphthol, CAS 30478-88-7
- mPAH1 (Synthesised by and bought from ENAMINE Ltd., Kyiv city, Ukraine)

5.1.2 pH Jump

Components used to measure pH jump of photoacids are listed in table 5.1. 1mM photoacid (HPTS, G-acid, R-acid and 6-cyano-2-naphthol) were illuminated for 5 minutes, then illumination was removed.

Table 5.1: List of chemicals and devices used to measure a photo induced pH jump

Application	Device	Manufacturer
pH Indicators	Bromcresol Green (CAS:76-60-8) Bromcresol Purple (CAS:115-40-2) Neutral Red (CAS: 553-24-2) Phenol Red (CAS:143-74-8), Cresol Red (CAS:1733-12-6),	Sigma-Aldrich Chemie GmbH, Taufkirchen, Germany
Micro pH electrode	SenTix® Mic-D	Xylem Analytics Germany Sales GmbH & Co. KG Weilheim, Germany
Spectrometer	High-Sensitivity UV Spectrometer Maya	Ocean Optics Largo, USA
Microtiter plate 96 well	Microtiter plate	BRAND GMBH + CO KG, Wertheim, Germany
Poket pH meter	H138 Minilab	Hach Company Loveland, United States

5.1.3 Irradiation Sources

LED Arrays

All devices which were used to build the different versions of the LED arrays are listed in table 5.2.

Table 5.2: List of used devices to build the LED Arrays

Device	Technical Data	Manufacturer
Medium power LED on 1x1 cm PCB chip	0.7 W, 365 nm	All Bright International Co. Ltd, Tainan City, Taiwan
High power LED on 8 mm PCB chip	3 W, 365 nm	All Bright International Co. Ltd, Tainan City, Taiwan
High power LED on 1x1 cm PCB chip	0.7 W, 405 nm	LUMITRONIX LED-Technik GmbH, Hechingen, Germany
High power LED on 1x1 cm PCB chip	3 W, 405 nm	LUMITRONIX LED-Technik GmbH, Hechingen, Germany
Microcontroller	Arduino Uno	Arduino Uno,AZ-Delivery Vertriebs GmbH, Deggendorf, Germany
LED driver LDD 700 L	700 mA	Meanwell Enterprises, New-Taipeh, Taiwan
Axial fan	12 V DC, 500 mA	Conrad Electronic SE, Berlin, Germany
Radial fans	12 V, DC, 50x50x15mm	YOTINO Co Ltd, Shenzhen, China
Thermal conductive adhesive tape	0.9 W/mK	Akasa Ltd, Greenford, UK
Thermal conductive adhesive paste	0.925 W/mK	Stars Co. Ltd., Taoyuan, Taiwan
Thermal conductive paste	0.9 W/mK L	Conrad Electronic SE, Berlin, Germany).
TEC1-12706 Peltier Element	60 W	Hebei I.T. (Shanghai) Co., Ltd, Shanghai, China
TEC1-12710 Peltier elements	85 W	Hebei I.T. (Shanghai) Co., Ltd, Shanghai, China
Transformator	12V, 30 A	Superlight Ltd, Sydney, Australia
3D Printer	Makerbot 2	Makebot Replicator GmbH, Rheinmünster, Germany
3D printing material	Acrylonitrile Butadiene Styrene	Makerbot Replicator GmbH Rheinmünster, Germany

5.1.4 Chemicals

General chemicals used in the laboratory were bought from Sigma Aldrich (Taufkirchen, Germany). TCI Chemicals (USA) or Carl Roth GmbH + Co. KG (Karlsruhe, Germany) with the purity grade "for analysis". For gel electrophoresis SERVA DNA Stain Clear G from SERVA Electrophoresis GmbH (Heidelberg, Germany) was used.

5.1.5 Enzymes

S1 Nuclease

10,000 units S1 Nuclease were purchased from roboklon GmbH (Berlin, Germany) in storage buffer consisting of the following components: 20 mM Tris-HCl (pH 7.5 at 22oC), 50 mM NaCl, 0.1 mM ZnCl2and 50% (v/v) glycerol.

Acid Phosphatase

Acid phosphatase from potato type IV (EC 3.1.3.2) was purchased from Sigma Aldrich (Germany) as lyophilized powder with 3.6 U/mg solid.

5.1.6 Oligonucleotides

All oligonucleotides used were purchased in high purity salt free HPSF or high pressure liquid chromatography (HPLC) from Eurofins Genomics in Ebersberg, Germany or metabion international AG, Steinkirchen, Germany. Oligonucleotides were dissolved as 100 µM stock solution using TE Buffer (1 mM TRIS und 0,1 mM EDTA, pH 8 at 25 °C) or HPLC grade water. To avoid contamination and multiple thaw -freeze cycles, 10 µM aliquods of stock solution were prepared and stored at -20°C.

5.1.7 Hardware

All used devices, which are not standard laboratory equipment are listed in table 5.3.

Table 5.3: List of used devices

Application	Device	Manufacturer
Microplate reader	iControl Infinite 200Pro	Tecan, Männedorf, Swiss
Thermocycler	PCR Thermocycler Mastercycler Personal	Eppendorf, Hamburg, Germany
Fluorimeter	Qubit 2.0	Thermo Fisher Scientific, Waltham, USA
IR camera	Model Ti100	Fluke Cooperation, Eindhoven, Netherlands
3D Printer	Makerbot Replicator 2	Makerbot Replicator GmbH Rheinmünster, Germany
Spectrometer	Mini spectrometer STS-VIS	Ocean Optics Largo, USA
Fragment Analyser	5200 Fragment Analyzer	Agilent Technologies Deutschland GmbH Waldbronn, Germany
NanoDrop	NanoDrop 2000c	Thermo Fisher Scientific (Bremen) GmbH Bremen, Germany
Gel electrophoresis Imaging	Fusion FX EDGE	Labtech International Ltd Heathfield, England
Temperature Measurement	302 K/J	Omega Engineering GmbH Deckenpfronn, Germany

5.1.8 Software

Fluke Connect Software to analyse infra red images taken by camera
Arduino IDE Software to program micro controller Arduino Uno

5.2 Methods

5.2.1 Photoacids

Absorption and emission spectra were recorded with the Tecan Infinite® 200 PRO, which is a multimode plate reader. Dilutions of all photo acids were done in HPLC grade water purchases from Carl Roth GmbH + Co. KG, Karlsruhe, Germany. All absorption and emission spectra were recorded using 100 µM photoacid, buffers used are listed in table 5.4 and were produced using HPLC grade water as a solvent.

Table 5.4: Buffers used for measuring pH dependent absorption and emission spectra of photoacids

pH	Buffer Solution
4 - 6	45 mM Citrate Buffer
7 - 9	45 mM TRIS-HCl Buffer
12	3 M NaCl

5.2.2 pH Jump

Photoacids were illuminated with illumination devices as listed in table 5.5. pH of all photoacids used was adjusted to 7 before starting any pH measurements.

Table 5.5: List of used devices to measure a photo induced pH jump

Photoacid	**Illumination**
HPTS	405 nm MP, HP LEDs, 450 MP, HP nm LEDs
Naphthol Derivates	365 nm HP LEDs
mPAH	450 MP, HP nm LEDs

pH indicators

First, 100 μM pH indicator were added to buffers of pH 8, 6.8, 5.9 and 4.5 with buffers as listed in table 5.4 to an overall volume of 200 μl in a reaction tube. 100 μM pH indicator were added to 1 mM photoacid respectively. All components were solved in HPLC grade water. Final volume was 100 µl in a 200 μl reaction tube. Samples were illuminated sideways with version 1 of the LED array for 1 -5 minutes.

Micro pH electrode

1 mM photoacid was dissolved in HPLC grade water in 200 µl final volume in a 200 µl reaction tube. Samples were illuminated for different times sideways using LED array

version 1. Micro pH electrode was dispensed into solution and pH value was measured while photoacids were illuminated.

Fluorescence Measurements

1mM HPTS was dissolved in HPLC grade water, 200 μl was filled into a 1 ml quartz cuvette. Sample was exited using a focussed 0.7 W 450 nm LED as a light source. Light was coupled into the sample by using a glass fibre. Perpendicular to the sample a Maya spectrometer was used to measure fluorescence at 512 nm. Emission was measured with a 0.1 ms resolution, which was the fastest measurement interval of the spectrometer. The schematic setup is displayed in figure 5.1.

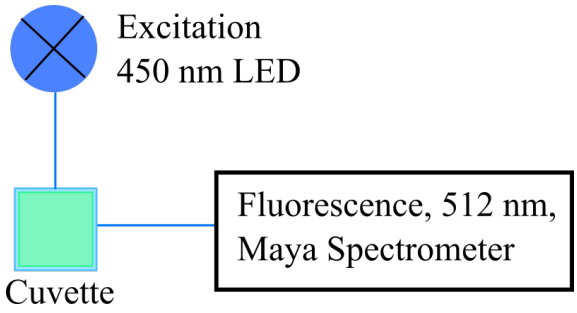

Figure 5.1: Schematic setup to measure absorption while HPTS is excited with a 405 nm LED

Absorption Measurements

1mM HPTS was dissolved in HPLC grade water, 200 μl was filled into a 1 ml quartz cuvette. Maya spectrometer was used to measure absorption at 450 nm, using a 0.7 W LED as a light source. Light was coupled into the sample by using a glass fibre. Perpendicular, the sample was illumined using a glass fibre coupled, focussed beam from a medium power 405 nm LED with 0.7 W. Absorption was measured with a 0.1 ms resolution, which was the fastest measurement interval of the spectrometer. The schematic setup is displayed in figure 5.2.

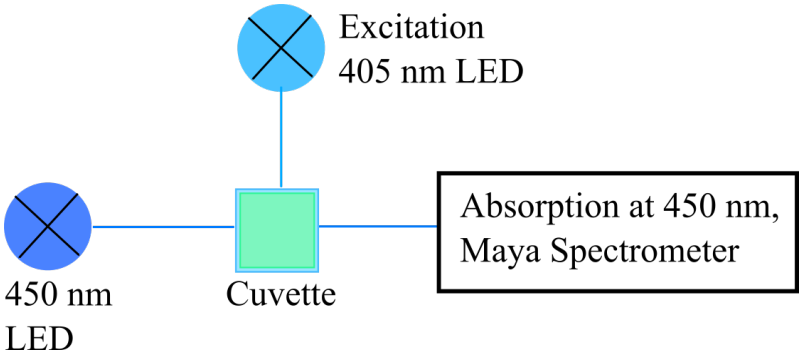

Figure 5.2: Schematic setup to measure absorption while HPTS is excited with a 405 nm LED. The excitation takes placed orthogonal to the absorption measurement

5.2.3 LED Array

Materials used are listed in detail in table 5.2. All LEDs had a silicon lens with a radiation angle of 120° and were powered by LDD700L constant current sources with a constant current output of 700 mA, if not mentioned otherwise. The constant current sources had built-in pulse width modulation (PWM) dimming option, allowing pulsed operation mode with a frequency up to 1 kHz. A 5 V signal is needed to disable or enable the current flow of the LDD700L constant current sources and thus trigger the PWM. The external 5 V PWM signal, to control overall runtimes, in pulsed or continued mode, was generated by a microcontroller. The schematic, how the constant current sources were connected to the LEDs and the microcontroller can be found in the appendix, figure 8.1.

Version 1

Three LEDs on a 8 mm PCB chip were placed on a 10 cm x 1cm x 1 cm aluminium heat sink block using thermal conductive tape. The LEDs were directly powered by a laboratory power supply. A schematic overview of version 1 of the LED array is displayed in figure 5.3.

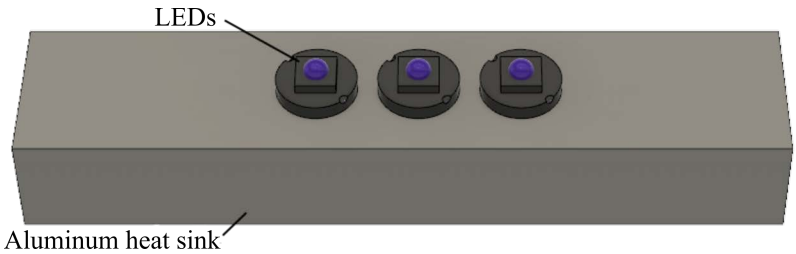

Figure 5.3: Schematic overview of LED array version 1, the three LEDs are mounted on a simple aluminium block using thermal tape

Samples were in 200 μl reaction tubes which were placed into a 3D printed plate with suitable wholes for the reaction tubes. The plate as well as the aluminium block with the LEDs on it were then clamped and adjusted to each other on two separate stands. Samples were illumined sideways, as shown in figure 5.4.

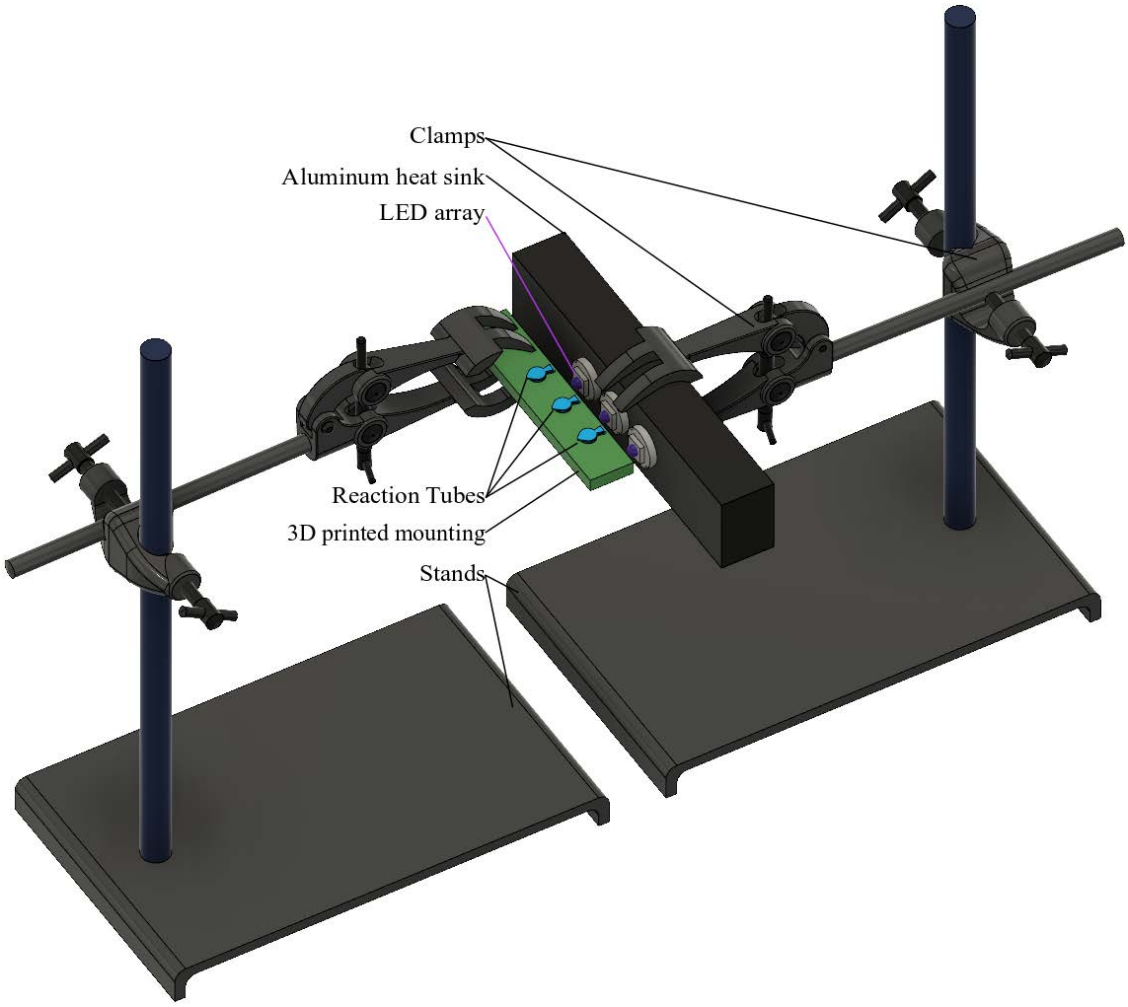

(a) Slanted view from above

(b) Detailed view from the right side

(c) Detailed slanted view from above

Figure 5.4: Illumination and mounting of LEDs and samples using version 1 of the LED "array". The reaction tubes are placed in a 3D printed holder mounted by one clamp. The LEDs are mounted in the second clamp

Temperature measurement in 100 µl volume was done in a sample which was illuminated for 5 minutes using HP 365 nm LEDs.

Version 2.1

The next setup consisted of a simple CPU aluminium heatsink with a suitable fan, 12 V DC and 500 mA, underneath the aluminium block. LEDs were mounted on the aluminium block using thermal conductive double sided adhesive tape (Akasa Ltd) with a thermal conductivity of 0.9W/mK. The tape will be further referred to as thermal tape for convenience. A cavity was milled into the aluminium heat sink in which the LEDs were fixed, as can be seen in the schematic overview. The cavity enables the user to place a microtiter plate on top of the setup and illuminate the plate from the bottom, making the sample - LED distance always the same and reproduceable. A schematic overview of LED array version 2.1 can be seen in figure 5.5.

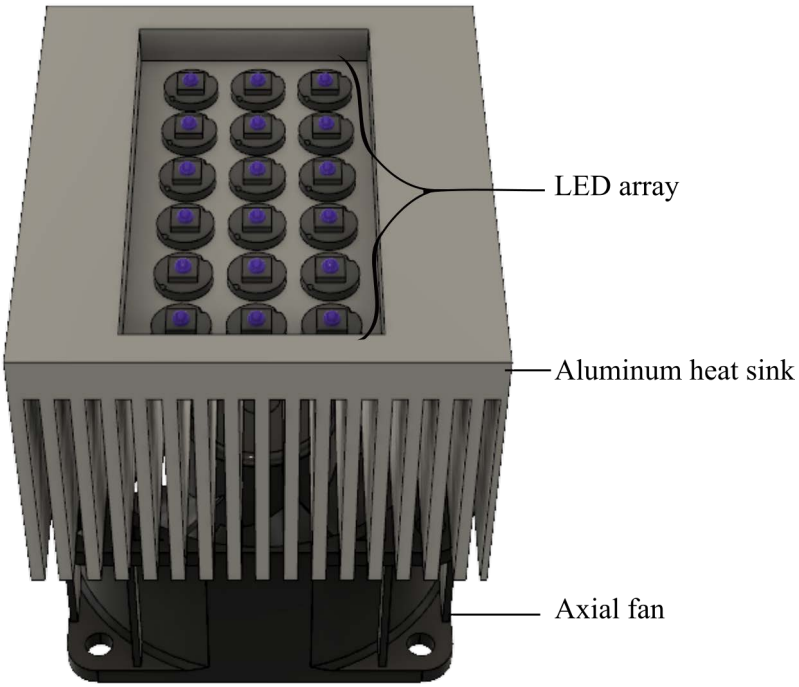

Figure 5.5: Schematic overview of LED array version 2.1, from [14]. 18 samples can be illuminated in parallel.

The microtiter plate position had to be adjusted manually to the LEDs.

Version 2.2

Both, the thermal tape and thermal conductive adhesive paste with a thermal were used to mount LEDs on a 20cm x 20cm x 0.05cm aluminium plate. LEDs were placed using a 3D- printed matrix suitable to fit the wells of a 96 well microtiter plate. Underneath the aluminium plate four TEC1-12706 Peltier Elements were coupled using thermally conductive paste. Peltier elements were powered using a transformer. A 10x10x5 cm aluminium heat sink was placed underneath each Peltier element. Heat sinks were actively cooled, using a CPU fan for each heat sink. A mounting was constructed in Solid Works and printed (Material: acrylonitrile butadiene styrene) using a 3D printer to place the

microtiter plate above the LEDs with a distance of 8 mm. A schematic overview of the LED array version 2.2 can be seen in figure 5.6.

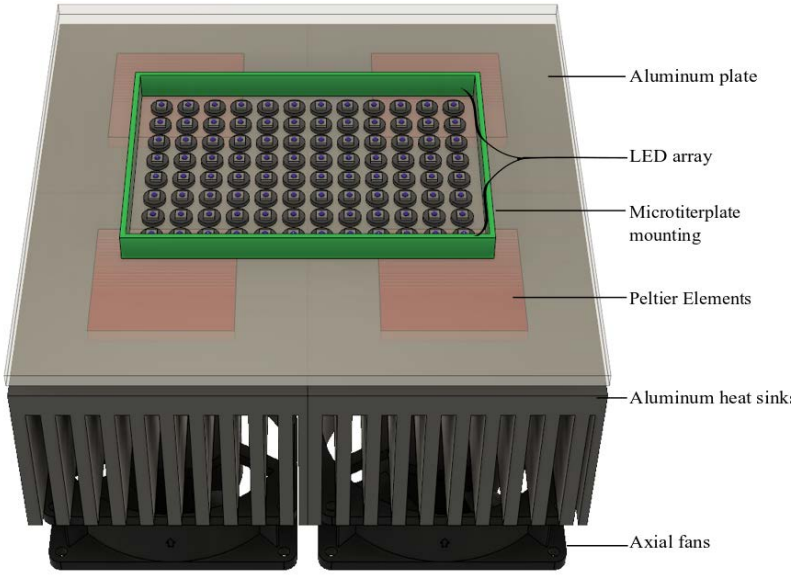

Figure 5.6: Schematic overview of LED array version 2.2, from [14]. 96 samples can be illuminated in parallel, the LED matrix matches a 96 well microtiter plate

Because of the 3D printed mounting for the microtiter plate the plate-LED distance and position were always the same.

Version 2.3

LEDs were mounted on a 20 cm x 20 cm x 0.05 cm aluminium plate using thermal conductive adhesive paste. Underneath the aluminium plate, four stronger peltier elements TEC1-12710 were mounted and thermally coupled under the aluminium plate using thermal conductive paste. Peltier elements were powered using a transformer. A 10x10x5cm aluminium heat sink was placed underneath each Peltier element using thermally conductive paste. Heat sinks were actively cooled using a CPU fan. Furthermore, a new microtiter plate mounting was designed and 3D- printed to allow the integration of three radial fans. In order to avoid light scattering a crossbrace between each LED row was added. Three radial fans were integrated to ensure a constant air flow between the microtiter plate and the LEDs. The radial fans use a current of 0.23A and have a power of 1.8W. A schematic overview of LED array version 2.3 can be seen in figure 5.7.

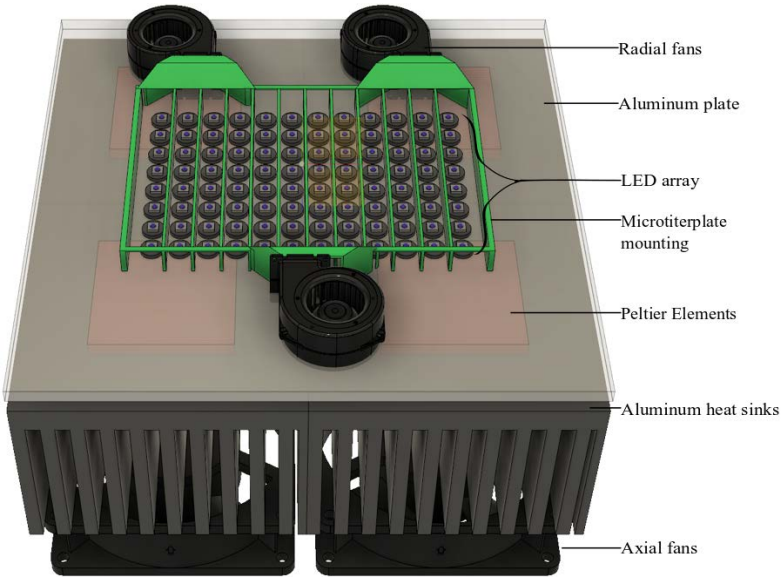

Figure 5.7: Schematic overview of LED array version 2.3, from [14].96 samples can be illuminated in parallel, the LED matrix matches a 96 well microtiter plate

Temperature measurement in 100 µl volume was done in a sample which was illuminated for 5 minutes using HP 365 nm LEDs.

Intensity Mesaurements

LED intensities were analyzed using an STS-VIS miniature spectrometer (Ocean Optics, Ostfildern, Germany). An adapter which fits exactly in one well of a standard 96 well flat bottom microtiter plate and the mini spectrometer was designed. The dimensions of a standard microtiter plate are 127.71 mm x 85.43 mm (LxW), detailed dimensions are listed in a manual by the supplier of microtiter plates used (Brand GmbH, Wertheim, Germany) [23][23]. The microtiter plate was placed on top of the LED array and the adapter was fixed on the microtiter plate lid while intensities were measured. Emission intensities of LEDs were at 365 nm, while the LEDs were switched on in three cycles for 5 minutes continuous illumination. LED intensities were recorded using U= 3.4 V as the LED forward voltage and 700 mA per LED. "On time" of each LED was 5 minutes continuous illumination which was recorded for 3 cycles with 1.5 minutes "off time" between each cycle. A photo of how LED emission intensity were measured with the mounted microtiter plate is shown in figure 5.8.

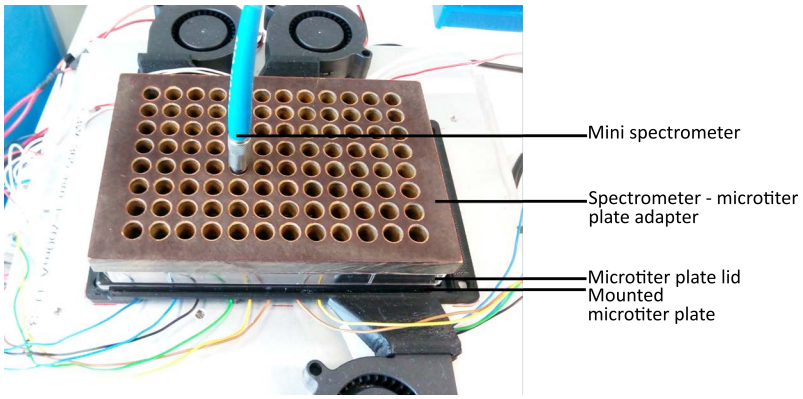

Figure 5.8: Schematic overview of LED emission intensity measurement setup, adapted from [104].

Important Note: LEDs used, emit strong UV light, thus that eye shield protection and skin protection must be worn at all times when working with high power UV light.

5.2.4 Enzymatic assays

Average temperature was measured in 100 µl volume was done in a sample which was illuminated for 5 minutes using HP 365 nm LEDs (for Version 1 and version 2.3).

S1 Nuclease

S1 nuclease requires an acidic environment to cut nucleic acids. Supplied **5x reaction buffer** contains: 150 mM sodium acetate (pH 4.6 at 25°C), 1.4 M NaCl, 5 mM $ZnSO_4$. The **storage buffer** is 20 mM Tris-HCl (pH 7.5 at 22°C), 50 mM NaCl, 0.1 mM $ZnCl_2$ and 50 % (v/v) glycerol [94]. Aliquots of 10 μl were produced and stored at -20 °C. All Samples that were not illuminated were incubated at 37°C.

Nomenclature of samples used are listed in table 5.7. Sample names, final concentrations with their corresponding sample abbreviation are:

Table 5.6: Overview of sample concentrations and abbreviations

Sample	Concentration	Abbreviation
70mer ssDNA	21 ng / μ l	ssDNA
S1 Nuclease	1 U/ml	S1
Reaction Buffer	1x	RB
Acetate Buffer	45 mM	AB
Thermopol Buffer	45 mM	TP
$ZnSO_4$	1 mM	Zn
HPTS	1 mM	HPTS
G-acid	1 mM	G-acid

Table 5.7: Overview of final sample compositions

Sample Name	ssDNA	S1	RB	AB	TP	Zn	HPTS	G-acid
pH 8.8	x				x	x		
RB pH 4.5	x		x					
AB pH 4.5 pH 4.5	x			x		x		
S1 pH 8.8	x	x			x	x		
S1 RB pH 4.5	x	x	x					
S1 pH 8.8	x	x			x	x		
S1 AB pH 4.5	x	x		x		x		
HPTS pH 4.5	x			x		x	x	
S1 + HPTS pH 4.5	x	x		x		x	x	
HPTS pH 8.8	x			x		x	x	
S1 + HPTS pH 8.8	x	x		x		x	x	
G-acid pH 4.5	x			x		x		x
S1 + G-acid pH 4.5	x	x		x		x		x
G-acid pH 8.8	x			x		x		x
S1 + G-acid pH 8.8	x	x		x		x		x

Standard Assay

First, the standard assay, supplied by the company roboklon GmbH was conducted: 1 x reaction buffer, with the 70mer single stranded oligonucleotide with the following sequence:

5'-ATGCCGCTCATCCGCCACATATCCTGATCTTCCAGATAACTGCCGTCA
CTCCAGCGCAGCACCATCACCG - 3'

was incubated at 37°C for 10 minutes using 1 U/µl enzyme. Amount of single stranded 70 mer oligonucleotide was quantified using the fragment analyser with the standard broad range kit assay. Relative fluorescence units were recorded.

Next, reaction buffer from supplier was replaced using 30 mM pH 4.5 acetate buffer and 1 mM $ZnSO_2$. Samples were incubated at 37°C for 10 minutes using 1 U/µl enzyme. Amount of single stranded 70 mer oligonucleotide was quantified using the fragment analyser with the standard broad range kit assay. Relative fluorescence units were recorded. Controls are incubated in pH 8.8 thermopol buffer from Sigma Aldrich.

Inhibition by Photoacids

After establishing the standard assay, the reaction buffer was replaced using acetate buffer adjusted to pH 4.5 by titration NaOH and HCl into the buffer, also $ZnSO_4$ was added separately. The adjusted assay conditions were: 40 mM acetate buffer, 1 mM $ZnSO_4$, 1 u/µl S1 nuclease and 21 ng / µl 70 mer oligonucleotide. The inhibition of S1 nuclease by

photoacids was tested by adding 1 mM photoacid. The experiments were conducted with HPTS and G-acid. Assay conditions were 40 mM acetate buffer, 1 mM $ZnSO_4$, 1 U/µl S1 nuclease and 21 ng/µl ssDNA 70 mer oligonucleotide and 1 mM photoacid. Negative controls with acetate buffer were adjusted to a pH of 8.8 using 3M NaOH.

Illumination Assay

Samples were illuminated for 10 minutes continuously with the following assay conditions: 1 mM $ZnSO_4$, 1 u/ µl S1 nuclease and 21 ng / µl 70 mer oligonucleotide and 1 mM photoacid, pH of 1 mM photoacids was adjusted to pH 4 by adding HCl / NaOH. For the excitation of G-acid a 365 nm LED, 0.7 W was used. For HPTS a 405 nm LED, 1W was used. For gel- electrophoresis Serva DNA Stain Clear G was used. It has an excitation maximum at 490 nm [105] and is excited at 470 nm using the Fusion FX EDGE for gel electrophoresis imaging.

Acid Phosphatase

Acid phosphatase from potato was stored at -20 °C. For each experiment acid phosphatase (AP) was prepared freshly in cold HPLC grade water, as recommended by supplier. Stock concentration was 30 u/ml, this was further diluted to the enzyme concentration needed for the experiment. All experiments were conducted at 40°C.

Standard Assay

Standard assay was conducted with 100 µM pNPP, and a low and a high acid phosphatase concentration respectively. Low acid phosphatase concentration was 0.12 U/ml and high acid phosphatase concentration was 0.21 U/ml. Experiments were conducted in 45 mM citrate acid buffer with a pH ranging from 4 - 6.5. All experiments were conducted with 100 µl per well and stopped with 100 µl 3 M NaOH after the incubation time, resulting in an overall volume of 200 µl per well. For blank, enzyme was added after 100 µl 3 M NaOH. Samples were incubated for 1-10 mins and stopped each minute.

Inhibition by photoacid

Assay was conducted with 100 µM pNPP, 700 µM G-acid and low and high AP concentration respectively. Experiments were conducted in 45 mM citrate acid buffer with a pH from 4 - 6.5. All experiments were conducted with 100 µl per well and stopped with 100 µl 3 M NaOH after the incubation time, resulting in an overall volume of 200 µl per well. For blank, enzyme was added after 100 µl 3 M NaOH. Samples were incubated for 1-10 mins and stopped each minute.

Illumination Assay

Sample illumination was done using the self-constructed LED array, version 2.3, suitable for a 96 well plate format as described in section 5.2.3. Assay conditions were as following for low concentration AP and high concentration AP: 100 µM pNPP, 700 µM G-acid and 0.12 U/ml AP and 100 µM pNPP, 700 µM G-acid and 0.21 U/ml AP in a final volume of 100 µl. Different illumination conditions were tested. All assays had an overall incubation time of 10 minutes and a light exposure time of 1-5 minutes. Samples were left in dark after illumination to an overall time of 10 minutes each. Reaction was then stopped using 100µl 3 M NaOH. Following illuminations were tested: a) Continued illumination with a light exposure time of 1-5 minutes b) Cycled illumination with 1 minute on – off alternatingly with 1-5 minutes light exposure time) Cycled illumination with 0.5 minutes on-off alternatingly with 1-5 minutes' light exposure time. Starting pH for all samples was 8.1- 8.3. Negative controls were left in dark at a pH of 8.1 - 8.3 for 10 minutes. Product of the enzymatic reaction, p-Nitrophenol, was detected by measuring the absorption in a 96 well microtiter plate with a total volume of 200 µl /well at 405 nm using a plate reader Infinite 200 PRO® (Tecan, Männedorf, Switzerland).

6 Results

6.1 Identification of Suitable Photoacids

First, pH dependent absorption and emission spectra of all photoacids and buffers used were recorded to determine suitable absorption peaks in the UV-VIS spectra. If not referred to otherwise all samples had a concentration of 100 µM.

6.1.1 Buffers

Absorption spectra of buffers used for experiments were analysed. All buffers absorb in the UV region only until ca. 360 nm, independent of their pH (Fig.6.1).

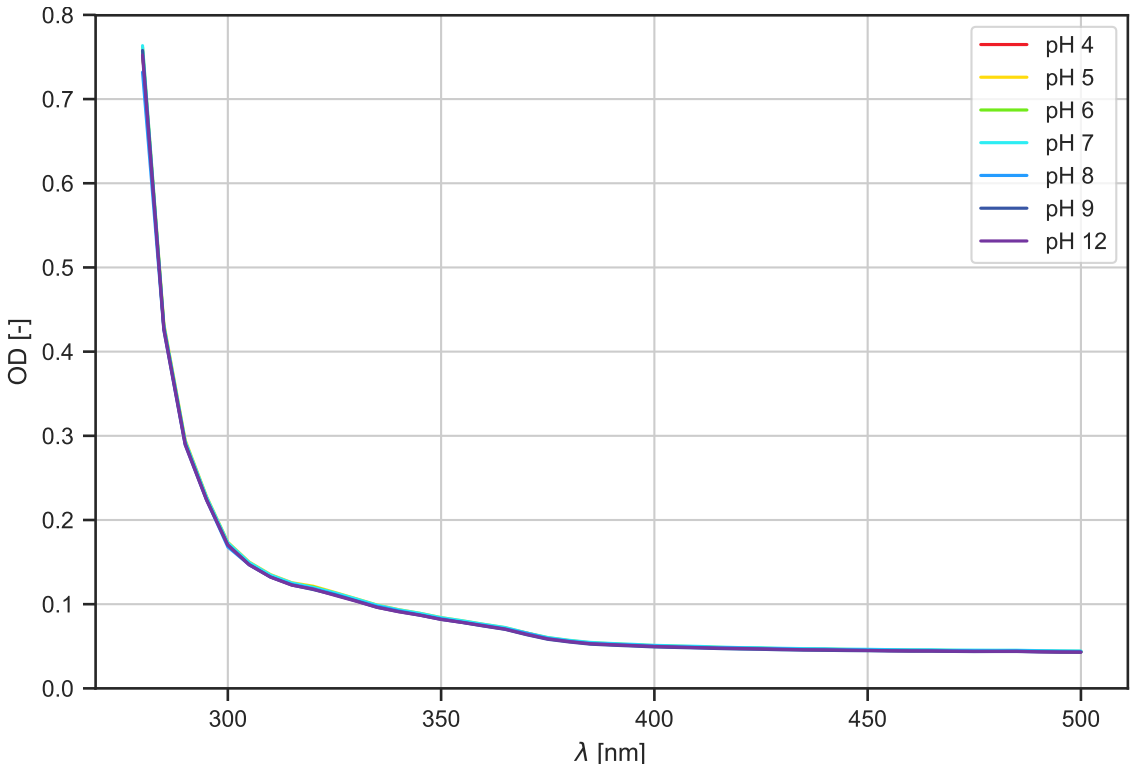

Figure 6.1: pH dependent absorption spectra of pure buffers, as described in table 5.4. Buffer absorption does not change with the pH value and the absorption spectra for the different pH values overlap

6.1.2 HPTS

HPTS has two absorption peaks in the range between 280 - 500 nm. The absorption depends on the pH value. The first absorption peak at acidic pH values from 4-6 (deprotonated form) is at 405 nm. The second at neutral to alkaline pH values from 7- 12 (protonated form) is at 450 nm. The isosbestic point is at 415 nm (Fig. 6.2).

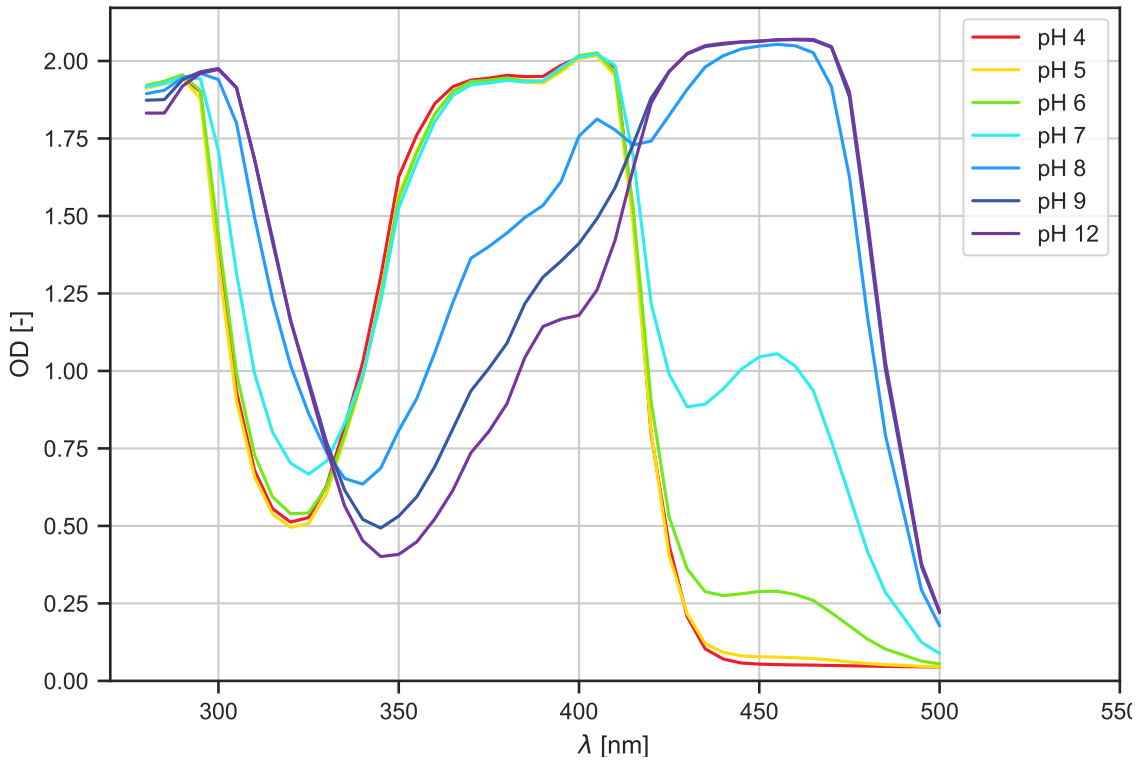

Figure 6.2: pH dependent absorption spectra of 100 µM HPTS, dissolved in buffers, as described in table 5.4. HPTS strongly changes its absorption from pH 4 to 12: For acidic pH (4-6) the absorption peak is at 405 nm, this shifts to 450 nm for neutral to alkaline pH (7-12)

6.1.3 G-Acid

G-acid absorbs mainly in the UV region until ca. 410 nm. The photoacid has a pH dependent absorption with a peak at 365 nm at alkaline pH values ranging from pH 8-12. The peak at 365 nm is highest at a pH of 12. At ca. 320 nm a change in absorption spectra, dependent on the pH, can be observed: The absorption also rises with the pH (Fig. 6.3).

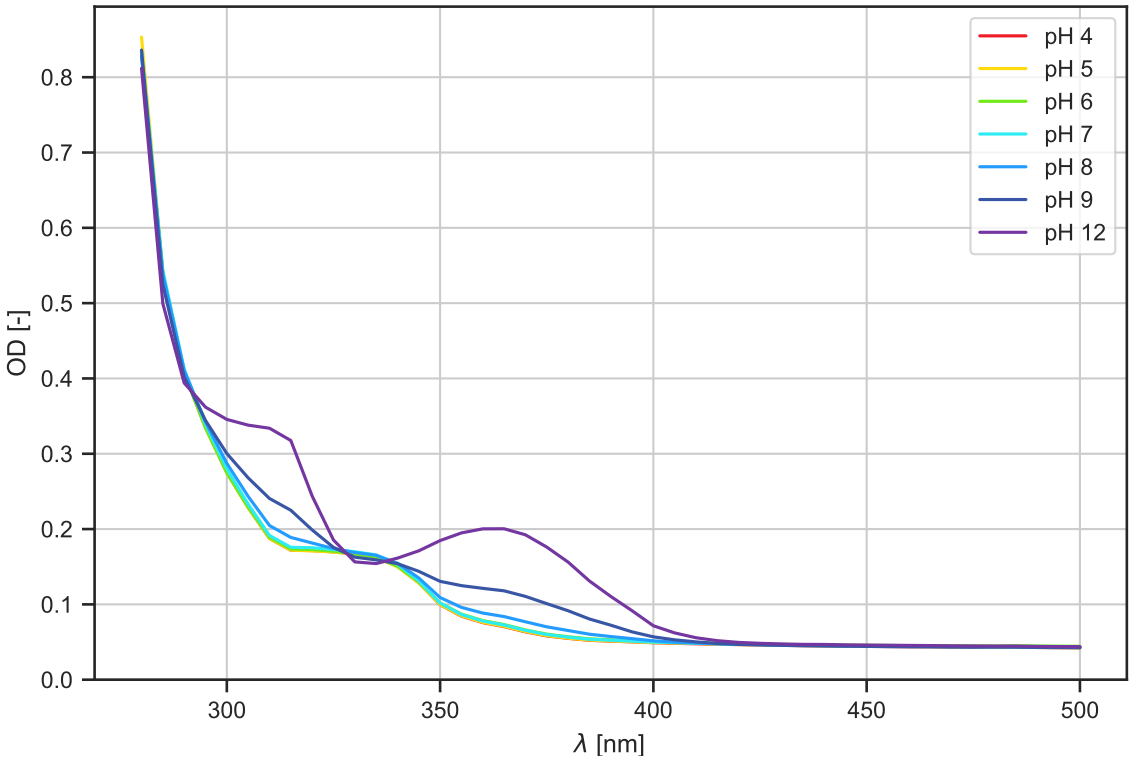

Figure 6.3: pH dependent absorption spectra of 100 µM G-acid, dissolved in buffers, as described in table 5.4. G-acid changes its absorption from pH 4 to 12: A peak at 365 nm and 320 nm is visible for alkaline pH values

6.1.4 R-Acid

R-acid has a similar absorption spectra as G-acid. The absorption is pH-dependent and mainly in the UV spectra, reaching into the visible spectrum until ca 410 nm. A peak at 365 and 320 nm nm is present at alkaline pH values from 9-12, being the highest at a pH of 12. The absorption peak at 365 nm is lower for R-acid than it is for G-acid (Fig. 6.4).

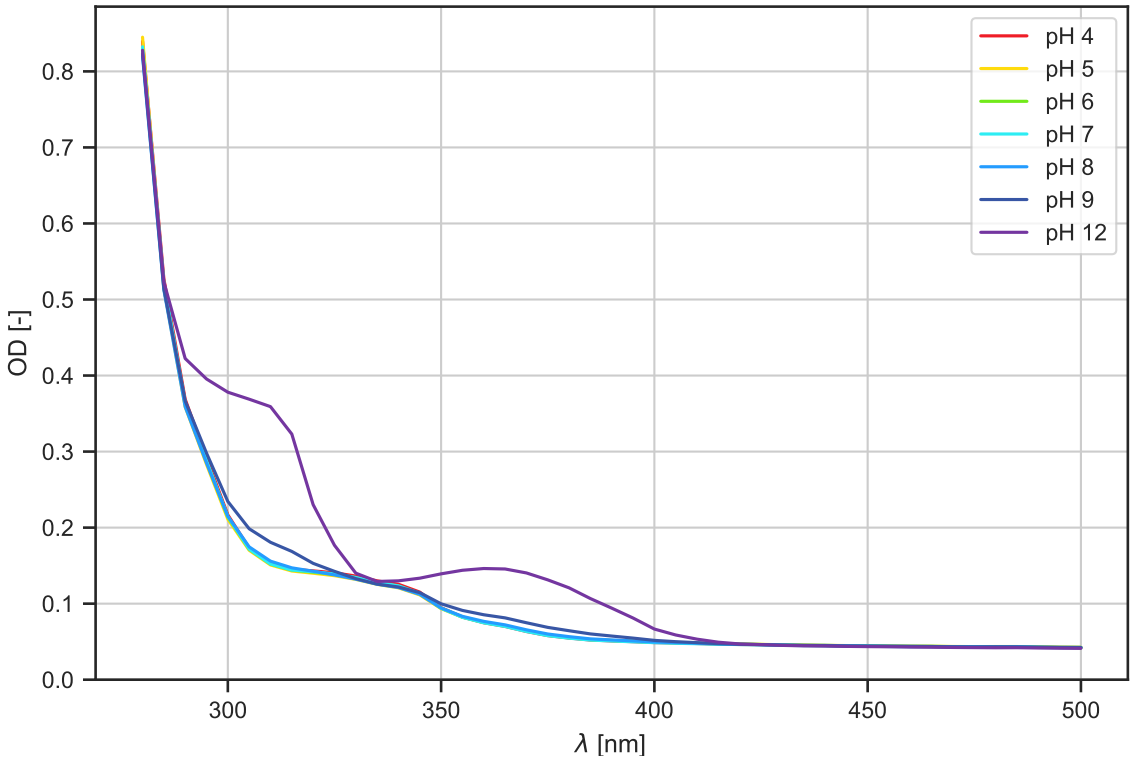

Figure 6.4: pH dependent absorption spectra of 100 µM R-acid, dissolved in buffers, as described in table 5.4. R-Acid changes its absorption from pH 4 to 12: A peak at 365 nm and 320 nm is visible when at alkaline pH values (9-12)

6.1.5 6-Cyano-2-Naphthol

The absorption spectra of 6-cyano- 2-naphthol is strongly pH dependent. The naphthol derivative has an absorption peak at ca 300 nm for acidic pH values from 4-5. The second absorption peak at ca 325 nm is present at pH values 9 and 12 (Fig. 6.5).

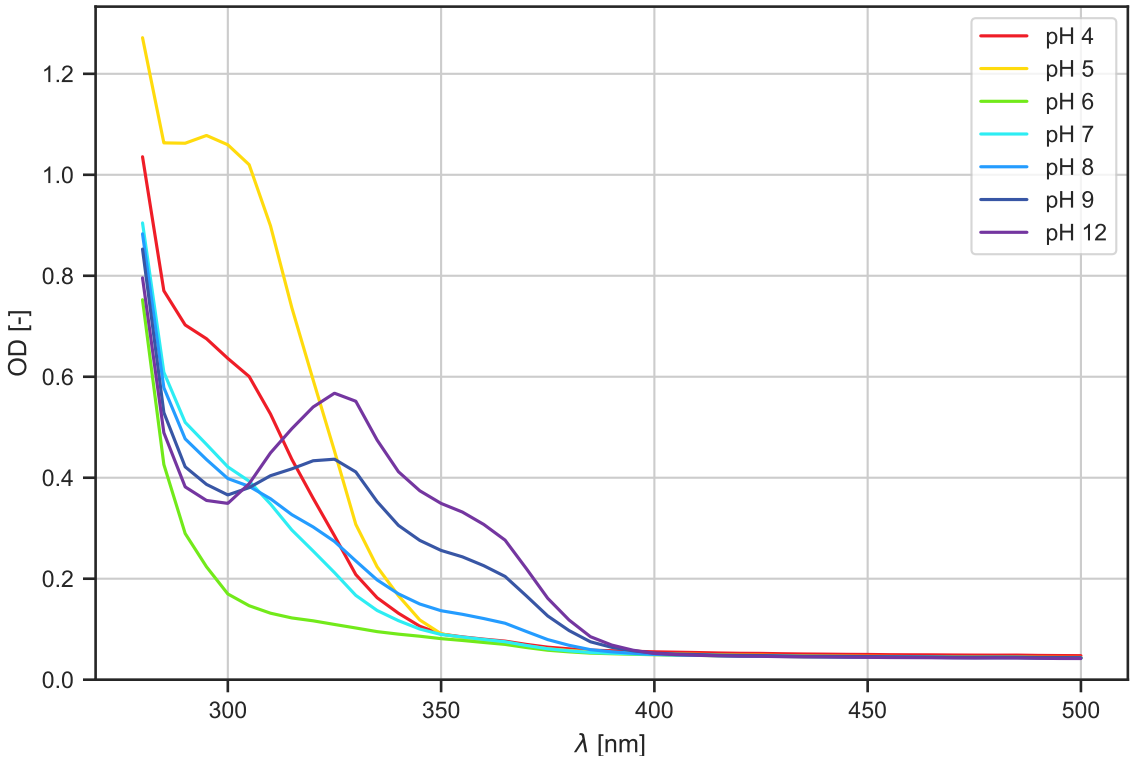

Figure 6.5: Absorption spectra of 100 µM 6-cyano- 2-naphthol, dissolved in buffers, as described in table 5.4. The absorption is strongly pH dependent, a peak at 325 nm and a shoulder is present at ca. 355 nm (pH 8-12). For acidic pH (5-4) a peak at 300 nm can be observed

6.1.6 3- Amino-2-Naphthol

The absorption of 3-amino-2-naphthol is also pH dependent. It hat two pH dependent absorption peaks, the first being at ca 330 nm at acidic pH values 4-5. The second is at ca 340 nm at a pH of 12. The photoacid absorbs in the UV region until a maximum wavelength of ca 360 nm (Fig. 6.6).

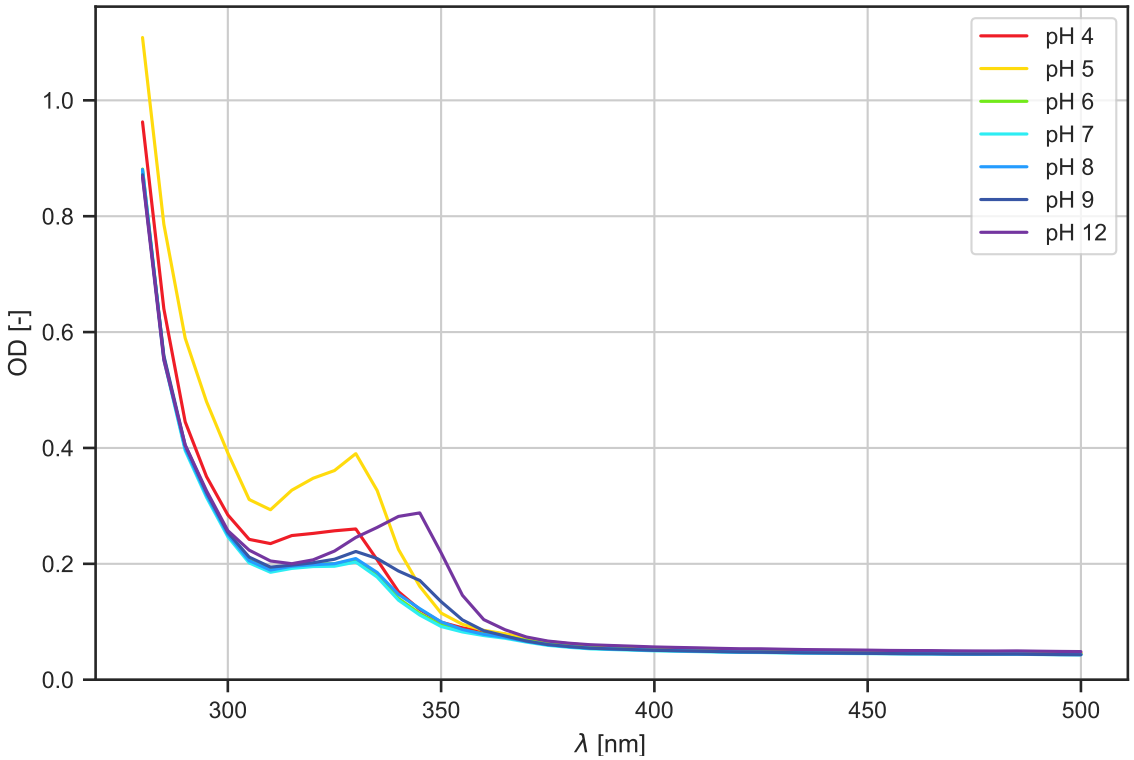

Figure 6.6: pH dependent absorption spectra of 100 µM 3-Amino-2-naphthol, dissolved in Buffers, as described in table 5.4. The absorption peak shifts from ca. 330 nm (pH 4) to 340 nm (pH 12)

6.1.7 3-Bromo-2-Naphthol

The absorption of 3-bromo-2-naphthol is pH dependent. It has a pH dependent absorption. The photoacid absorbs in the UV region until a maximum wavelength of ca 380 nm. The peak at 350 nm is visible at pH 12 (Fig. 6.7).

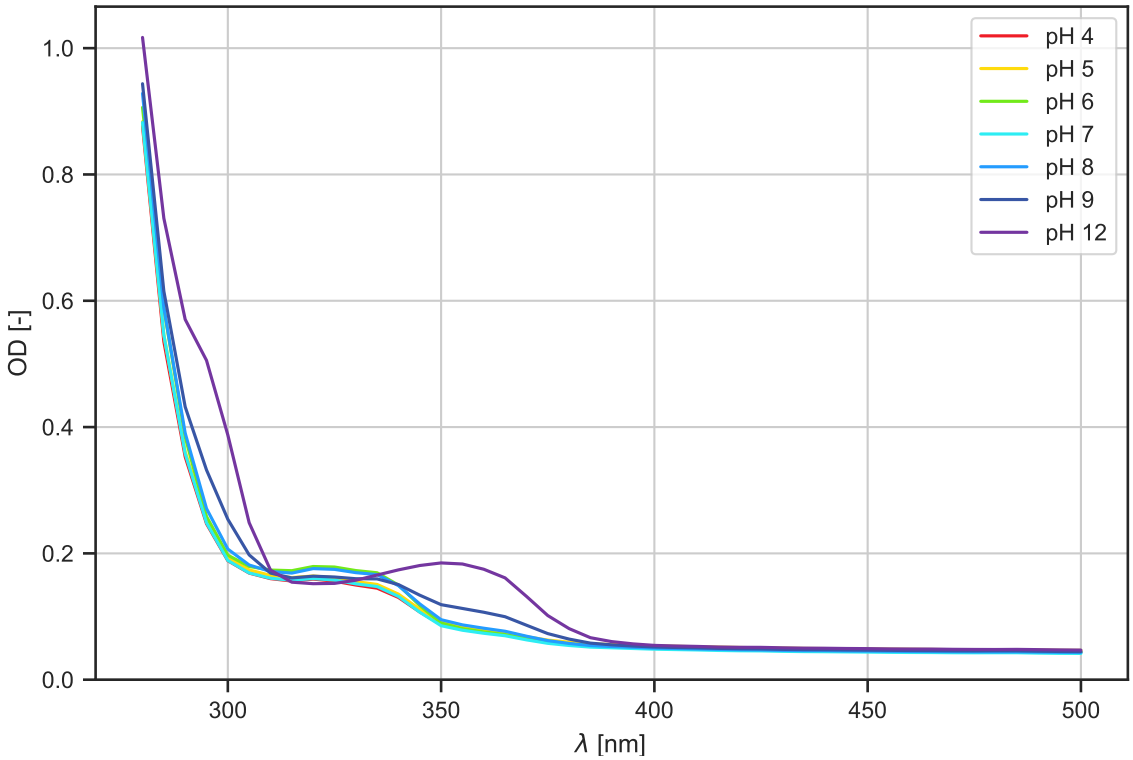

Figure 6.7: pH dependent absorption spectra of 100 µM 3-bromo-2-naphthol, dissolved in buffers, as described in table 5.4. With alkaline ph values a peak at ca 350 nm appears.

6.1.8 mPAH1

Absorption spectra of mPAH1 were recorded in different solvents: HPLC grade water, 100 % methanol and 100 % ethanol. When solved in HPLC grade water the absorption spectra displays a peak at 340 nm, 420 nm and at 520 nm. Sample illuminated for 2 minutes has the same absorption spectra as mPAH in HPLC grade water in darkness. When illuminated for 10 minutes with two different distances the absorption spectra shifts slightly and absorption is lower at 420 nm. It does not make a difference whether the sample is illuminated with 1cm distance between LEDs and sample or 0.1cm (Fig. 6.8). As mPAH1 was originally dissolved and tested in methanol by the group who first synthesised it (see reference [6]), the same was done here to test if absorption changes would occur when choosing methanol as a solvent.

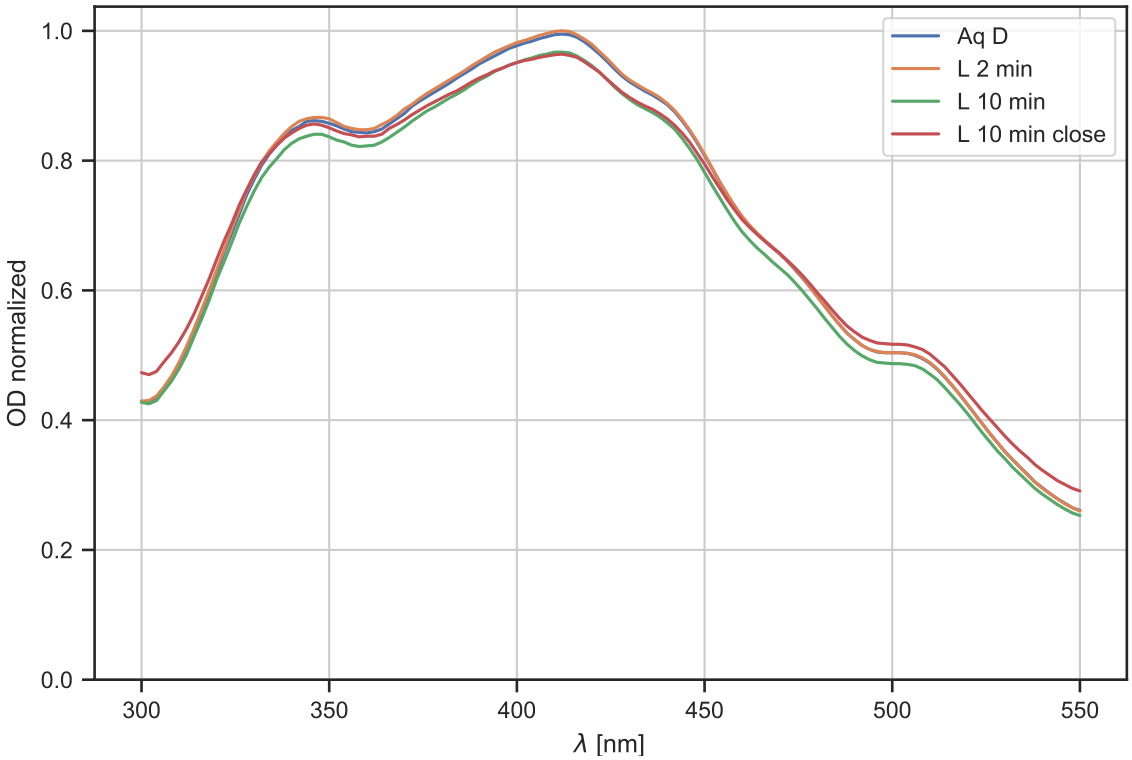

Figure 6.8: Absorption spectra of 100 µM mPAH1, dissolved in HPLC grade water. Sample was illuminated for 2 and 10 minutes using HP 405 nm LEDs. When dissolved in water no significant absorption change is observed, regardless of the illumination time

mPAH 1 was dissolved in 100 % methanol. The peaks are partially red-shifted when compared to the spectra where mPAH1 was dissolved in HPLC grade water. The first peak is at ca 350 nm, the main peak is at 420 nm and the third peak at 520 nm. When the sample is illuminated for 2 minutes the absorption lowers indicating a conformation change. Sample was also illuminated for 10 minutes. This increased the downward shift in absorption intensity (Fig. 6.9). To further test alcohols as a solvent for mPAH1, it was also dissolved and illuminated in ethanol.

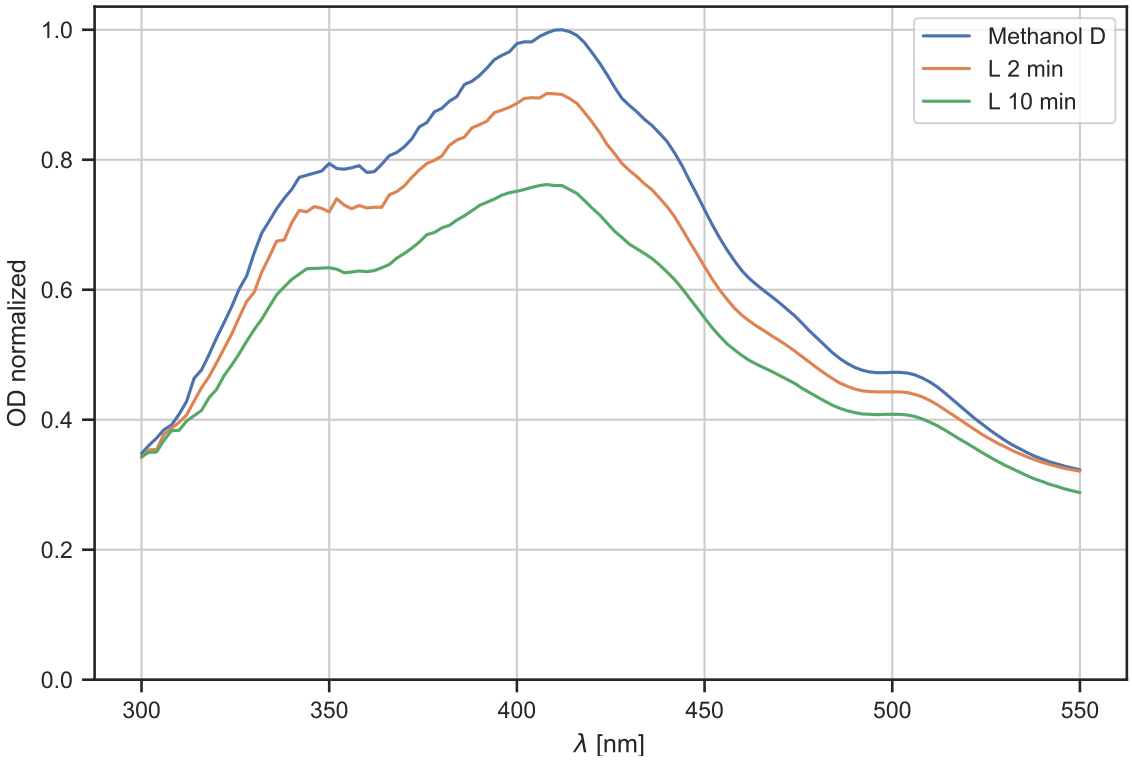

Figure 6.9: Absorption spectra of 100 µM mPAH1, dissolved in methanol. Sample was illuminated for 2 and 10 minutes using HP 405 nm LEDs. When dissolved in methanol a significant absorption shift can be observed: The peak at 410 nm decreases further with longer illumination times

Absorption spectra for mPAH1 was now recorded with ethanol as a solvent. Here the metastable photoacid has an absorption peak at ca. 345 nm and an absorption peak at 450 nm. When being illuminated the peaks shift: The absorption of the 450 nm peak lowers significantly and a new peak appears at ca. 320 nm after two minutes illumination time (Fig. 6.10).

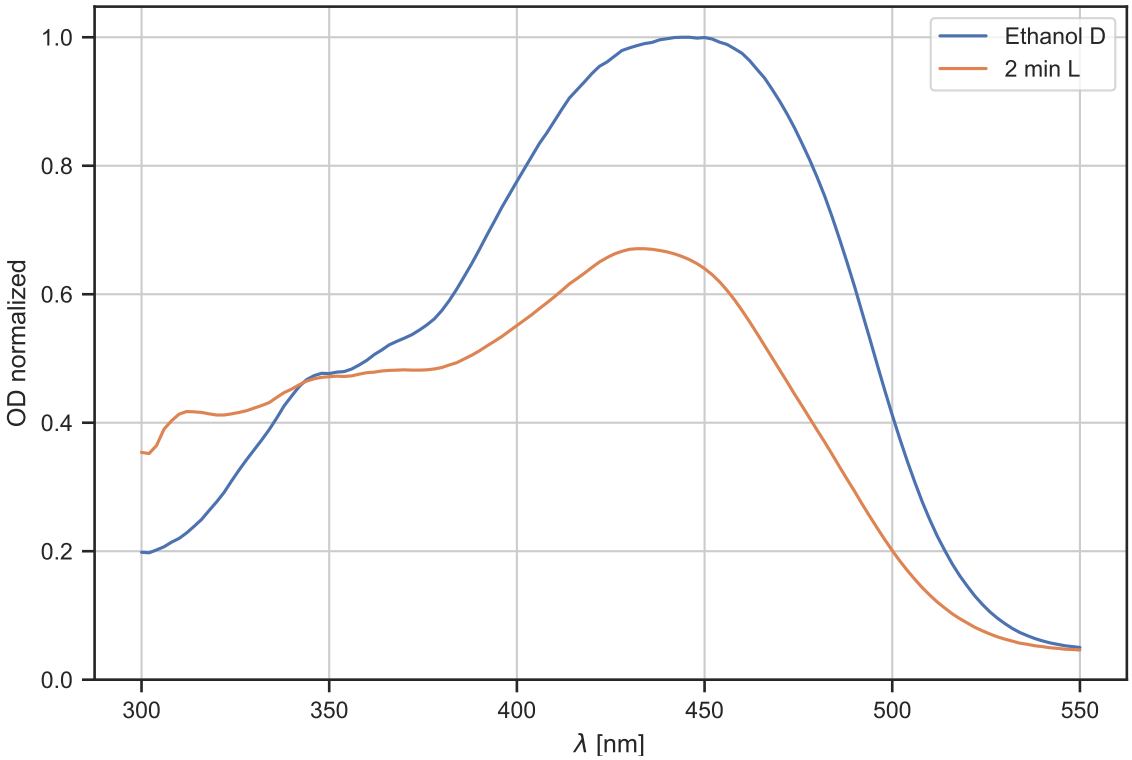

Figure 6.10: Absorption spectra of 100 µM mPAH1, dissolved in ethanol. Sample spectra was recorded before illumination (blue) and after two minutes illumination (orange) using HP 405 nm LEDs. Absorption significantly changes upon illumination, indicating a conformation change of mPAH

6.1.9 pH Jump

pH indicators

PH indicators were tested without the addition of photoacid to determine the best pH indicator with a significant colour change between the pH values 4.5- 8. Cresol red has almost no colour shift in the range of pH $8 - 4.5$, just as mCresol purple. Phenol red has a slight colour shift from reddish at pH 8 to a more yellowish appearance at pH 4.5, neutral red has a significant colour change from pH 8 (orange) to pH 6.8 -4.5 (red). Strongest colour change is observed for neutral red (Fig. 6.11).

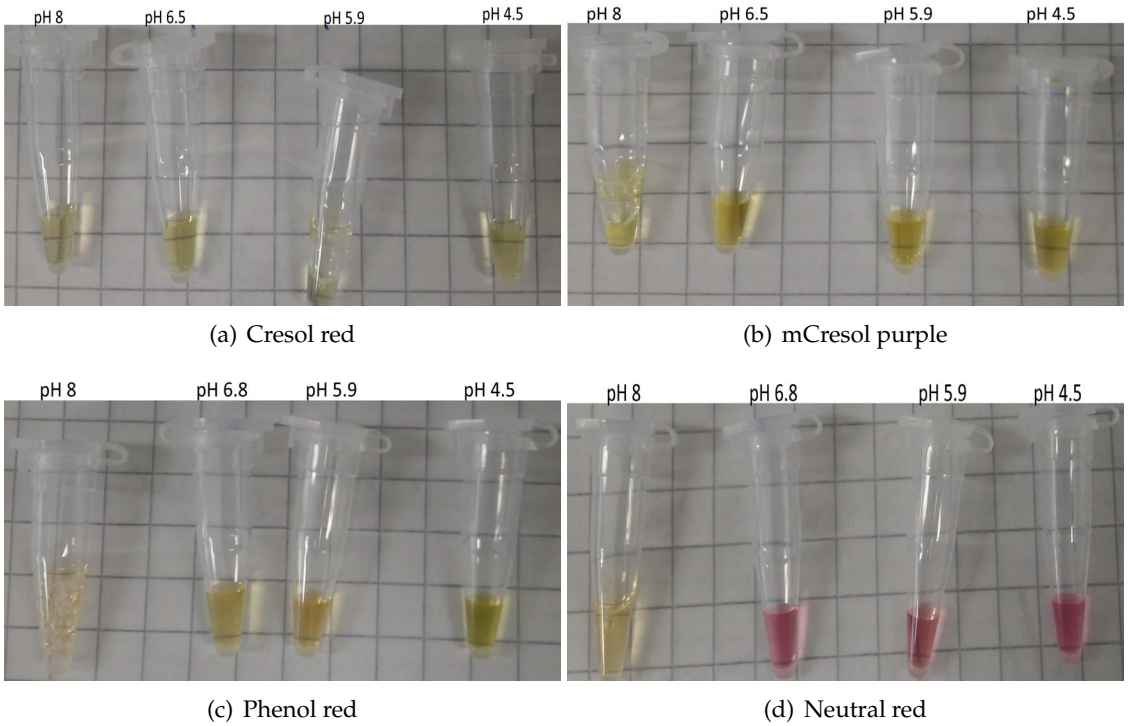

(a) Cresol red (b) mCresol purple

(c) Phenol red (d) Neutral red

Figure 6.11: Colour change of different pH indicators at different pH values in buffers as listed in table 5.4. The pH value of each buffer is listed above the tubes respectively. Only neutral red has a significant pH shift in the desired pH region

As the analysed pH indicators did not show a significant colour change in the desired pH region alternative pH indicators ,bromcresol purple and bromcresol green, were analysed the same way. Bromcresol purple has a significant, multicoloured pH change from blue (pH 8) to purple (pH 6.8) to yellow (pH 5.9-4.5) and pink when the pH is 0. When mixed with 1 mM HPTS the colour changes are neutralized and pH values from 8-4.5 all appear light green to yellow. Bromcresol green has a colour change from blue (pH 8-5.9) to green (pH 4.5) and to yellow (pH0). When mixed with 1 mM HPTS the colour change is from green (pH 6.8) to light blue (pH 5.9) to light green (ph 4.5), see figure 6.12.

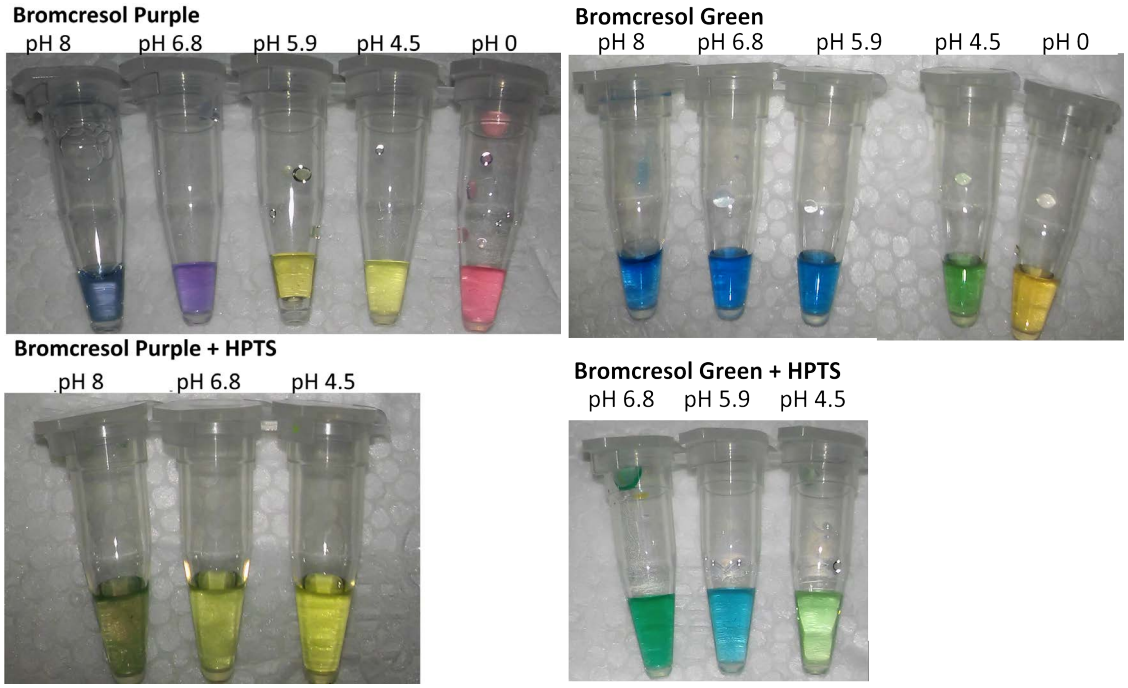

(a) Bromcresol purple (top) and bromcresol purple + 1mM HPTS (bottom)

(b) Bromcresol green (top) and bromcresol green + 1mM HPTS (bottom)

Figure 6.12: Colour change of different pH indicators at different pH values in buffers as listed in table 5.4 with and 1mM HPTS. Both indicators display a significant colour change in buffer at different pH values. However only bromcresol Green still changes its colour significantly when 1 mM HPTS is added.

As bromcresol green was the only pH indicator with a significant colour change from pH 7 to 4.5 it was chosen to continue illumination experiments using bromcresol green. As a control, bromcresol green solved in HPLC grade water was illuminated for one minute. Starting pH was set to pH 7. No colour change of bromcresol green before and after illumination is observed (Fig. 6.13).

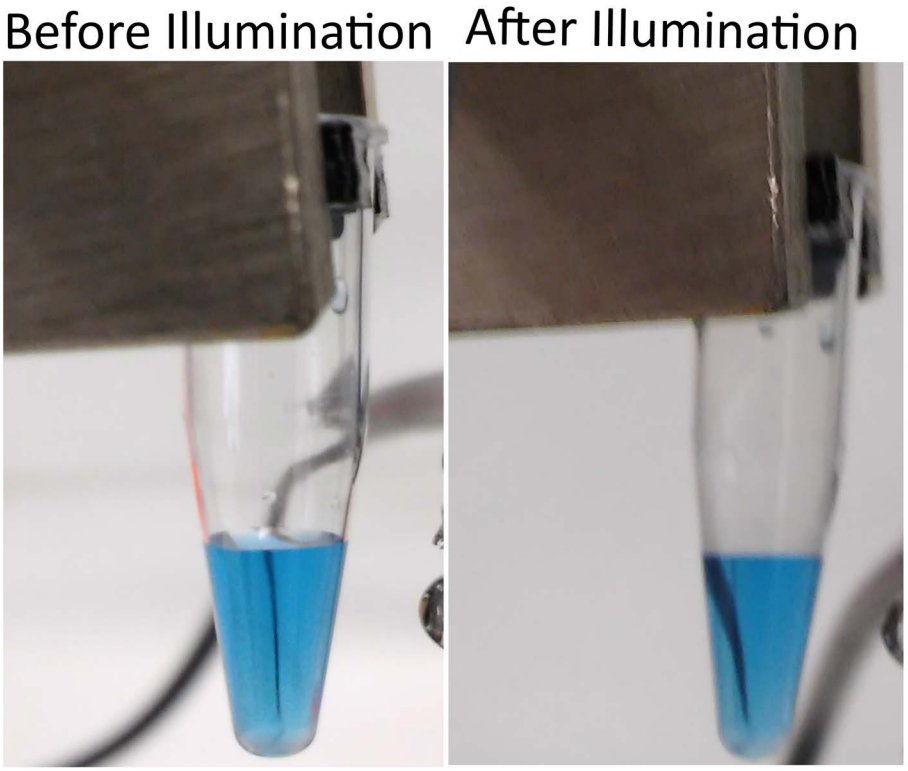

Figure 6.13: Bromcresol green before and after 1 minute illumination with 405 nm HP LEDs dissolved in HPLC grade water, pH before illumination was adjusted to pH 7

To test the pH change upon illumination, when photoacid is present bromcresol green together with 1 mM HPTS was illuminated for one minute with a starting pH of 7.5 using HP 405 nm LEDs. The colour changed from blue (pH 7.5) to a light green, indicating a pH change to about 4.5. (Fig. 6.14).

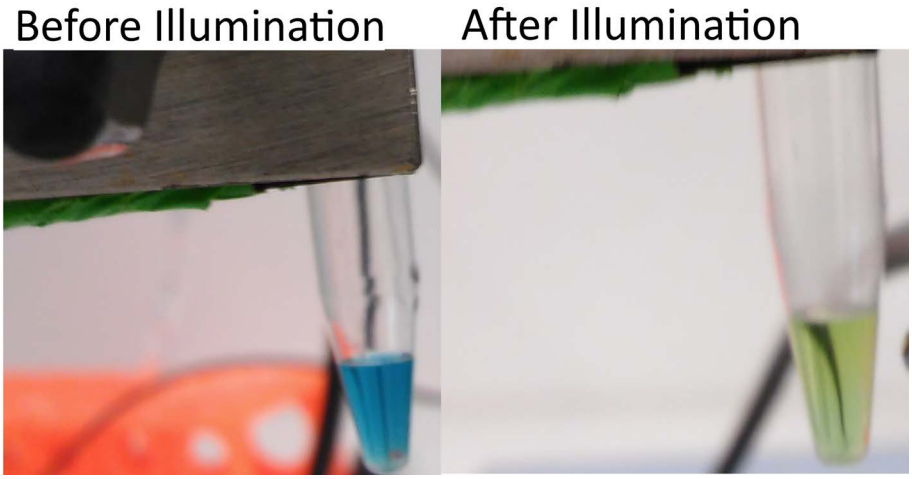

Figure 6.14: Bromcresol green + 1mM HPTS before and after 1 minute illumination with 405 nm high power LEDs dissolved in HPLC grade water, pH before illumination was adjusted to pH 7.5. After illumination the colour changes to a light green, indicating a pH change to about 4.5

The same samples were left in darkness for three minutes and the colour change was again recorded. The colour changed from light green after illumination to a darker green after the sample was kept in darkness for 3 minutes. This indicates a rise of the pH value to a pH between ca. 6.8 - 5.9. (Fig. 6.15).

Figure 6.15: Bromcresol green + HPTS before 1 minute illumination (left) and bromcresol green + HPTS after 1 minute illumination with 405 nm high power LEDs dissolved in HPLC grade water and 3 minutes dark time. pH before illumination was adjusted to pH 7. The green of bromcresol green gets darker, indicating that the pH is returning to ca 6

Micro pH electrode

First, response time of the pH micro electrode was measured in 100 mM and 1 mM buffer, as listed in table 5.4. The pH electrode was dipped into one buffer until pH value was set. Then pH electrode was directly dipped into the other buffer. An overview of the response time from pH 8 to pH 4 and from pH 4 to pH 8 in different buffer concentrations is listed in table 6.1. For all measurements using the pH micro electrode the micro electrode was calibrated. As per manufacturer data sheet (Xylem Analytics Germany Sales GmbH & Co. KG), the error margin is $\pm$ 15 mV at room temperature and a pH change by one unit corresponds to a voltage change of 59.16 mV, also at room temperature. Hence, absolute error due to the measurement device is ca. 25 % per pH unit, when measuring pH value at room temperature, as done in conducted experiments.

Table 6.1: pH micro electrode response time in different buffer concentrations. The response time of the pH micro electrode rises when the buffer concentration is lower

	pH 8 to pH 4	**pH 4 to pH 8**
100 mM buffer	ca. 20 sec	ca. 20 sec
1 mM buffer	ca. 40 secs	ca 40 secs

The response time of the pH micro electrode doubles with the lower buffer concentration, thus the response time of the electrode is ca. 40 seconds for the following experiments where 1 mM photoacid is used. This has to be taken into account for the online pH measurements using the micro electrode. Afterwards, the influence of irradiation intensity

was tested on HPTS using a) medium power 405 nm LEDs and b) high power 405 nm LEDs. Starting pH was ca. 7.3, samples were illuminated until pH lowered to ca. 6.6, time was measured in seconds until pH 6.6 was reached (Fig.6.16).

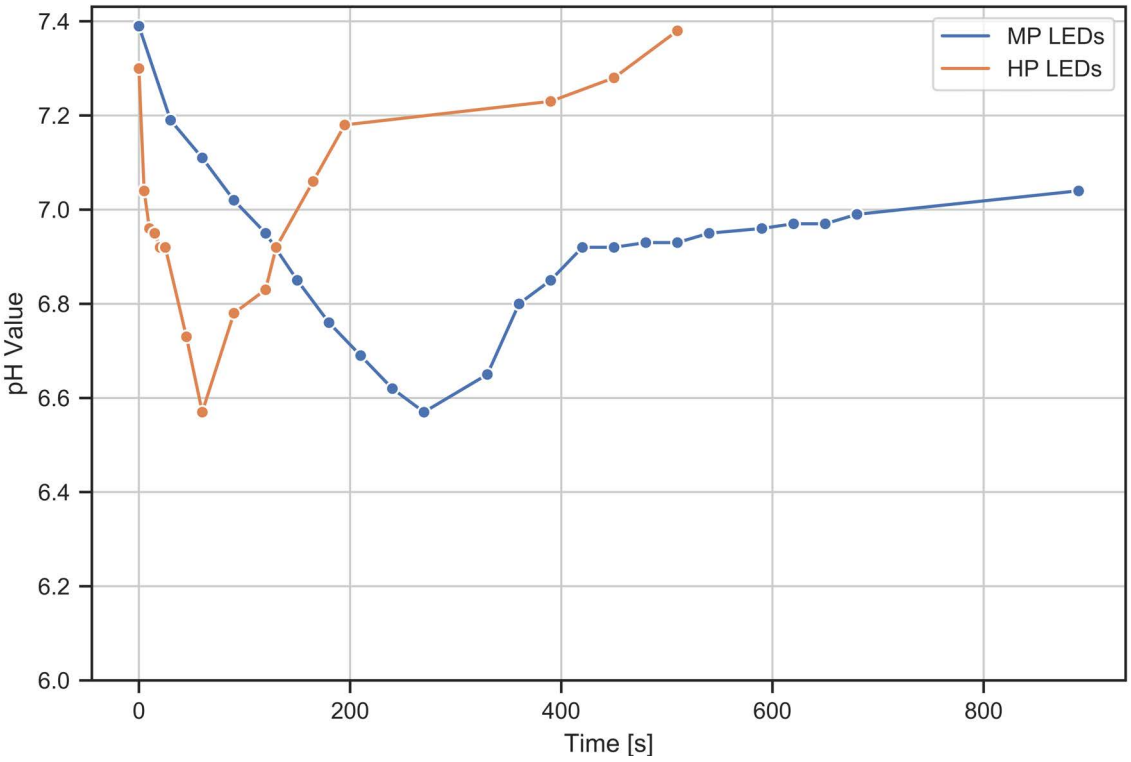

Figure 6.16: pH change over time of 1mM HPTS dissolved in HPLC grade water when being illuminated with 405 nm medium power (MP) LEDs and with 405 nm high power (HP) LEDs. Starting pH of both samples is ca. 7.3. Illumination is removed after pH 6.6 is reached.

PH change from ca 7.3 to ca. 6.6 took ca. 270 seconds (4.5 minutes) when medium power LEDs were used as an illumination medium. This also seems to damage the photoacid, as the reverse progress when light is switched off using MP LEDs is significantly slower than the reverse process when HP LEDs are used. This is also implied by results in figure 6.18. The same pH change was achieved in ca. 60 seconds when using HP LEDs as illumination source. Next, influence of HPTS concentration on pH change was analysed (Fig. 6.17).

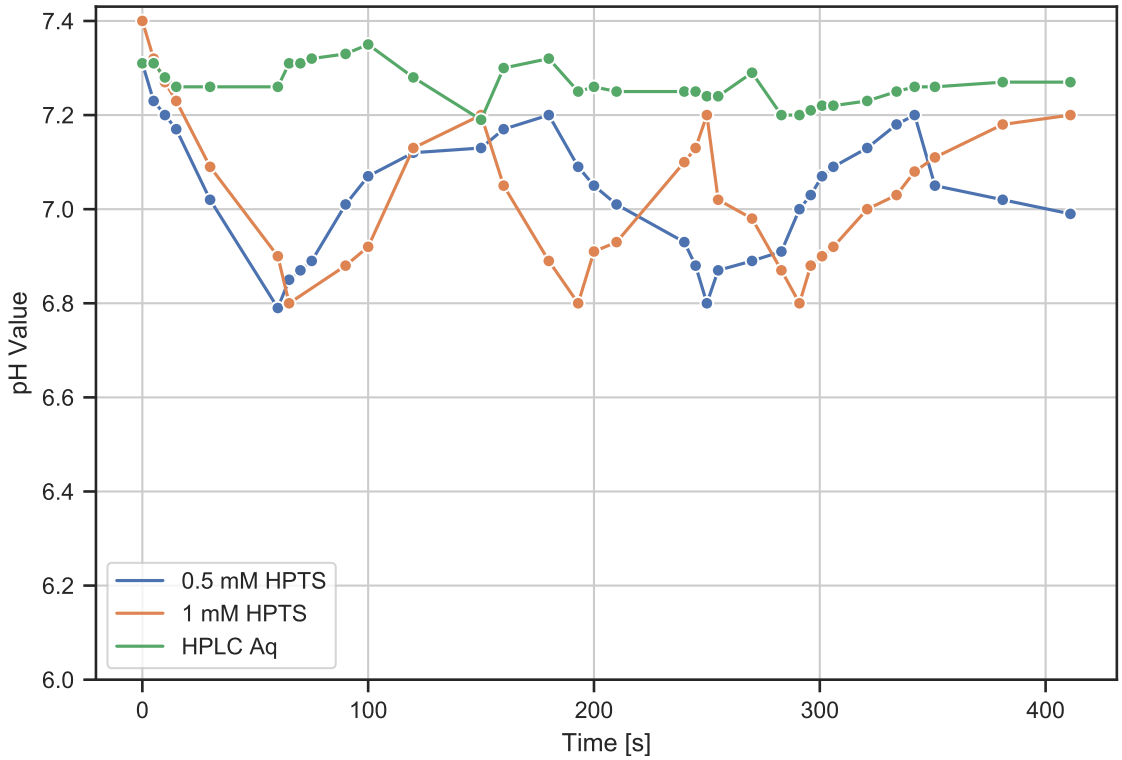

Figure 6.17: pH change over time of 1mM HPTS dissolved in HPLC grade water when being illuminated with 405 nm high power (HP) LEDs and 0.5 mM HPTS. Starting pH of both samples is ca. 7.3. Illumination is removed after pH 6.8 is reached and is switched back on after pH 7.2 was reached while samples are in dark. The higher concentration can be cycled quicker than the lower photoacid concentration. Water, as a control, does not significantly change pH value upon illumination

PH change from 7.3 to 6.8 was achieved 3 times when using 1 mM HPTS and 2 times when using 0.5 mM HPTS in an overall time of ca 7 minutes. Thus the pH change can be achieved faster when using a higher concentration of photoacid. Furthermore, both photoacid concentrations can be used to cycle the pH value, using light as a controlling mechanism. Water was illuminated by 405 nm HP LEDs and pH was measured as a control. Water does not change the pH significantly when being illuminated.

After testing the light intensity influence on the pH cycling, the influence of light exposure time was tested. Two illumination times with MP LEDs and 1 mM HPTS were tested. The magnitude of the pH jump is 0.62 when HPTS is illuminated for 5 minutes and 2.63 when illuminated for 10 minutes. The pH value returns to ca 7.3 for the sample that was illuminated for 5 minutes, but does not significantly rise again for the the sample that was illuminated for 10 minutes (Fig. 6.18). Thus a maximum of 5 minutes light exposure time was chosen for all following experiments.

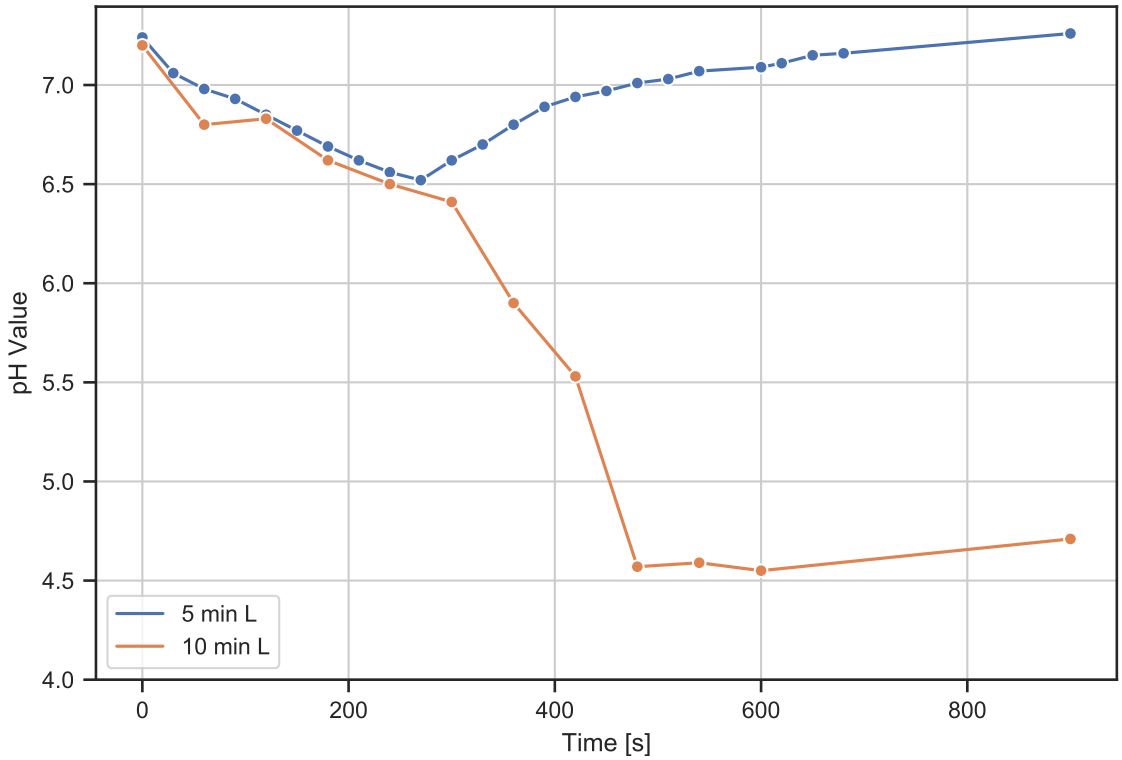

Figure 6.18: pH change over time of 1mM HPTS dissolved in HPLC grade water when being illuminated with 405 nm MP LEDs for 5 minutes and 10 minutes illumination time. When being illuminated for 10 minutes HPTS does not return to the original value of ca. 7.3 but does stay at ca. 4.5, indicating a photo destructive process when being illuminated too long

A similar experiment was conducted for the naphthol derivatives: Samples starting pH was ca. 7.3 - 7.5, samples were illuminated for 5 minutes, using the found optimized parameters: Maximum of 5 minutes illumination time and HP 365 nm LEDs. The pH change over time while samples were illuminated for 5 minutes and light was switched off afterwards is recorded. HPLC grade water, as a control, did not change the pH over time significantly. Neither did 6-cyano-2-naphthol. R-acid does change the pH from ca. 7 to 6.5 and stays at this pH value, also when irradiation is removed and thus does not seem to be reversible. G-acid's pH significantly lowers when illuminated from 7.3 to ca 4.8 in 5 minutes light exposure. the pH returns to pH 7 in ca. 600 seconds (10 minutes), see figure 6.19. Thus G-acid seems to be the most suitable photoacid of the naphthol derivatives. All further experiments are continued using HPTS and G-acid as those photoacids could be optically controlled to reversibly changed pH value.

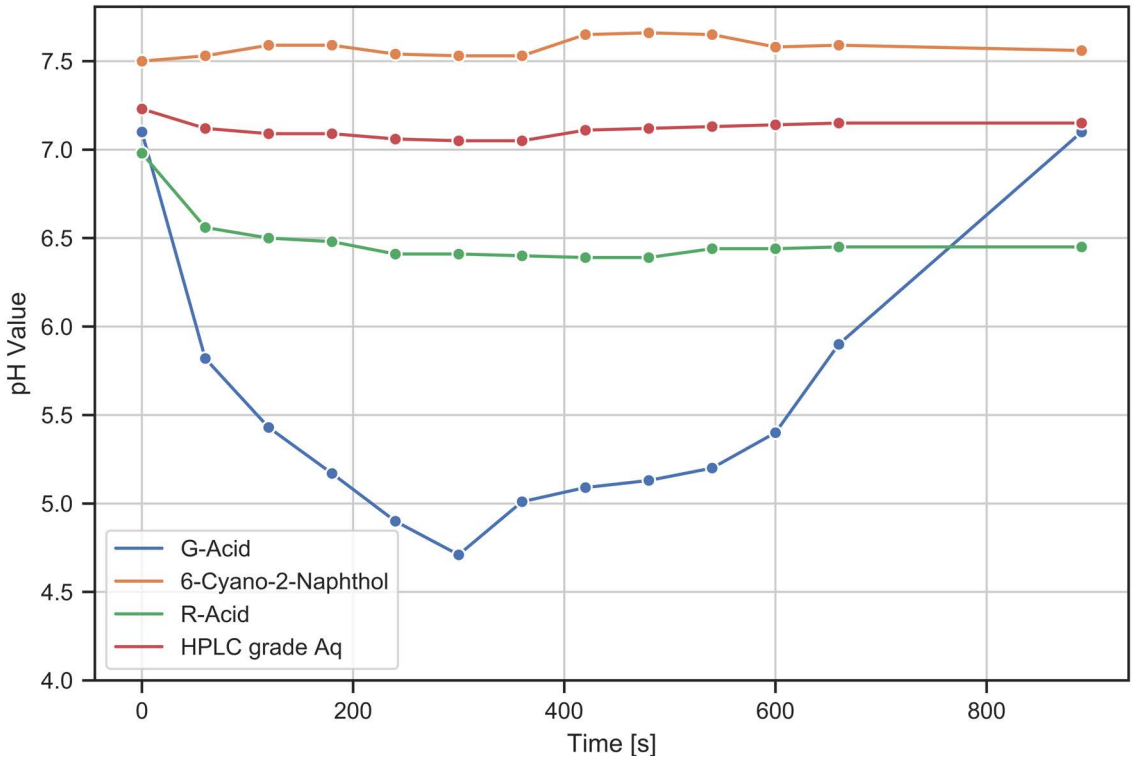

Figure 6.19: pH change over time of 1mM G-acid, R-acid and 6-cyano-2-naphthol dissolved in HPLC grade water when being illuminated with 365 nm high power LEDs. Starting pH of all samples is ca. 7.1- 7.4. Illumination is removed after 5 minutes. As a comparison pH of HPLC grade water is also recorded under same conditions.

Absorption and Fluorescence Measurements

To develop an alternative method of the pH change over time, fluorescence and absorption measurements were conducted. When excited with 405 nm HPTS has a strong fluorescence with a peak at 512 nm (Fig. 6.20). The excitation with 405 is near the isosbestic point at 410 nm.

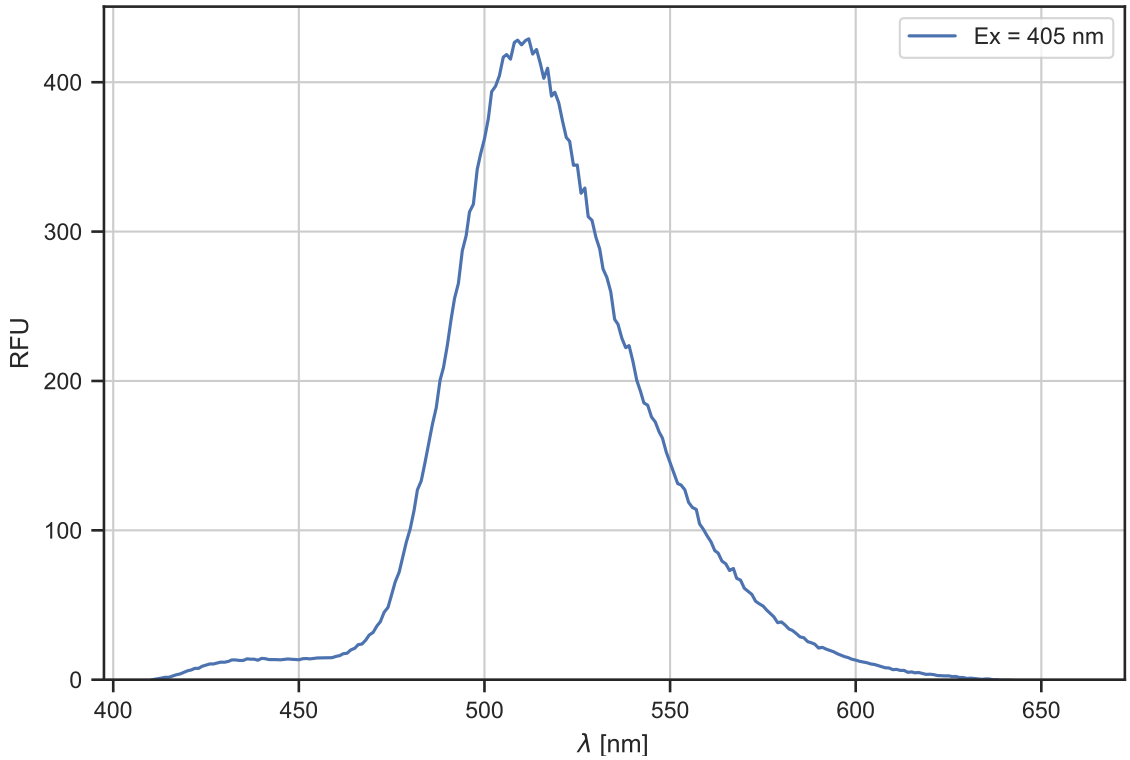

Figure 6.20: Emission spectrum of 1mM HPTS in TRIS- HCl buffer at a pH of 7. Sample is excited at 405 nm for 10 minutes using HP LEDs, however no change in emission can be detected over this period of time, indicating that this measurement method is not suitable to detect an online pH change

HPTS has a strong, pH dependence fluorescence depending on the excitation wavelengths, the wavelength of the detector is set to 512 nm. HPTS exhibits a strong , pH dependent fluorescence with a maximum at 512 nm. The emission intensity depends on the pH value and the excitation wavelength: When excited at 405 nm the fluorescence increases with decreasing pH, if excited in at 450 nm, the fluorescence increases with increasing pH. Maximum emission only differs in intensity, the emission peak of 512 nm does not shift (Fig. 6.21).

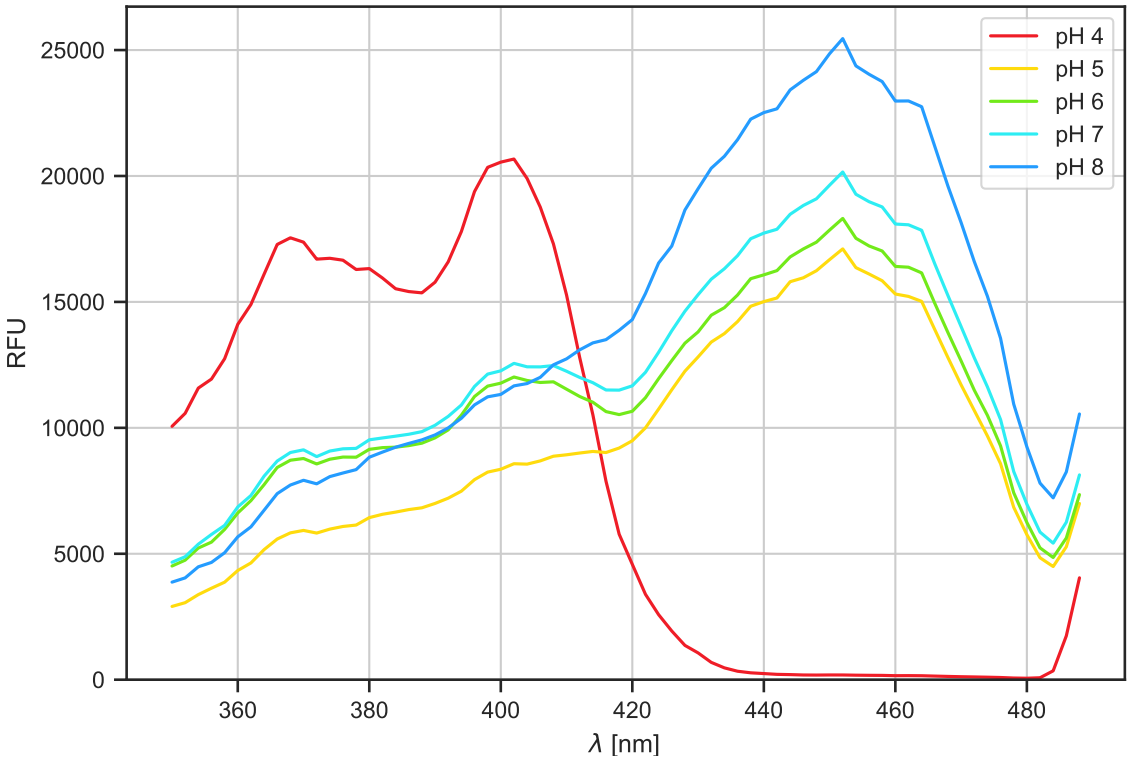

Figure 6.21: pH dependent excitation of 1mM HPTS in TRIS- HCl and citrate buffer, detection wavelength is set to 512 nm. Depending on th pH, the fluorescence is either stronger when excited at 400 nm (pH 4) or when excited at 450 nm (pH 5-8)

A cuvette was illuminated and used for the absorption and fluorescence measurements to detect a pH change by recording (a) the absorption at 450 nm while exciting HPTS in the cuvette using a high power 405 nm LED and (b) by recording the fluorescence at 512 nm while exciting HPTS using a high power 405 nm LED. The fluorescence intensity at 512 nm, as well as the absorption at 450 nm was recorded over time, but no change could be detected for both. The cuvette's sample volume could not be fully illuminated using the applied techniques (Fig. 6.22), which might be a reason. If the cuvette is not fully illuminated the photoacid itself serves as a buffer.

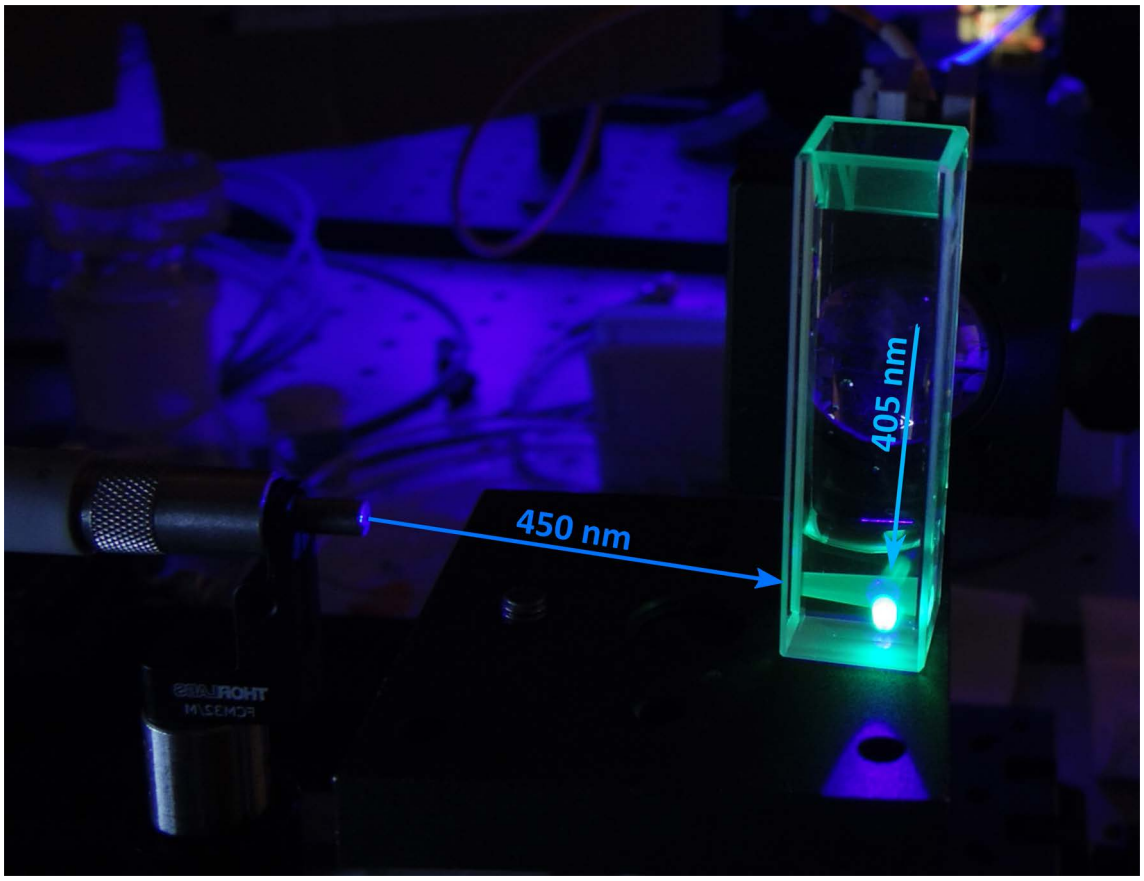

Figure 6.22: Illumination of HPTS to record fluorescence and absorption spectra when illuminating with 405 nm high power LEDs. Cuvette could be only partially illuminated with the chosen setup. 405 nm is used for excitation for fluorescence measurement and 450 nm is used to record absorption

Next, as the second suitable photoacid G-acid was chosen to be tested the same way. G-acid also has a strong, pH dependent fluorescence when excited at 365 nm. The fluorescence with a peak at 475 nm decreases with decreasing pH value. It is at it's maximum at pH 9 for the recorded spectra (Fig. 6.23).

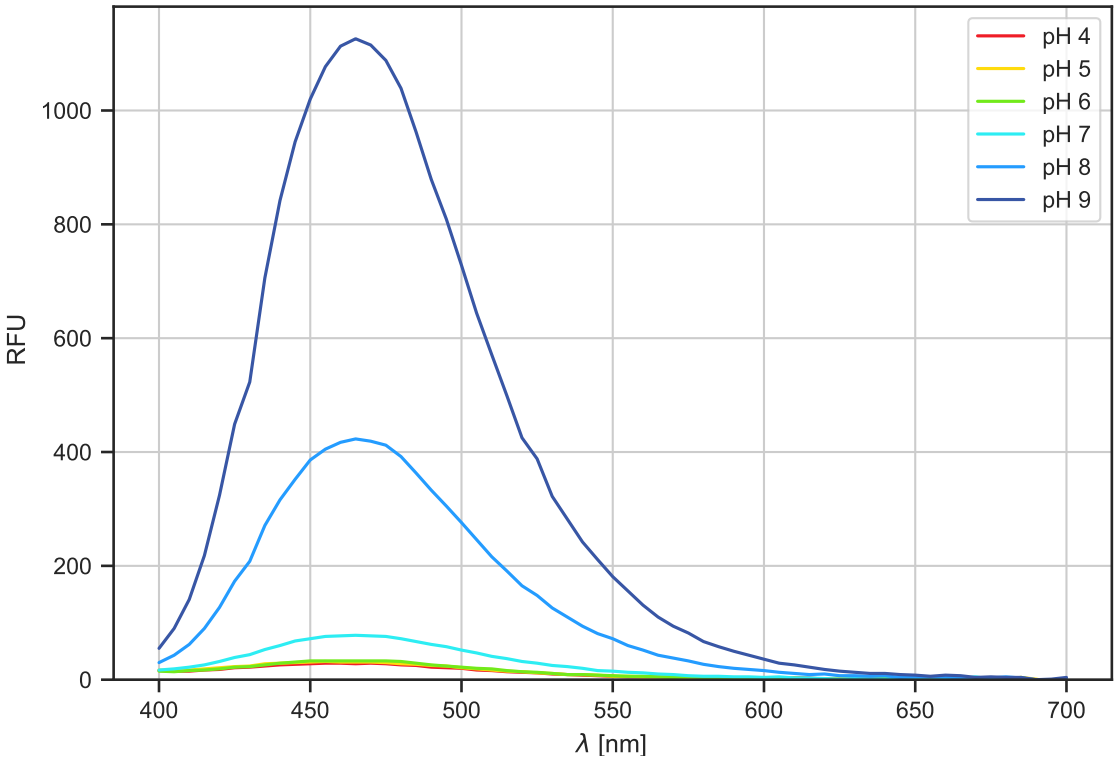

Figure 6.23: pH dependent rmission spectra of 100 µM G-acid, dissolved in buffers, as described in table 5.4. Excitation wavelength is 365 nm. The emission has its peak at ca 475 nm and significantly lowers with the pH value

However, G-acid turned out to exhibit very strong photobleaching. This was tested by illuminating G-acid using 365 nm HP LEDs for 5 minutes. The fluorescence was recorded using a mini spectrometer on top of the setup, as displayed in figure 5.8. 1 mM G-acid looses more than 40 % of its original fluorescence signal within 5 minutes light exposure time in TRIS-HCl ph 8 buffer (Fig. 6.24).

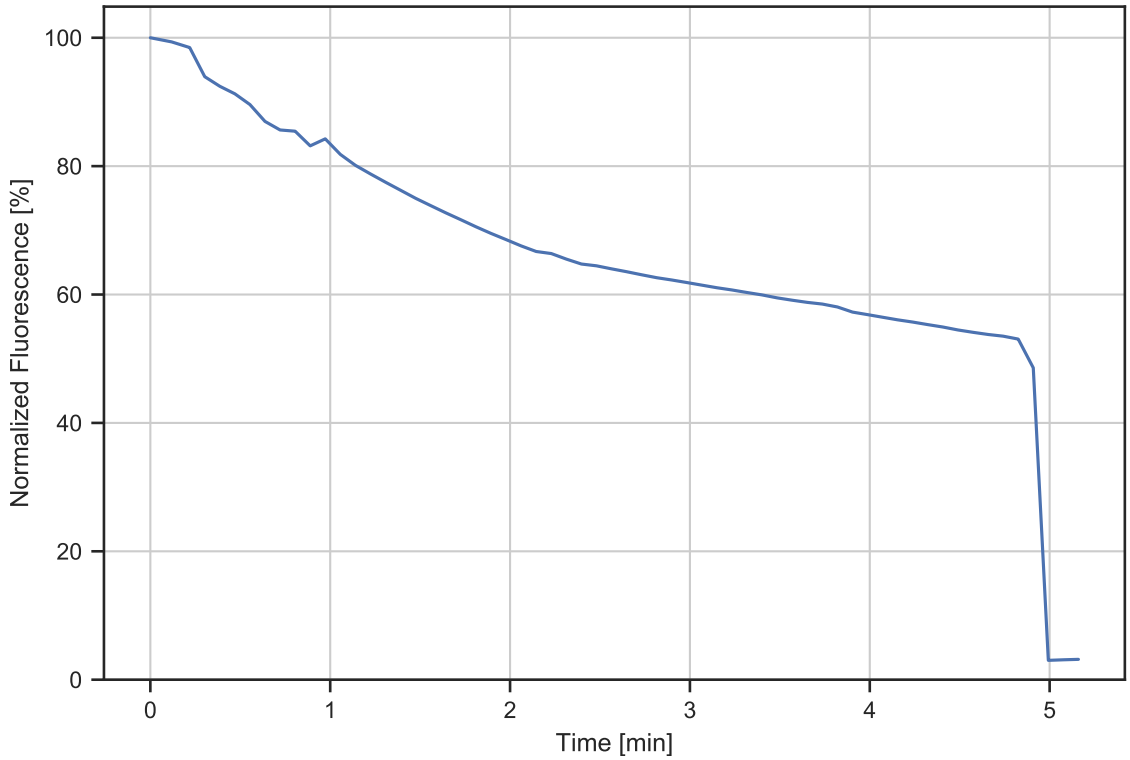

Figure 6.24: Photobleaching of G-acid recorded when being illuminated for 5 minutes using 365 nm HP LEDs. G-acid was dissolved in 45 mM pH 8 TRIS-HCl buffer to keep pH stable and losses more than 45 % of its fluorescence during this illumination time

Thus, due to its strong photobleaching G-acid is unsuitable for online pH measurement, where it is mandatory to detect a decreasing fluorescence with decreasing pH.

6.2 Development of a High Power LED Array

LEDs were mounted in two different ways in the LED array prototype development: Using thermally conductive adhensive tape and thermally conductive adhensive paste. The influence of the LED mounting method on temperature development was analysed. Used were thermal conductive tape and thermal conductive paste, as described in section 5.2.3. Afterwards the influence of the mounting method on the LED light intensity and LED heat management was analysed.

6.2.1 LED mounting and Cooling

LEDs were mounted with thermal conductive tape in version 2.1 and version 2.2. In LED array version 2.3 all LEDs were mounted using thermal adhesive paste. Influence of the mounting methods is visualized by IR images as shown in figure 6.25.

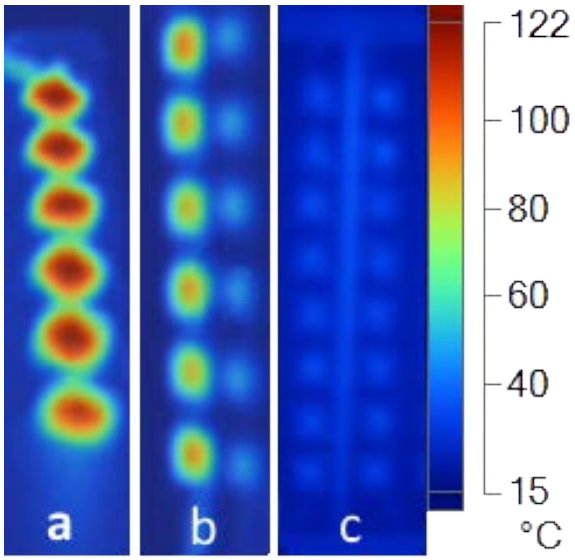

Figure 6.25: Temperatures recorded using a IR camera while LEDs were switched on for 5 minutes. Images are taken from (a) version 2.1 (mounted with thermal tape), (b) version 2.2 mounted with thermal tape (left) and mounted with thermal paste (right), (c) version 2.3 mounted with thermal paste and with radial fans turned on. Clearly the mounting method has an influence on the LED temperature: LEDs mounted with thermal tape are overheating whereas LEDs mounted with thermal paste have a temperature from 40 - 60 °C

There is a clear correlation between the mounting method and the casing temperature of the LEDs: In version 2.1 (Fig. 6.25 (a)) all LEDs were mounted using thermally adhesive tape. LED casing temperature is 122°C or higher. In version 2.2 LED mounted with thermal adhesive tape (Fig. 6.25 (b) left) have an average temperature of ca. 90°C. When mounted with thermal adhesive paste (Fig. 6.25 (b) right), the temperature lowers to an average of ca. 60°C. In version 2.3 only thermal adhesive paste was used (Fig. 6.25 (c)). The average LED temperature is ca. 40°C. Generally, temperature could be lowered to an average of ca. 40°C after 5 minutes irradiation time for version 2.3 (see figure 6.26), thus this prototype was finally used for later experiments.

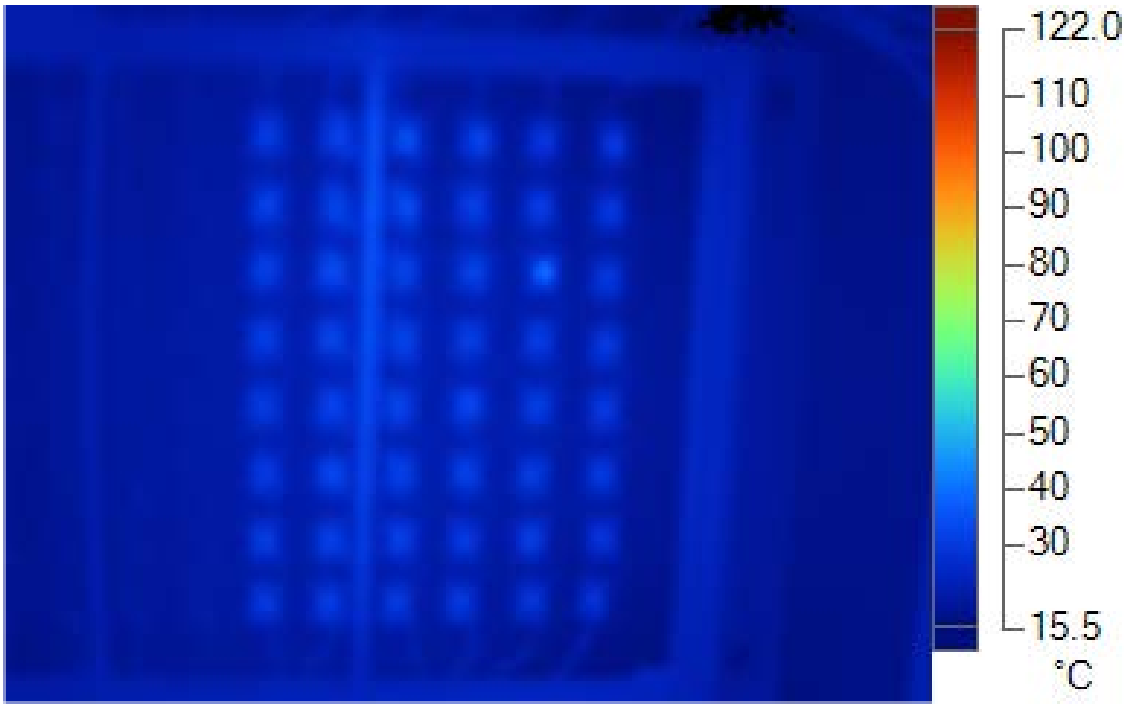

Figure 6.26: Temperatures recorded using a IR camera of version 2.3 with radial fans turned on

The LED casing temperature is directly correlated to LED intensity stability: When LEDs overheat the intensity is not stable and drops significantly. The intensity drop over time (5 minutes) is recorded and analysed in the next section in order to obtain reproduceable illumination intensities.

6.2.2 Light Intensity and Heat Management

The light intensities over time of LED array version 2.1-2.3 changes, depending on the cooling efficiency of each setup (Fig. 6.27), which was analysed in the previous section.

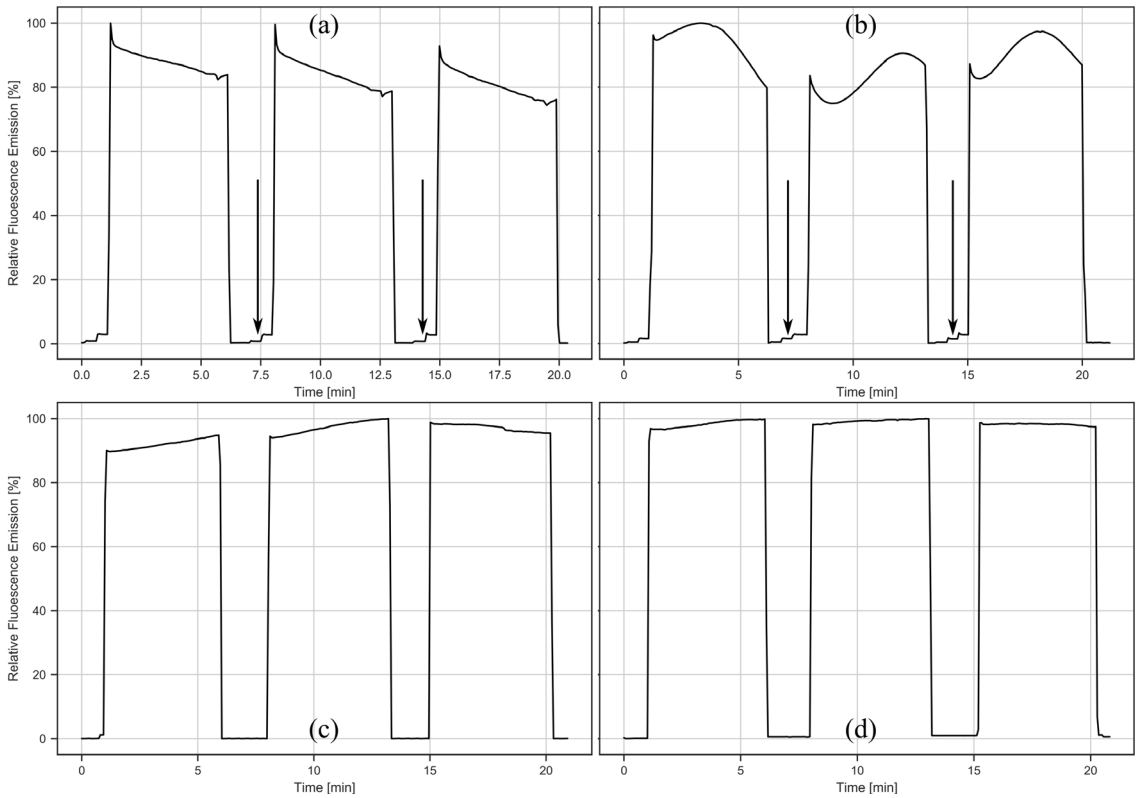

Figure 6.27: Light intensities recorded of (a) version 2.1, (b) version 2.2 , (c) version 2.3 without radial fans turned on and (d) version 2.3 with radial fans turned on. It is clearly visible, that in version 2.1 the intensity drops due to LED overheating. This is reduced in version 2.2 where LEDs are fixed with thermal paste. A stable illumination intensity is achieved when LED array version 2.3 is used and radial fans are switched on

The mounting method influences the LED light intensity as a consequence. For version 2.1 (Fig. 6.27 (a)) the intensity loss over 5 minutes continuous illumination is ca. 20% - 25%. Also, a 4% intensity drop can be observed during each cycle. This loss was slightly reduced to an average of 18% in version 2.2 (Fig. 6.27 (b)), where the emission intensity was recorded when LEDs were fixed with thermal conductive adhesive paste. Due to the stronger cooling of the peltier elements and the thermally more efficient fixing method in version 2.2, the thermal management improved and the intensity losses due to self-heating decreased. The long- term downward drifts disappear and LEDs alternately overheat and cool, resulting in intensity fluctuations and 2% output loss in each cycle when measuring at maximum intensity in each cycle. Ca 3% scattering light can be measured as a side effect, when neighbouring LED rows were switched on, for both version 2.1 and version 2.2. This is indicated by the arrows in figure 6.27 (a) and (b). Scattering light was suppressed by using crossbraces version 2.3 (Fig. 6.27 (c) and (d)). Without radial fans switched on in version 2.3 the long-term intensity drop was 8% (Fig. 6.27 (c)) . This was reduced to 3% when radial fans were on (Fig. 6.27 (d)). The average output loss from cycle to cycle was reduced to ca. 0.5%. LED mounting with thermal tape and thermally conductive paste both resulted in homogeneous temperatures for all three setups.

Apart from the LED illumination stability, the temperature reached inside each well of the microtiter plate is also important when conducting enzymatic reactions. Enzymes are temperature dependent, thus the influence on the sample temperature was analysed next

when LEDs are switched on for 5 minutes. In LED array version 2.1 the temperature rises from 22 °C to 63°C peak temperature after 5 minutes exposure time (Fig. 6.28).

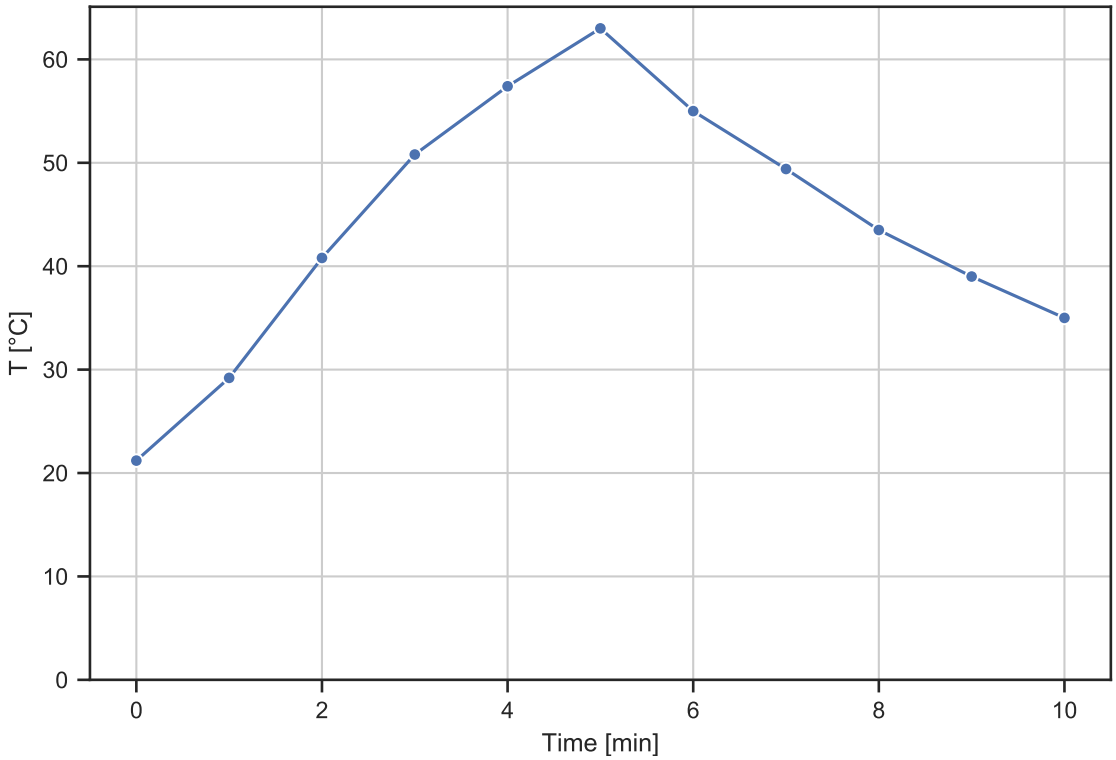

Figure 6.28: Temperature recorded for 10 min while HP LEDs were switched on for 5 minutes and switched off afterwards for 5 minutes in 100 µl sample volume in a microtiter plate placed on LED array version 2.1

The same measurement was done for the LED array version 2.3 with the more efficient cooling method. For LED array version 2.3 the temperature was measured for 3 ON/OFF cycles of 7 minutes, respectively.

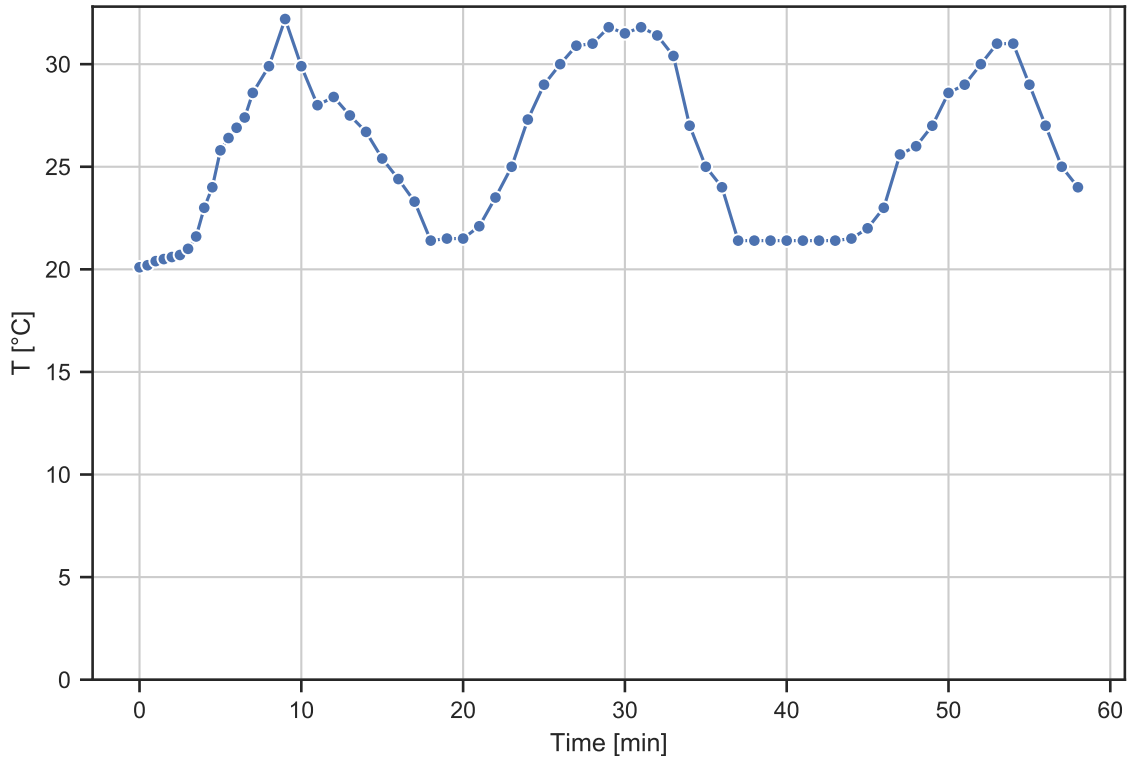

Figure 6.29: Temperature recorded for 3 cycles while HP LEDs were switched on for approximately 7 minutes and switched off afterwards for 7 minutes in 100 µl sample volume in a microtiter plate placed on LED array version 2.3. The temperature rises to a maximum of 32°C for each cycle.

In the first illumination cycle the temperature rises from 20°C to ca. 31°C while sample is illuminated. The temperature lowers to ca 22°C and rises to ca. 32°C in the second cycle. From there the temperature lowers again in the dark time to ca. 22°C. In the third cycle temperature rises from ca. 22°C to ca. 32°C while the sample is illuminated. The average temperature rise during illumination was lowered from ca. 43° in LED array version 2.1 while sample was illuminated to ca. 12 °C in LED array version 2.3, (Fig. 6.29). Thus LED array version 2.3 was successfully developed and is used for future biochemical reactions in this thesis.

All in all, three prototypes were developed in this thesis of which version 2.3 was finally used for successful experiments. An overview of the developed LED arrays is given in figure 6.30.

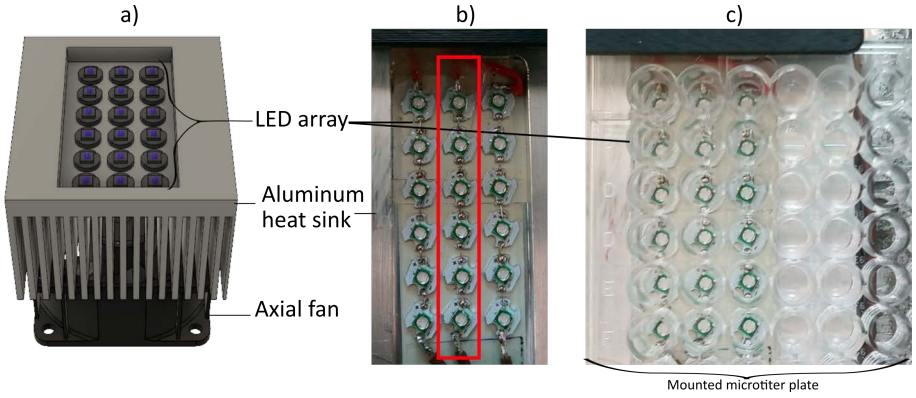

(a) Version 2.1

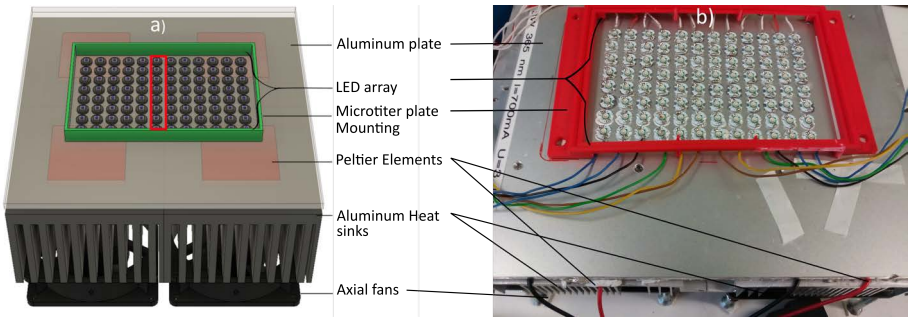

(b) Version 2.2

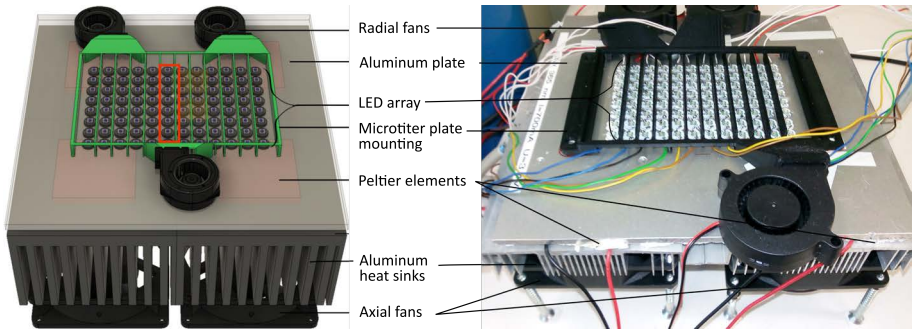

(c) Version 2.3

Figure 6.30: Development of 3 prototypes in CAD design (left) and a photograph of the actual setup (right)

6.3 Establishment of Enzymatic Reactions Using Photoacids

This section analyses the establishment of enzymatic assays using photoacids. First of all, standard enzymatic assays are conducted and then compared to assays when photoacid is added. Finally illumination assays are established using both, the enzyme and photoacid.

6.3.1 S1 Nuclease

An overview of the nomenclature of samples and its respective composition can be found in section 5.2.4.

Standard assay

The assay conditions are summarized in tables 5.6 and 5.7. First of all the standard assay using the reaction buffer of Roboklon GmbH was optimized. Assay conditions are listed in section 5.2.4.

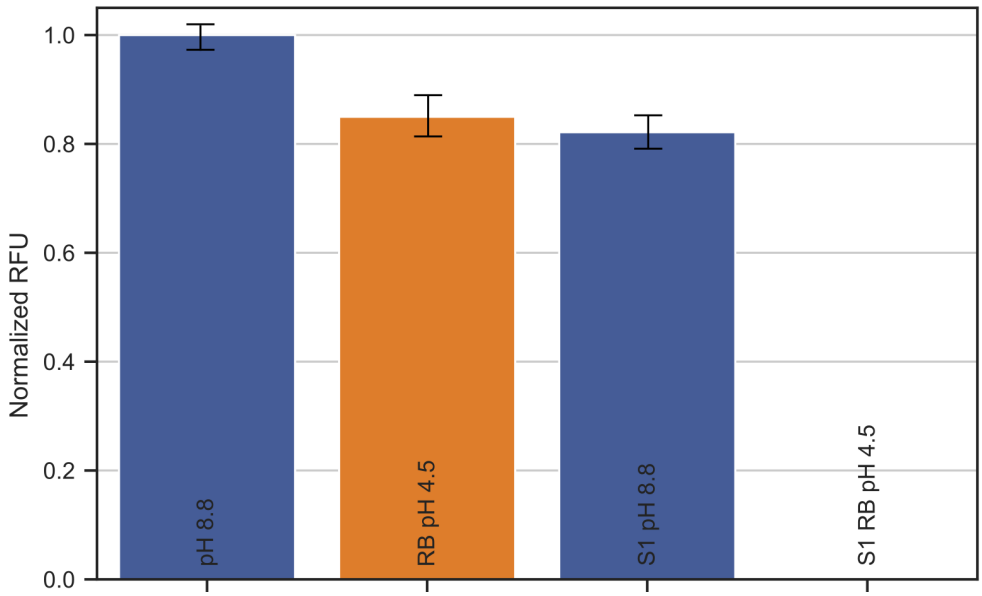

Figure 6.31: S1 Nuclease in a standard assay using the recommended reaction buffer by supplier. pH values 8.8 and 4.5 are compared. The enzyme has a very low activity at pH 8 (17 %) and is fully active at pH 4. When no enzyme is present the fluorescence at a pH of 4.5 in reaction buffer is slightly reduced to 83 %. Experiments are conducted in triplicates (n=3)

The following assay conditions using the reaction buffer of the provider were found after optimization: 30 mM sodium acetate, 28 mM NaCl, 1 mM $ZnSO_4$, 1 U/µl S1 nuclease and 21 ng/µl 70 mer oligonucleotide. S1 nuclease is only slightly active at an alkaline pH of 8.8 (Fig. 6.31). At a pH of 4.5 the enzyme fully hydrolyses the ssDNA. The fluorescence signal of the ss DNA RB + 4.5 sample without S1 nuclease present is almost 20% lower than the negative control at pH 8.8 To avoid possible proton scavenging by the reaction buffer it was exchanged for acetate buffer, zinc needed for reaction was added. See table 5.7 for assay concentrations. A comparison of the assays is done between the original supplier reaction buffer and the "self made" acetate buffer with added zinc.

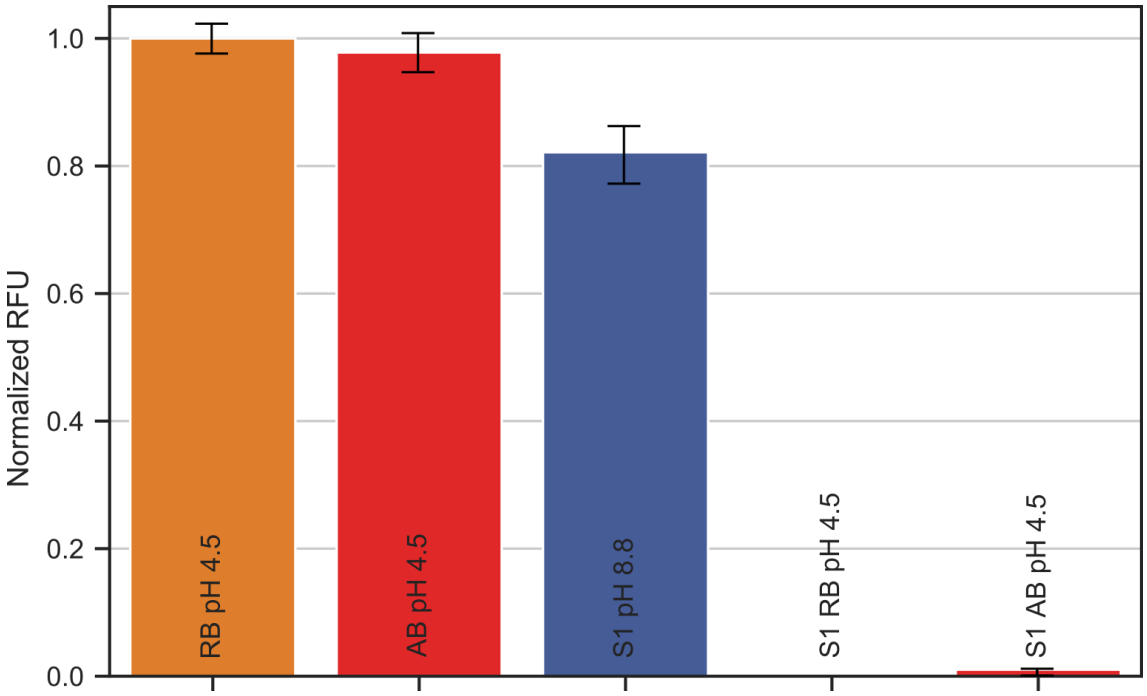

Figure 6.32: Comparison of S1 nuclease activity in 1x reaction buffer (RB) from supplier vs. 45 mM acetate buffer (AB) + 1 mM $ZnSO_4$ added for samples containing acetate buffer. The fluorescence signal of ssDNA only with the two different buffers is nearly equal, S1 nuclease has an activity of 17 (%) at a pH of 8.8. When using 1x RB S1 nuclease activity is 100 % and 99 % when using AB. Experiments are conducted in triplicates (n=3)

There is almost no difference between S1 nuclease activity when using supplied 1x reaction buffer or acetate buffer. The enzyme is inactive at a pH of 8.8 and fully hydrolyses ssDNA in reaction buffer (RB) and 99 % ss DNA in acetate buffer (AB) (Fig. 6.32). Thus acetate buffer with added zinc can be used to exchange reaction buffer. After establishing the standard assay the effect of photoacid on the enzyme was tested next.

Inhibition by Photoacids

Potential inhibition of S1 nuclease by photoaids HPTS and G-acid was tested. Negative controls were adapted to a pH of 8.8 using 3M NaOH. Acetate buffer was replaced when photoacids were present and the pH was adjusted to either 8.8 or 4.5 using 3M NaOH or 1 M HCl.

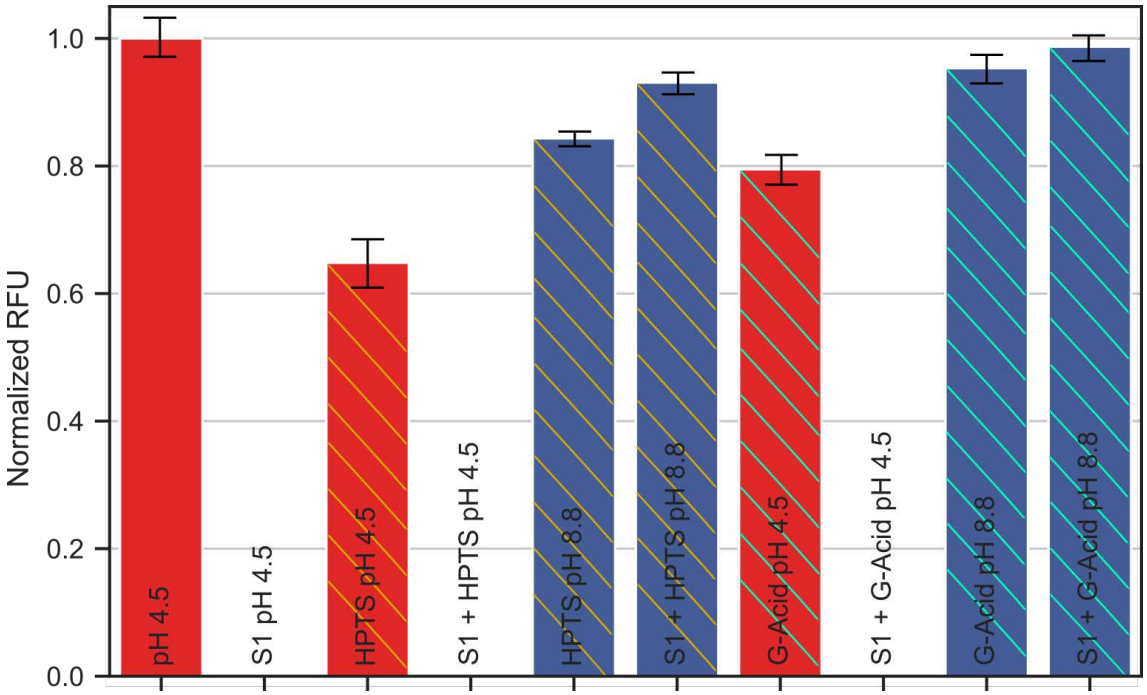

Figure 6.33: Potential inhibition of S1 nuclease by 1 mM HPTS and 1 mM G-acid. Only ssDNA in AB at pH 4.5 is taken as reference. When S1 is present 100% ssDNA is hydrolysed, also when photoacids are present. When HPTS and ssDNA are prensent in the sample at pH 4.5 the fluorescence is reduced to 63%, indicating that HPTS might damage or influence the ssDNA measurement. When G-acid and ssDNA only is present the fluorescence at a pH 4.5 is reduced to 79%, indicating a potential ssDNA damage as well. S1 nuclease has a maximum activity of 86% when pH is 8.8, also when photoacids are present. Experiments are conducted in triplicates (n=3)

Up to 1 mM photoacid did not inhibit the S1 nuclease's activity. This was true for both, HPTS and G-acid. ssDNA only at a pH of 4.5 was taken as a control. Positive control with S1 nuclease at pH 4.5 fully hydrolysed ssDNA. The fluorescence signal of ssDNA with 4.5 and 1 mM HPTS was ca. 40% lower than ssDNA only at pH 4.5. The enzyme fully hydrolysed ssDNA when 1 mM HPTS was present. For samples containing 1mM HPTS at a pH of 8.8 no hydrolysis was detected when S1 nuclease was present compared to negative controls without enzyme at a pH of 8.8 containing HPTS. The same is true for samples containing G-acid (Fig.6.33). As the enzyme is not inhibited in its activity at a pH 4.5 by both photoacids, next step is to establish an illumination assay to regulate the pH value by light using the photoacids as proton donors.

Illumination Assay

All samples were adjusted a starting pH of 8.8 before illumination using 3M NaOH. Samples were illuminated for 1 or 10 minutes. A signal decrease of ca. 18% illuminating HPTS and sDNA alone is observed. This rises to more than 80% when the sample is illuminated for 10 minutes . When S1 nuclease is present the signal decreases to ca. 15% when illuminated for 1 minute and to ca. 12% when illuminated for 10 minutes. Signal of samples in the dark with an incubation time of 10 minutes at a pH of 8.8 resulted in a

decrease of ca 18% when only HPTS and ssDNA is present. When HPTS and S1 nuclease is present with ssDNA at a pH of 8.8 signal decreases to ca 75% (Fig. 6.34). These results indicate, that photoacid seems to damage the ssDNA when illuminated.

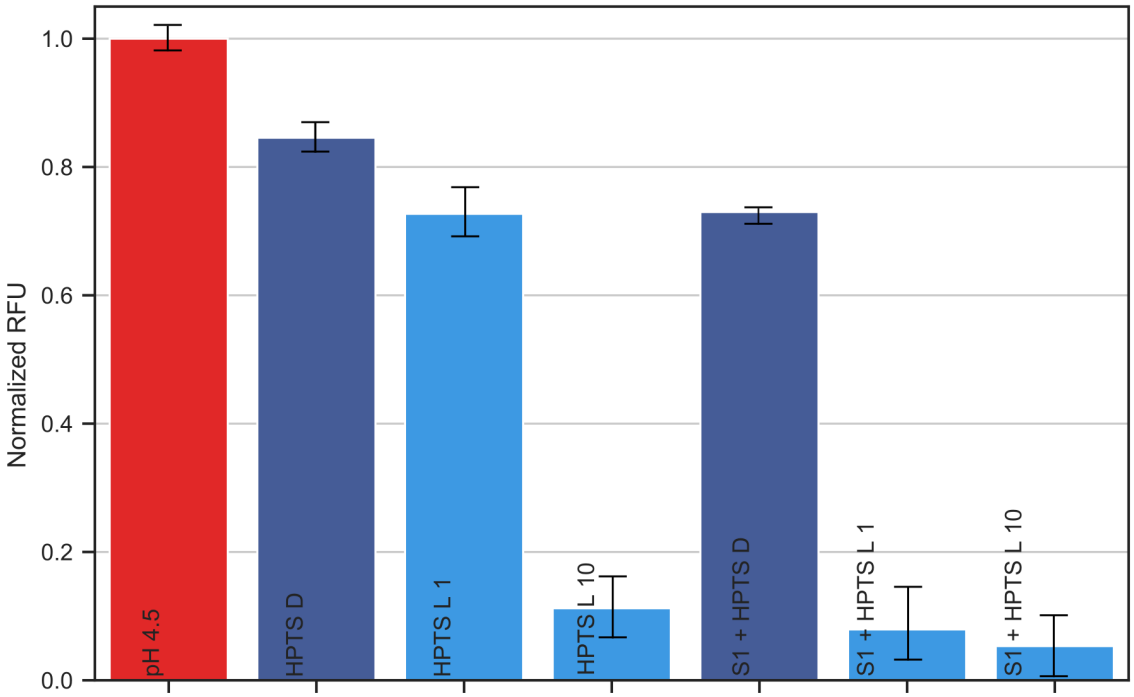

Figure 6.34: S1 nuclease with 1 mM HPTS illuminated for 10 min. An L indicates "Light", a D indicates "Dark" serving as negative controls. The fluorescence signal of ssDNA with HPTS only significantly decreased when samples are illuminated. This is also true when S1 nuclease is present. This indicated a ssDNA damage when samples are illuminated together with HPTS. Negative controls at a pH of 8.8 in Darkness are 83 % when ssDNA and HPTS are present and 77 % when S1 Nuclease, ssDNA and HPTS are present. Experiments are conducted in triplicates (n=3)

Alternatively, as second method to control results from the fragment analyser (Fig. 6.34), the illumination assay was carried out again and a gel electrophoresis was used. The used dye for gel electrophoresis (Serva DNA Stain Clear G) is excited at 470 nm where HPTS also absorbs. Samples with HPTS had a very strong fluorescence and could not be analysed using gel electrophoresis with Serva DNA Stain Clear G. Thus, only the fragment analyser is suitable to analyse samples containing HPTS of the tested devices.

The same experiment was repeated using G-acid. Analysis using G-acid in gel- electrophoresis is possible, when exciting samples at 470 nm. These results confirm the results from the illumination assay with HPTS (Fig. 6.34). The ssDNA seems to be hydrolysed by the combination of photoacid and light. The light-hydrolysis in combination with a photoacid happened with both photoacids used (Fig. 6.35).

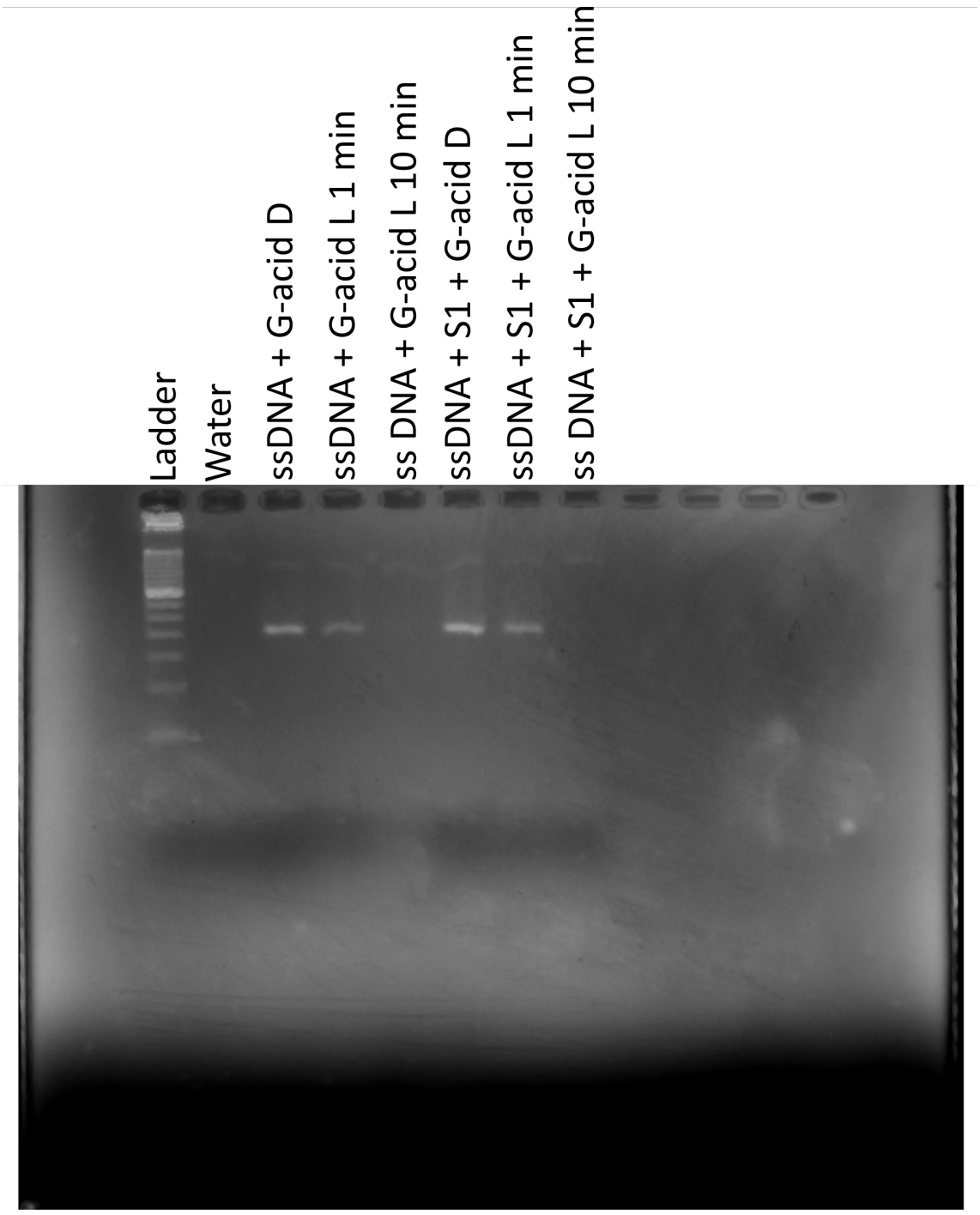

Figure 6.35: ssDNA after 10 minutes incubation or illumination time with G-acid in gel-electrophoresis. An "L" indicates light, a "D" indicates darkness. Results obtained with the fragment analyser and HPTS are confirmed by this gel-electrophoresis: ssDNA degrades when illuminated for 10 minutes and photoacid is present. When samples are in darkness (D) ssDNA is clearly visible in the gel, without and with enzyme

To confirm ssDNA degradation when illuminated with photoacid, rising G-acid concentrations were illuminated for 10 minutes together with ssDNA of the same concentrations. ssDNA degraded proportionally to G-acid concentration when samples are illuminated for 10 minutes with 365 nm HP LEDs. When no photoacid is present and ssDNA is exposed

to UV 365 nm light, survival rate is at ca 95 % (Fig. 6.36).

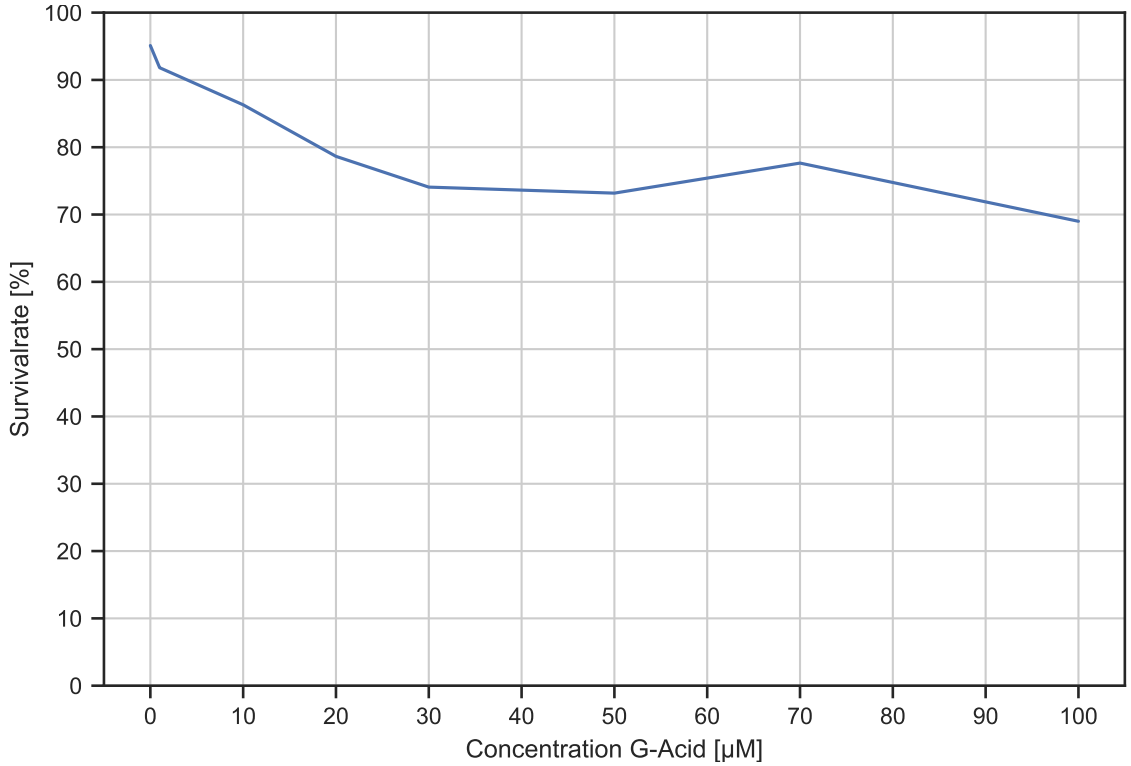

Figure 6.36: ssDNA survival rate with different G-acid concentrations after 10 minutes illumination time

6.3.2 Acid Phosphatase

As a second approach to control enzymatic activity with light acid phosphatase was chosen. To avoid DNA degradation an absorption assay was chosen using pNPP, which is hydrolysed to pNP by acid phosphatase. pNP has an absorption peak at 405 nm at pH 12. Two enzyme concentrations were tested using 100 µM pNPP. The substrate absorb in the UV region until ca 375 nm. Both enzyme concentrations (0.12 U/ml - AP low and 0.21 U/ml - AP high) absorb less in the UV range than pNPP. Both enzyme concentrations also absorb slightly until 375 nm. G-acid has a peak at 340 nm and absorbs most at 365 nm at a pH of 8.3 (Fig. 6.37). As the absorption of G-acid is higher at 365 nm than that of the other components, G-acid seems to be suitable to use for an assay establishment. HPTS was excluded from this experiments due to its strong absorption at 405 nm - the absorption peak at 405 nm needed to detect the enzymatic reaction product was covered be HPTS absorption.

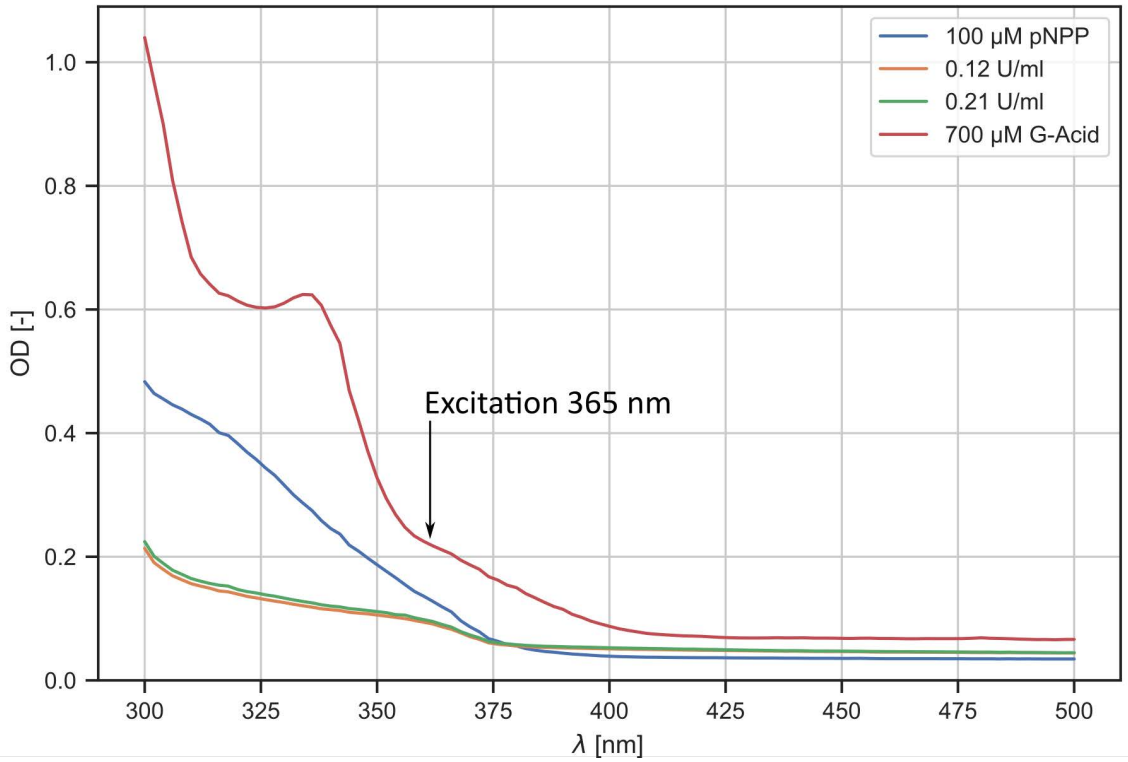

Figure 6.37: Absorption spectra of all components used at pH 8.3. orange line: 0.12 U/ml acid phosphatase (low AP), green line: 0.21 U/ml acid phosphatase (high AP), blue line: 100 µM pNPP, red line: 700 µM G-acid. G-Acid has the highest absorption at 365 nm and can thus be excited in this region.

All of the following absorption measurement were obtained at 405 nm at a pH of 12 and in an overall volume of 200 µl.

Standard Assay

First of all a standard assay was established and inhibition of 700 µM G-acid was tested for both enzyme concentrations. Acid phosphatase is not inhibited by G-acid. G-acid causes a slight increase by ca. 0.14 absorption units for all incubation times and both concentrations (Fig. 6.38). Inhibition was tested in a standard assay in 45 mM pH 5.5 citric buffer.

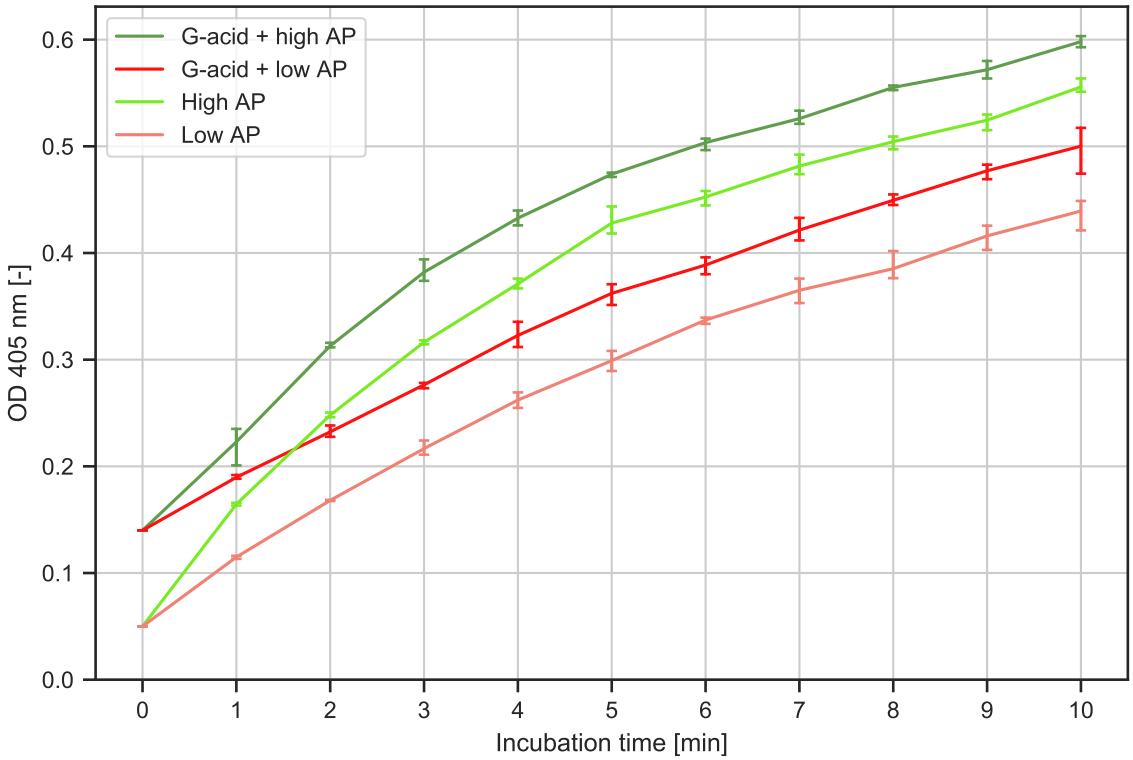

Figure 6.38: Acid phosphatase incubated for 10 minutes in a standard assay with and without G-acid to demonstrate that acid phosphatase is not inhibited by G-acid. The assay is conducted with a high and low acid phosphatase concentration. Slight increase in absorption at 405 nm can be detected. Experiments were conducted using triplicates (n=3)

Citric acid buffer was exchanged for HPLC grade water and pH dependent activity of acid phosphatase was recorded for different pH values by adjusting the sample pH value using 3 M NaOH or 1 M HCl. The low AP concentration has it's optimum activity at a pH ranging from 5-5.5. The activity is lower at a pH of 4-4.5 and further decreases with increasing pH. At a pH of 8 there is no significant activity (Fig. 6.39).

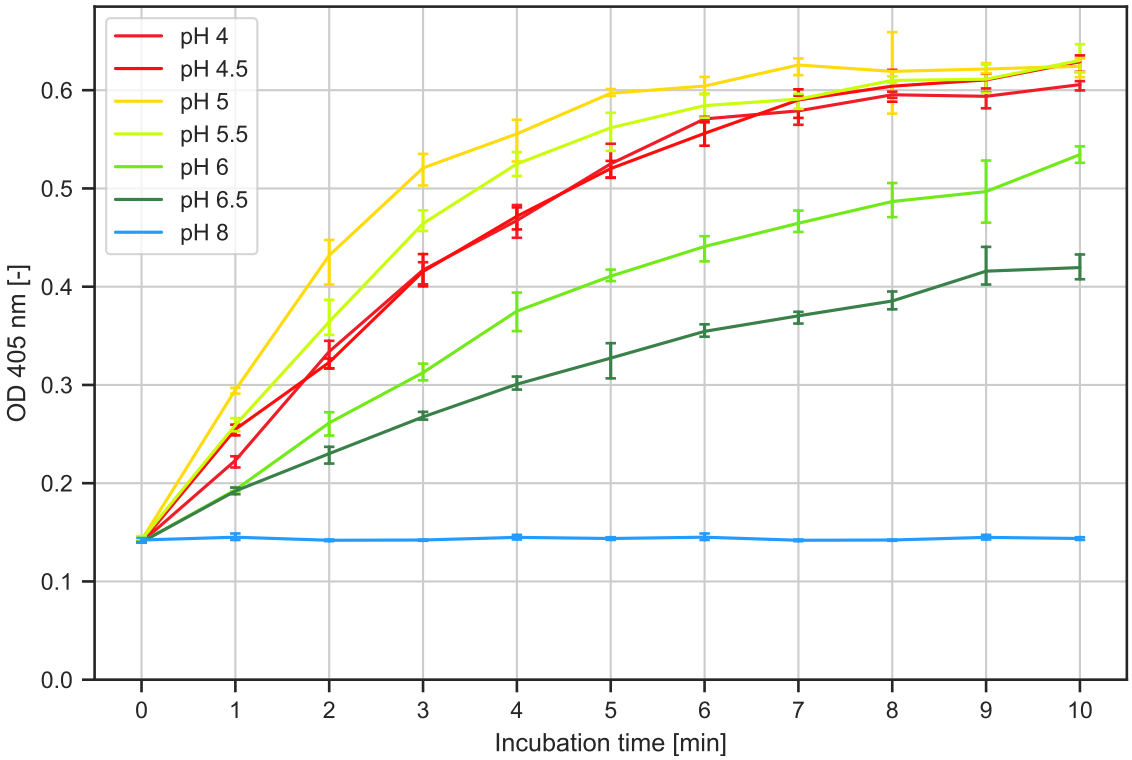

Figure 6.39: Acid phosphatase kinetic 0.12 U/ml + 100 µM pNPP + 700 µM G-acid incubated in 45 mM citrate acid buffer at pH values from 4 – 6.5. The optimum activity is at pH 5-5.5, acid phosphatase is nearly inactive at pH 8. Experiments were conducted using triplicates (n=3)

High AP concentration also has it's maximum activity at a pH of 5-5.5 and is generally higher than the low AP concentration. The activity lowers at a pH of 4-4.5 and further decreases with increasing pH. There is no significant activity at a pH of 8 (Fig. 6.40).

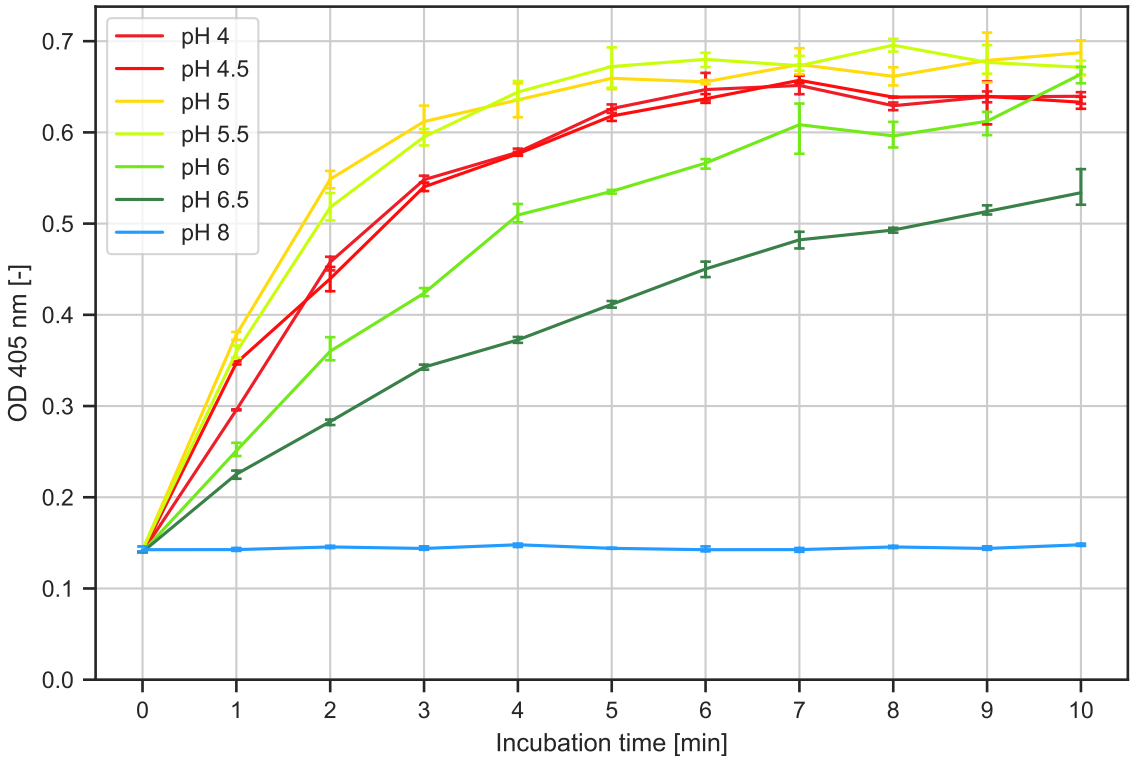

Figure 6.40: Acid phosphatase kinetic 0.21 U/ml + 100 µM pNPP + 700 µM G-acid incubated in 45 mM citrate acid buffer at pH values from 4 – 6.5. The optimum activity is at pH 5-5.5, acid phosphatase is nearly inactive at pH 8. Experiments were conducted using triplicates (n=3)

After successfully testing that AP is not inhibited by G-acid and recording the enzyme kinetics, illumination assays were established using 700 µM G-acid, 100 µM pNPP and the high and low AP concentrations. Also the inhibition of the enzyme by UV light only was tested in the next step.

Illumination Assay

Inhibition of AP by 365 nm HP LED UV light was tested. Both enzyme concentration were incubated in 45 mM pH 5.5 citric acid buffer. Samples were illuminated for the first 4 minutes incubation time, LEDs were then switched off. A slightly lower activity of acid phosphatase when exposed to UV light can be detected. The decrease for both enzyme concentrations is ca. 0.5 absorption units (Fig. 6.41) in contrast to the assays conducted under the same conditions without illumination. As the illumination with UV light did not significantly hamper the AP activity, an illumination assay in which the pH value is controlled by optical means using photoacid is established.

Potential Acid Phosphatase Inhibition by UV- Light

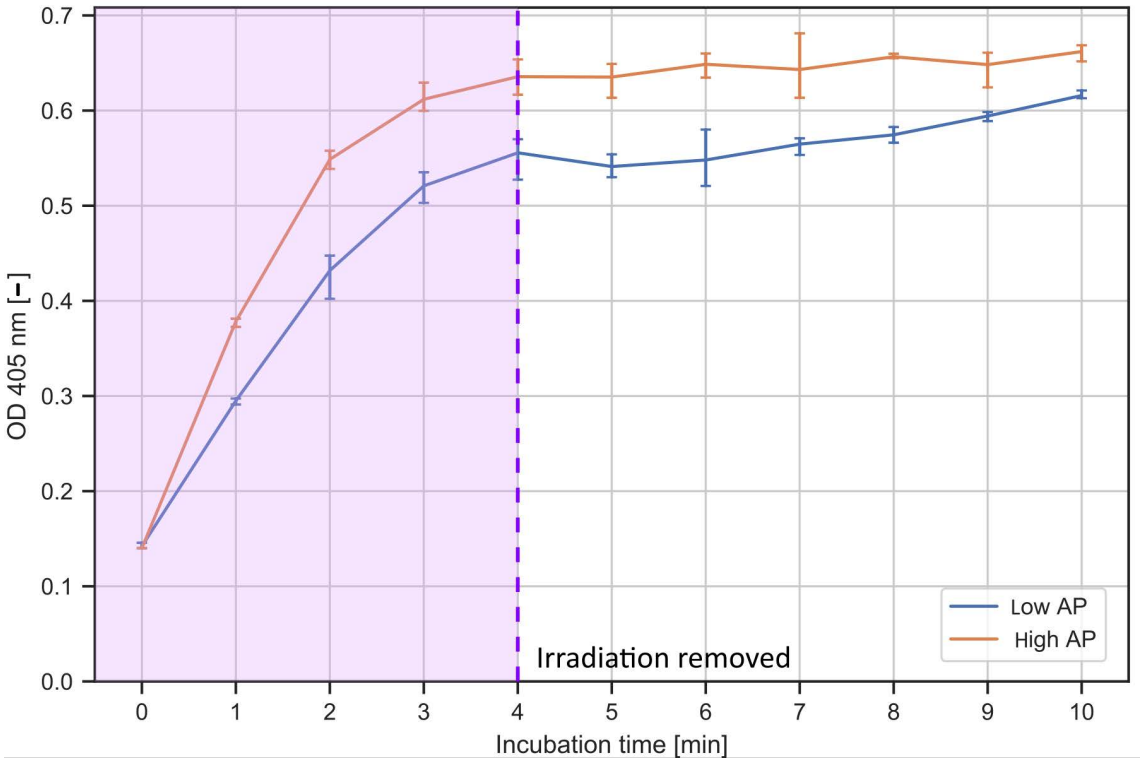

Figure 6.41: Testing irradiation influence on the enzymatic activity in a standard assay in citrate acid buffer at pH 5.5. Samples were illuminated starting until 4 minutes incubation time, illumination was then switched off. A slight decrease in AP activity is observed when compared to the assays conducted in darkness. Experiments were conducted using triplicates (n=3)

Continuous Illumination

Samples were illuminated for 0-5 minutes. Starting pH of all samples was adjusted to 8.3 and overall incubation time for all samples was 10 minutes (Samples were left in darkness after illumination time to an overall time of 10 minutes). Acid phosphatase is not active at a pH of 8 in darkness for both enzyme concentrations. A slight rise in absorption due to UV irradiation in absence of enzyme is recorded. When samples are exposed to UV light activities correlate to enzyme concentrations: The activity is lower for the low AP concentration and is higher for the high AP concentration (Fig. 6.42).

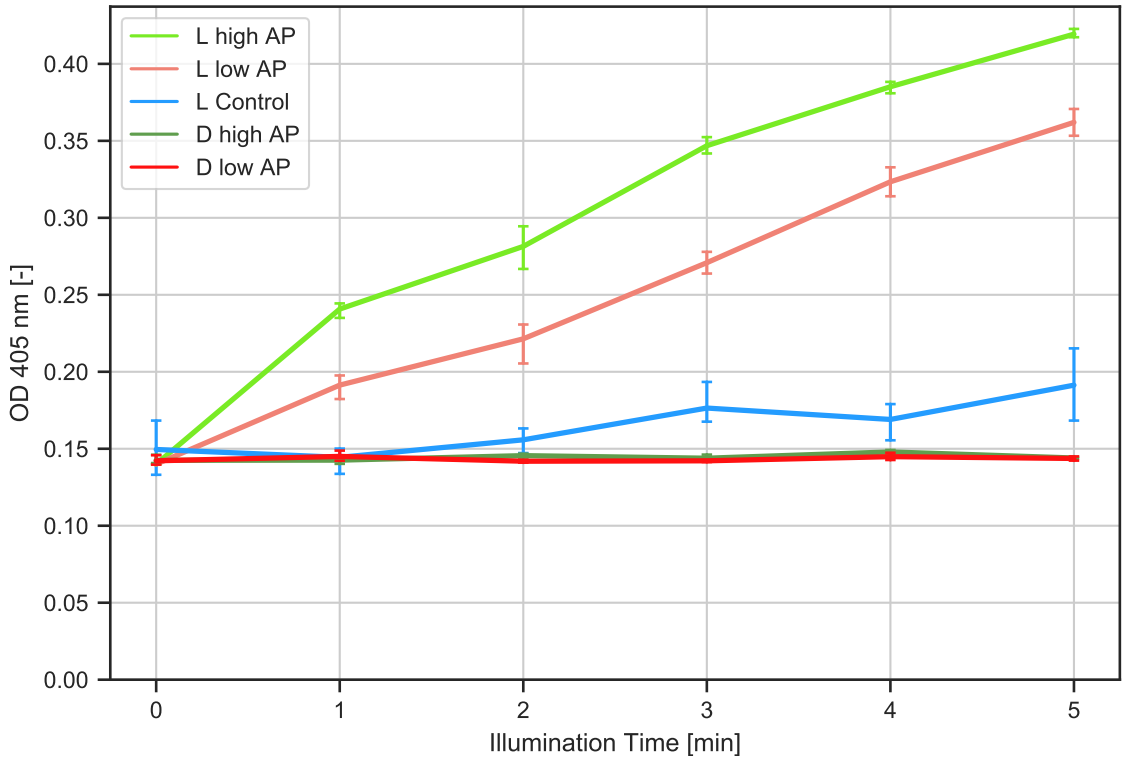

Figure 6.42: Absorption at 405 nm vs. exposure times 1 – 5 min at 365nm. The overall incubation time for all samples is 10 minutes (Samples are left in darkness after illumination to an overall incubation time of 10 minutes). Enzyme concentrations were low AP concentration (0.12 U/ml) and high AP concentration (0.21 U/ml) and a control without enzyme. L indicates light; D indicates absence of illumination (darkness). The enzyme is not active in darkness for both enzyme concentration. When illuminated the enzyme activity is proportional to the light exposure time. A slight UV hydrolysis can be observed in absence of enzyme due to the UV irradiation. Experiments were conducted using triplicates (n=3)

For continuous illumination the enzyme activity is proportional to the light exposure time, as the pH is lowered while the photoacid is excited. As a next step, samples were illuminated in cycles with switching times of one minute and 30 seconds and compared with the continuous illumination in the following sections. This shall prove that the enzyme activity is dependent on the light exposure time only, regardless if the light is applied continuously or in a cycled manner. The overall illumination time is still the same as for the continuous illumination.

Cycled Illumination

Light exposure time was the same as in the continuous illumination assay, this time varying the switching sequence. Hence the illumination was now cycled. Two switching times were chosen: 1 minute and 0.5 minutes. The enzyme activity is the nearly the same and within the error margins for all three types of illumination for both AP concentrations (Fig. 6.43).

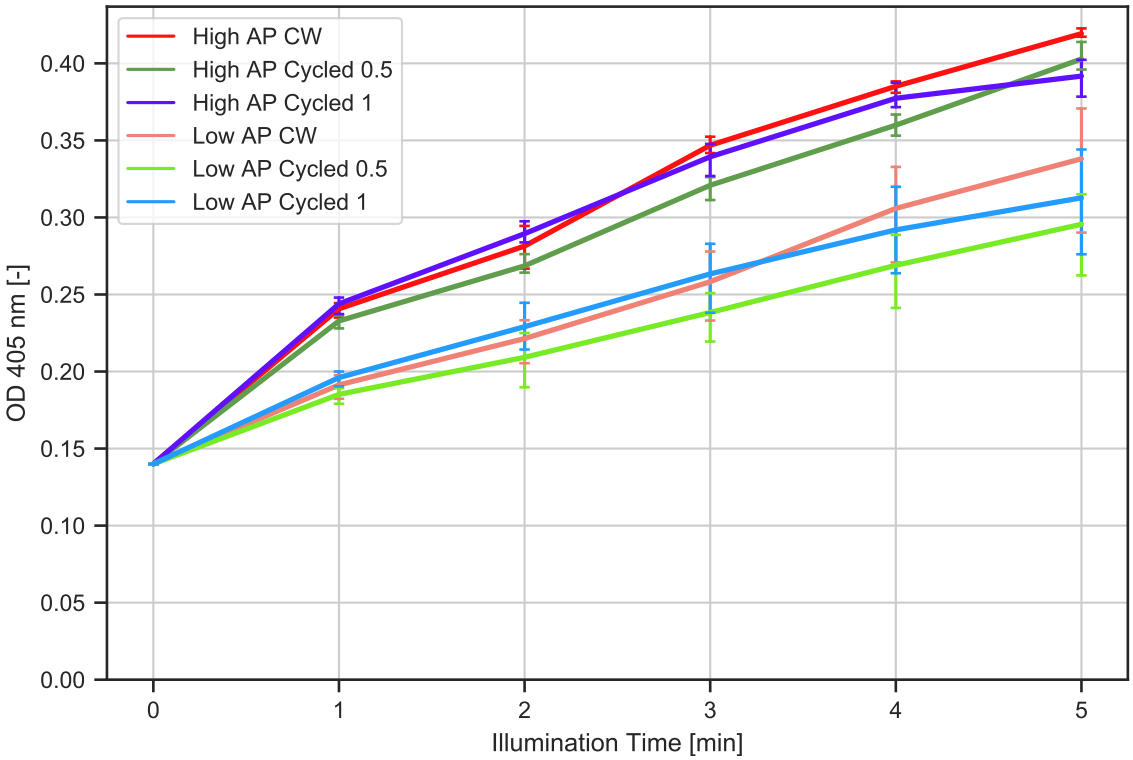

Figure 6.43: Comparison between continuous light vs. cycled exposure times. Absorption was measured at 405 nm, exposure was at 365 nm from 1- 5 minutes with an overall incubation time of 10 min for all samples. Enzyme concentrations were low (0.12 U/ml) and high (0.21 U/ml). CW = continuous illumination; cycled 0.5 and cycled 1 indicates switching times of 30 seconds vs. 1 min. To better compare the results of the illumination assay using continuous illumination are displayed in the figure again. Experiments were conducted using triplicates (n=3)

7 Discussion

Goal of this thesis was to optically and reversibly control the pH value using photoacids and establish and assay in which the pH dependent activity of an enzyme could be switched on and off photoactively. In order to achieve a photoinduced pH control, three partial goals had to be established: 1. Analysing and characterizing a suitable photoacid which can be reversibly controlled optically. 2. Develop a versatile, adaptable experimental setup, which provides the optical photoacid control is solely done by automatically controlled LED irradiation switched in suitable, short illumination intervals. This setup must ensure that factors, such as temperature, do not interfere in switching the photoacid. 3. Demonstrate the optical, reversible pH cycling by using photoacids in an example: The pH-dependent enzyme activity is optically controlled in a non- invasive manner by a photo-induced, reversible pH jump. Factors that influence the assay and obtained results from this thesis will be discussed, compared with literature values and reasons for selections done will be given in the following sections.

7.1 Photo-induced pH Jumps Using Photoacids in Biochemical Applications

Depending on the application, a suitable photoacid has to chosen. Important parameters to be considered are:

- Possible ΔpH (pH jump)
- pH jump control
- pH jump duration
- Illumination sources (intensity, wavelength)
- Photoacid's absorption spectra (pH value dependent)
- Solubility in water
- Biological compatibility / toxicity

Magnitude of the photo-induced pH jump

The ΔpH is defined by the ΔpK_a (equation 3.1). The larger the difference between the ground state and the excited state, the larger the expected pH jump. A summary of

ΔpH of photoacids used in this work is given in table 3.1. One group of photoacids with a significantly large ΔpH is called "Super photoacids" [52, 49, 7]. The used photoacid 6CN2 is also considered to be in this group. Due to its large ΔpH 6CN2 seems the most promising photoacid for biological applications. However it has not been used for pH jumps experiments yet. Only ESPT studies have been conducted with this photoacid and its pH-dependent absorption spectra have not published. Hence, establishing pH jumps experiments to determine the ΔpH in a solvent as water was first goal of this thesis. HPTS, G-acid, R-acid, 6-cyano-2-naphthol and mPAH were chosen to be tested for pH jumps experiments. Their pH-dependent recorded absorption spectra were suitable to be excited with available high power LEDs. Thus these photoacids (HPTS, G-acid, R-acid, 6-cyano-2-naphthol and mPAH) were chosen for further analysis. The remaining two photoacids were excluded due to their absorption below 360 nm. Taking the previously done ΔpH considerations into account G-acid, 6CN2 and mPAH are expected to induce the largest pH jump due to their large ΔpH. However, no photo-induced pH change for 6CN2 could be measured by the applied techniques. This was also true for R-acid: A pH change upon illumination from pH 7 to 6.5 was recorded. However, when irradiation was removed, the pH did not rise again but stayed at ca. 6.5. The largest ΔpH by 2.52 units was detected for G-acid after 5 minutes irradiation and 0.62 for HPTS. The experiments to determine the ΔpH were conducted using a micro pH electrode.

Alternatively, pH indicators, such as bromcresol green, can be used for a second-order diffusion controlled reaction to measure the actual ΔpH achieved in solution: The photo-induced proton ejected from a photoacid changes the formation of the pH indicator and allows a spectroscopic determination of pH change. This was demonstrated by Gutman et al. [11, 13]. They showed that aqueous solutions could be acidified on a microsecond scale by exciting the photoacids HPTS and G-acid, using a short 347.2 nm laser pulse of 50 ns. The absorption change in bromcresol green (BCG) was detected perpendicular to the excitation at 632.8 nm (using a continuous He-Ne laser) or at 442 nm (using a He-Cd laser). The maximum ΔpH measured by Gutman et al. was 1.91 pH units from 6.2 (dark) to 4.29 (excited) for HPTS. Maximum pH jump achieved for G-acid was 4.14 units from 8.6 (dark) to 4.46 (excited). The achieved pH jump in this work might have been larger, if the volume was stirred, as done by Gutmann et al. As the bottom of the microtiter plate was used for illumination by the LED array and the top had to stay open in order to pipette, start or stop reactions, a stirring mechanism could not be implemented. This way the process relies on diffusion alone. However, the pH jump induced by the method in this thesis is still significant.

Using bromcresol green and HPTS, a colour change could be achieved by continuous LED illumination. However no online absorption detection was established. These were first experiments to test the photoacids functionality when using LEDs with continuous illumination as an excitation source (see section 6.1.9). Excitation in free solution using LEDs has not been done yet in literature. Hence this was a good test to see if the intended illumination system would suffice. A local pH change using surface-bound HPTS was achieved by a research group using LEDs. The photoacid (HPTS) was, fixed on silica nano-wires [35]. The group measured a local alteration of surface-bound HPTS by using a continuous low powered LED illumination (650mW for 400 nm LED). The magnitude of pH jump was ca 0.3 from 7.1- 6.8 and could locally trigger the activity of the enzyme pepsin.

Two outcomes were demonstrated in this work: 1. pH can be decreased by using LEDs as an irradiation source, no laser system is needed. 2. This is possible in solution and

no photoacid surface-binding step is necessary. Establishing an enzymatic assay in free solution has the advantage that a higher photoacid concentration can be used in contrast to a system where the photoacid is surface bound. Moreover it is a less complex approach where possibly no pre-treatment, such as surface binding, is required. On the other hand, when being fixed on a surface, the enzyme is not influenced by inhibiting factors and the photoacid does not potentially compete with the enzyme's substrate.

Furthermore, the pH jump can be measured by the established method using a micro pH electrode with a response time of ca. 20 -40 seconds in 200 µl volume. The established method greatly facilitates the pH jump measurement. This is not as accurate or fast as the previously discussed method using a spectrometer (ns scale), however it is sufficient for the intended biochemical applications (minute scale). Enzymes with a strong pH-dependent activity, such as S1 nuclease, pepsin or acid phosphatase, are active in a certain pH range. Their activity has a pH optimum, but is not limited to this very certain pH value alone [95, 34, 1].

Besides using a pH micro electrode, an optical approach for detecting a decreasing pH upon illumination was conducted. HPTS has a very strong, pH-dependent absorption and fluorescence. Hence, the photoacid can function as both: a pH indicator and a photoacid (see section 5.2.2 for experimental setup). Tested measurement in this thesis used a spectrometer to record the absorption and fluorescence changes upon HPTS illumination. However, this approach could not be established successfully. No changes in absorption or fluorescence were observed. Cuvette volume could not be fully illuminated in this process, which might be a reason. Testing G-acid with the same method was not possible, as G-acid undergoes strong photobleaching in the process of continuous illumination. Online pH measurement using spectroscopic methods could have been further optimized and established in this interdisciplinary project. However, it would have involved a complex optical setup with high-end spectrometers, which were not available in the institution and establishing a physically correct detection method was hardly possible considering given conditions. As the main goal of this thesis was to establish a photo-controlled enzymatic reaction it was decided to continue using biochemical methods, such as a pH electrode.

Apart from the reversible photoacids, it is also possible to induce an optical pH jump using metastable photoacids [2, 106]. The mPAH, also tested in this work, could achieve a pH jump of ca 1.7 from 6 to 4.7 in aqueous surrounding containing 10% DMSO and was determined by change in spectra following literature [63]. The spectra change could be reproduced in this work when using methanol or ethanol as a solvent. The photo-induced spectra change could not be achieved using HPLC grade water as a solvent alone. Methanol and ethanol are both unsuitable solvents for an enzymatic reaction, as they are inhibitory or lethal for the enzyme [107]. Hence the metastable photoacid was excluded for further experiments.

Control of pH jump

The magnitude of the pH jump can be influenced by choosing the optimum excitation wavelength and light exposure time. This is important for using photoacids in biochemical application, as not necessarily the largest possible pH jump shall be induced. Furthermore the magnitude of the pH jump can be influenced by changing either the photoacid concentration or the light intensity by which the photoacid is excited, thus enhancing the excitation yield [11].

Theoretically more protons can be emitted by the photoacid upon excitation when more photoacid is present. A more effective pH jump by enhancing the concentration from 0.1 mM to 1 mM HPTS is measured and displayed in figure 6.17. However, the PA concentration cannot be increased arbitrary, due to the following fact: One excitation-recombination Förster Cycle of the photoacid takes place on the scale of µs (section 3.1). Hence, only a certain amount of photoacid can be excited in this time. If more is present in solution the PA itself will serve as a buffer, when more molecules are present in the ground state. Moreover the first layer of photoacid will block the light for layers behind in a certain volume. Hence, it is important to take the volume, as well as its distribution into account. Preferable is a thin solution layer to lower light absorption effects in the volume. In addition,the concentration of many photoacids in water is limited by their solubility in aqueous media [63]. These facts influence the biochemical assay design as well. Components must be chosen in correct concentrations and buffering effects, layer thickness, sample carrier (microtiter plate, Petri dish, cuvette) and other hampering influences, such as absorption of used materials must be taken into account. To reduce proton scavenging by assay components lowest possible concentrations were chosen.

The illumination length also corresponds to the magnitude of the pH jump. When HPTS was illuminated for 10 minutes the magnitude of the pH jump was increased from 0.62 (5 minutes illumination time) to 2.63 (10 minutes illumination time). The increase of the pH drop with the excitation intensity is consistent with results observed in literature [11, 13]. However, when the sample was illuminated for 10 minutes the pH did not return to its original starting pH. Presumably the reversible photoacid undergoes a photo destructive oxidation process when the exposure time or excitation intensity surpasses a certain limit. The destruction of photoacids, when being illuminated for 10 minutes could also be observed as a change in colour for both, G-acid and HPTS. G-acid changed its colour from transparent to beige and HPTS from bright yellow to yellow-orange. This process could not be prevented by adding reducing reagents, such as ascorbic acid, neither. All in all, due to their absorption characteristics, the possible pH jump and the compatibility with tested enzymes HPTS and G-acid seem to be the best choice of tested photoacids, although absorption and fluorescence spectra have to be considered. HPTS could not be used for the experiments conducted in this thesis, due to its strong fluorescence cause by irradiation with visible light. This hampered analysing methods applied.

Biocompatibility

It is desirable to use a photoacid with a high pK_{a0} to achieve a pH jump starting in a neutral or alkaline environment. The starting pH must not be higher than the pK_{a0} of the proton emitter, otherwise the photoacid itself will function as a buffer and thus the number of liberated protons is reduced [11]. G-acid ($pK_{a0} = 8.29$) is suitable for experiments with a starting pH of 8 and higher, whereas HPTS ($pK_{a0} = 7.7$) is not. Furthermore an absorption of the photoacids in the visible or UVA spectra is desirable as many enzymes, as well as DNA, are damaged when irradiated with UVB light [108]. HPTS was already used in enzymatic reactions and does not inhibit the enzyme pepsin [35]. This was confirmed by experiments conducted in this work. Both enzymes used were neither inhibited by G-acid nor by HPTS. Apart from suitable absorption spectra and characteristics of the photoacids, also the absorption properties of all used components for an assay should be taken into account. An overlap in absorption of used assay compounds with the absorption of the photoacid will decrease the yield of protons emitted by the photoacids, as absorption for the photoacid is lowered by other compounds used. Buffer absorption do not interfere

with absorption bands of photoacids for the experiments conducted.

7.2 Use of an LED Array to Control Biochemical Reactions

When starting to establish reactions using photoacids, the system was not stable. No reproducible results could be obtained by using the first illumination setup, version 1 (see section 5.2.3). This setup used two mounting stands, one holding the LEDs, the other holding the samples. The alignment of these two stands inevitably slightly changes with each experiments, after the samples and the LEDs have been placed into the clamps. Biochemical reactions are very complex and depend on many parameters. Hence, experiments had to be parallelized in order to achieve comparable results. As a high power LED array is not commercially available, a development of it was mandatory in this thesis. With the developed array, suitable for a standard microtiter plate, comparable results with low error margins were finally achieved with LED array version 2.3. Using this automated, micro controller regulated setting, a rapid prototyping development was possible, facilitating making quick adoptions to the system. Several characteristics of the LED array will be discussed in the following section.

Temperature Influences

Enzymatic assays are usually strongly temperature dependent [109, 110, 111] or an enzyme can be inactivated by heat [112, 113, 114]. Thus it is important to take heat development caused by the illumination source into account. Apart from this, the pH measurement is also affected by temperature [115], e.g. when measured at room temperature a pH of 7 would change to ca. 6.63 when measured at a temperature of 50°C. This pH shift would significantly change the the activity of an pH-dependent enzyme.

This becomes even more demanding, when a microtiter plate is mounted on top of the LEDs, further enhancing heat accumulation effects. It is also important to note that suppression of scattering light might influence neighbouring samples. LEDs have a typical conversion efficiency of ca. 25% [75], when operated with a forward current of 700 mA and a forward voltage of 3.4 V, which corresponds to a thermal dissipation of 2.38 W per LED; summing up to a power of 228.48 W for the 96 LED array. As each LED is mounted on an 8 mm PCB chip this leaves a small surface of 50 mm² per LED. Thus an efficient thermal management is required, especially because both, the radiant flux and lifespan of LEDs are inversely related to its temperature. To analyse the influence of the mounting method of the LEDs, infra-red (IR) images were recorded (see section 6.2), using an IR camera. The junction temperature is directly proportional to the casing temperature, which can be measured by IR images. Using IR imaging as a method to obtain the surface temperature was chosen, as this was shown to be an accurate measurement [116]. Radiation emitted from the LEDs typically has a very low influence, as LED surfaces are fairly small and surface temperatures are relatively low (below 150°C) and are negligible [117, 118].

Temperatures using version 1 were not recorded as the results were not reproducible. As a consequence the development of the LED array versions 2.1- 2.3 was started. Even though, the thermal tape and the thermal conductive adhesive paste used for mounting the LEDs have very similar thermal conductivity, T_C is significantly higher when LEDs

are mounted using the tape. In version 2.1 T_C of ca. 122 °C was measured. In version 2.2, T_C could be lowered to ca. 92 °C using the thermal tape and cooling the setup by peltier elements. The improved LED stability, using peltier elements for cooling, was also demonstrated by Hoelz et. al using a HP 365 nm LED cooled by a peltier element [75]. The temperature increase in 100 µl sample could be decreased from 44 °C (version 2.1) to 10 °C (version 2.3) during 5 minutes illumination time. To take the temperature rise into account positive controls of enzymatic assays were incubated at the average temperature measured during illumination periods. Heat management was finally successful by optimizing the mounting method (thermal conductive paste), external active LED cooling (peltier elements) and a lateral airing, using radial fans, in order to avoid heat accumulation between the LEDs and the microtiter plate.

Stability and Intensity

As mentioned in the paragraph before, LED temperature is directly correlated with the emitting light intensity and stability [90]. An increase in temperature is to be avoided for both, samples and LEDs at all costs in order to minimize the influence on the enzymatic assay.

Recorded LED intensities for version 2.1-2.3 were measured (Fig. 6.27). For version 2.1 the intensity loss over 5 minutes continuous illumination was ca. 20% - 25%. The intensity loss is due to self- heating of the LEDs. Such a large intensity drop over 5 minutes illumination would influence the reproducibility of an enzymatic assay greatly. This loss was slightly reduced to an average of 18% in setup 2.2, where the emission intensity was recorded when LEDs were fixed with thermal conductive adhesive paste. Due to the stronger cooling of the Peltier elements and the thermally more efficient fixing method in setup 2.1, the thermal management improved and the intensity losses due to self-heating decreased. The long- term downward drifts disappear and LEDs alternately overheat and cool, resulting in intensity fluctuations and ca. 2% output loss in each cycle when measuring at maximum intensity in each cycle. Ca 3% scattering light can be measured as a side effect, when neighbouring LED rows were switched on. Scattering light was suppressed by using crossbraces in version 2.3. Without radial fans switched on in setup 3 the long-term intensity drop was 8% . This was reduced to ca. 3% when radial fans were on. The average output loss from cycle to cycle was reduced to 0.5%. LED mounting with thermal tape and thermally conductive paste both resulted in homogeneous temperatures in all three setups. Thus the thermal conductivity of both products seems consistent.

Finally a stable illumination could be achieved for this thesis and error margins in triplicates from the measured values of enzymatic assays could be reduced to an average of ca 2 %. Taking the large LED emission intensity drop of ca 25 % into account, it is not surprising that results were not comparable using the first LED array versions at the beginning. As the intensity is inversely proportional to the square of the distance from the illumination source it is crucial to ensure a constant illumination-sample distance for all experiments conducted. This is implemented in all setups by either a milled LED cavity or a 3D designed microtiter mounting.

In contrast to the LED array by Axion BioSystems [88], which offer LED arrays for up to 48 wells, the designed LED array offers illumination for a full 96 well format with 365 nm irradiation. Also, the array offers spatial control and not only a homogeneous irradiation of a single ultra-high power LED, as offered by Prixmatix Ltd [89]. The LED array can be

adapted to versatile assays, e.g. by exchanging LEDs to be able to illuminate with different wavelengths. Furthermore, LED intensities, as well as illumination times can be easily controlled and programmed by a simple and cheap microcontroller with the possibility to operate each LED row in different frequencies and runtimes. An example, of how the microcontroller (Arduino Uno) could be programmed is attached in the appendix.

7.3 Controlling Enzymatic Reactions Using a Photoacid

Restrictions in Enzyme Selection

First of all, to successfully establish a pH-dependent, enzymatic assay a suitable enzyme with a strong pH-dependent activity has to be selected. Pepsin for example is an enzyme with a sharp pH profile, however it belongs to the group of zymogen enzymes. Hence it is activated once by a pH drop, but does not reverse to inactivity once the pH rises. For activating zymogen enzymes a PAG would be a good choice. Adding to that pepsin is permanently inactivated once th pH reaches 8 or higher [34]. Thus enzymes need to have a pH activity that reversibly changes with the pH value to demonstrate the desired photo-induced enzymatic activity control of this work. Hence potential enzymes used must be relatively robust, not be damaged by the illumination source or chosen light intensity. Nor must the photoacid itself inhibit the enzyme. However, inhibitory effects of photoacids on enzymes was not an issue for both enzymes tested.

Moreover the enzyme has to be preselected in terms of reaction time which is needed to establish and analyse an enzymatic assay: It must not surpass a certain time frame. As mentioned earlier too strong or too long illumination does destroy the photoacid and the pH control is no longer reversible. Additionally the application itself determines the choice of photoacid and enzyme. Maybe there are situations in which only short, defined (enzymatic) reactions (ns-µs scale) shall be photo- controlled in contrast to controlling a longer enzymatic activity (minute scale). Apart from the enzymatic reaction time itself, it is also important to consider diffusion phenomena in solution. Impact of diffusion can be reduced by integrating a mixing aperture, by ensuring a very homogenous illumination and thin sample layers. Those phenomena could be further analysed significantly reducing system size, making a more detailed, separate analysis possible.

Buffering components from enzyme storage buffer might lower the assays efficiency by scavenging photo-induced, liberated protons of the photoacid. Hence, it is advisable to buy lyophilized powder with low buffering components or work with pure enzyme, e.g. by dialysing it from stock buffer. Alternatively, if the enzyme purification step shall be avoided, it is also possible to buy high enzyme stock concentrations. Thus, a high dilution can be done for final experimental concentrations. This will reduce the buffering component related influences in the final assay.

Considerations for Enzymatic Assay Establishment

In order to achieve a significant pH change compounds used in the enzymatic reactions must be carefully chosen and optimized in concerns of proton scavenging. Buffering effects should be examined not only for the enzyme selection, but for all components

used. They should have a low pK_a to reduce buffering effects for the pH jump and should preferably not absorb in the photoacid's excitation region. Materials used in the assay (microtiter plate, cuvette, Pertri dish) must be tested in terms of their absorption properties as not to reduce excitation light yield by absorbing at the excitation wavelength.

When establishing an enzymatic assay, analysing and detection methods for positive controls and results should be compatible with the photoacid. When working with ssDNA or dsDNA detection is often done by fluorescence assays using intercalating dyes and the photoacids fluorescence must not interfere with the fluorimetric DNA quantification assay. The Qubit™ ssDNA Assay Kit, which was also used to detect ssDNA digestion for S1 nuclease experiments in this thesis, is measured with the Qubit® 2.0 fluorometer. The fluorometer quantifies using the intercalating dye, which is then used in a fluorescence assay, exciting the samples at 450 nm and quantified the amount of ssDNA present in the sample. HPTS exhibits a much stronger fluorescence than the intercalating dye when being excited at 450 nm. This allows a standard measurement following the Qubit™ ssDNA assay impossible when HPTS is used. Also, HPTS is not suitable for uses with DNA detection dye in gel- electrophoresis. The excitation wavelength is 490 nm, where HPTS is still excited and emits a strong fluorescence. The only suitable device for analysing assays containing HPTS was the fragment analyser by Agilent Technologies Deutschland GmbH. In a DNA assay, HPTS can be removed from the samples by filtering the sample using spin columns or magnetic beads. However, using the short 70mer ssDNA oligo in this thesis, the yield after filtration was too small to obtain any significant results. This might be an option for assays with a different approach or longer oligonucleotides though. Sometimes measurements were not possible at all, because sample concentration was too low to be measured. G-acid could be used with all detection methods except NanoDrop detection, which is an absorption test at 260/280 nm, where both photoacids absorb, distorting the obtained results. Generally G-acid seems to be the more suitable photoacid to establish complex assays.

Moreover, it is important to test the assay to photo destructive processes. While PAG, mPAH and PAH are compatible and have been used with enzymes and biological compounds [2, 35, 1] without or only slight inhibition, use with ssDNA is rather unexplored. As shown in this thesis the used 70mer ssDNA was undergoing a destructive process when illuminated with HPTS or G-acid. The light irradiation itself or only the photoacids in darkness did not harm the used ssDNA. A reason could be, that the photoacid intercalate in the DNA structure and directly influence and destroy the structure upon proton release. However, it was demonstrated that ordered ssDNA structures, such as the i-motif form, can be switched by pH cycling [65] using a photobase. The ssDNA was present in an organized, stable structure. Even though it degraded continuously with the number of pH switching cycles as well. Hence, assays using (short), unstructured ssDNA oligonucleotides seem to be unsuitable for enzymatic assays using a photoacid.

In contrast to the experiment using S1 nuclease, the assay using pNPP for acid phosphatase was more suitable. The compounds used here were not significantly degrade by sample irradiation containing photoacid. pNPP also undergoes a slight hydrolysis when combined with G-acid and UV- light. However this is not significant compared with the enzymatic activity. HPTS absorbs strongly at 405 nm. This is also the absorption of the reaction's product pNP, which is the reason why experiments in the acid phosphatase assay were conducted with G-acid only. A substrate lack of pNPP is observed when measuring the acid phosphatase activity 6.3.2. The lack occurs due to the assay composition: If a higher pNPP concentration was chosen, the buffering effect of pNPP was too strong, thus the

substrate concentration had to be reduced to 100 µM.

Light-controlled Assays

Using a photo-induced pH jumps in light-controlled assays was successfully conducted before. For example by enhancing bacteria killing when using a photoacid to change the pH value [2]. Another example is HPTS that was fixed on a surface together with the enzyme pepsin on silica nanowires [35]. Both of the previous assays were not in free solution, but with the photoacids and other components fixed on a surface or infused into a gel. In this thesis an assay was established with all components in solution.

A light-controlled assay using a PAG in free solution was conducted by Kohse et al [1]. The activity of acid phosphatase could be successfully triggerd by irreversibly inducing one pH jump and then record enzymatic activity over time. The assay established here, successfully implemented a reversible pH control to reversibly control enzymatic activity of acid phosphatase. In all enzymatic assays in this thesis end point measurements for enzymatic activity detections were used. Enzymatic reaction was stopped after different reaction times. This requires a reliable method to stop enzymatic activity to be able to obtain time resolved results.

Hence it would be advantageous if an online assay could be developed7 to online track enzymatic activity or the pH jump or, ideally, both in parallel. The established online pH measurement using a pH micro electrode could not be done as the sample volume had to be reduced to 100 µl in the microtiter plate. Otherwise no effective assay could be established. However, 100 µl in a microtiter plate is not enough volume to measure the pH using the micro pH electrode. Establishing an online detection should use a fluorescence assay. Fluorescence can be detected from multiple angles and is more specific than absorption. For example to track the activity of acid phosphatase the coumarin derivative 6-chloro-8-fluoro-4-methylumbelliferone phosphate (CF-MUP) could be used, It is hydrolysed to 6-chloro-8-fluoro-4-methylumbelliferone (CF-MU) by acid phosphatase. CF-MU possesses strong fluorescence at ca. 450 nm with low pKa (4.7), high fluorescence quantum yield and pH independence in the physiological pH range. This new fluorescence dye, CF-MU, is a convenient tool for assays with buffer pH between 4.5 and 8 [22]. As CF-MU is excited at 450 nm photoacids would have to be chosen according to this excitation wavelength, excluding e.g. HPTS. Adding to that coumarin derivatives are known to have a relatively low photostability [119]. Photobleaching can be generally lowered by choosing optimal illumination conditions for the photoacid. When the photoacid is excited in the maximum absorption peak, excitation intensity can be reduced. This is only the case when other compounds of the assay do not interfere with the photoacids maximum absorption and reduce the light yield by also absorbing in the excitation range.

For online pH measurement, fluorescent dyes such as the SNARF indicators by Thermofisher [120] could be used. Those dyes have a fluorescence wavelength shift, depending on the pH value and should be considered for potential assay optimization. They are excited at 488 nm, which could again interfere with photoacid emission. Those pH-dependent fluorescent dyes also have the advantage that they are independent of the assay and track pH changes (whereas CF-MUP would be suitable for phosphatase hydrolysing assays only). A drawback of the SNARF indicators is that a significant pH-dependent fluorescence shift is taking place in the pH range of 9-6 only. Still, those dyes are a good approach as more dyes that are sensitive in acidic pH range might be developed.

This thesis succeed in establishing and optimizing a non-invasive, light-controlled assay. Choosing the correct parameters to fulfil the complex requirements were successfully fulfilled. Acid phosphatase's activity could be reversibly controlled by using G-acid as a photoacid and 365 nm HP LEDs as an illumination source. To achieve a successful experimental setup it was necessary to optimize the starting pH, so the enzyme is inactive and the photoacid absorbs sufficiently at this point. Both, G-acid an acid phosphatase are reversibly controllable and it was demonstrated that the enzyme activity depends on the light exposure time alone. The effective pH value in the illumination assay corresponds to a pH of 6.5, estimated by enzyme activity in a buffered assay conducted at a pH of 6.5 in darkness (for detailed results see section 6.3.2). The pH value in the illumination assay is an estimation, as enzymatic reactions also depend on ionic strength present in the buffer, such as salts or additives like magnesium etc. In the illumination assay G-acid (700 µM) was the strongest "buffering" component. For this reason the estimated pH is to be seen as a first approximation. The chosen example assay effectively demonstrates this thesis hypothesis: It is indeed possible to control enzymatic activity with light. Molecular modelling could generate optimal enzymes for such light-controlled assay, e.g. for a light-switchable polymerase chain reaction (PCR), significantly accelerating the process.

Generally the established method can be also used to control macro molecules by shifting the pH value using a photoacid. Hence, using enzyme free, highly controllable systems should also be possible. Self regulating macro molecule systems, such as DNA origami formation are stable and less complex than enzymatic assays. Thus a photoacid could be used to influence highly ordered DNA or nano structures by switching the pH value. For example DNA click chemistry, which does not require an enzyme, could also be a good application.

8 Summary & Future Prospects

In this work we could demonstrate the light induced, reversible control of the enzymatic activity of acid phosphatase in a non-invasive manner. Reversible photoacids offer a local control of pH, making them extremely attractive for miniaturizable, non-invasive and time-resolved control of pH dependent biochemical reactions. Photoacids thus have the potential for high throughput methods and automation. It was demonstrated that it is possible to control photoacids using commonly available LEDs, making their use in highly integrated devices and instruments more attractive.

The successfully designed 96 well high power UV LED array presents an opportunity for combinatorial analysis in e.g. photochemistry, where a high light intensity is needed for the investigation of various reactions. Heat management and a lateral ventilation system to avoid heat accumulation were established and a stable light intensity achieved. The array has the potential for miniaturized applications. It was designed for a standard 96 well microtiter plate and can be integrated into an automated robot assay system, such as a TECAN robot. The LED array can be practically built for every desired wavelength. Furthermore, an array with multiple wavelengths is possible and thus this design can be used and adapted for multiple applications in different areas. LED output could be further optimized by using a more complex setup, which includes a control feedback loop for regulating the cooling temperature, such as a PID controller. Furthermore spatial control is achieved as each well is illuminated by a single LED. By controlling each row individually using a micro controller different illumination parameters can be tested in a single microtiter plate assay. The spatial control could be enhanced by further reducing scattering light. This could be done constructing a new 3D printed mounting, creating a grid that embraces every single LED. Moreover, the LED array could be extended in functionality so that each LED could be controlled individually.

Furthermore, the spatial precision of the array could be further enhanced by using LED silicon lenses with a smaller irradiation angle. When photoacids are excited in their maximum absorption peak the proton emitting yield is greatly enhanced. The LED array designed in this thesis could be miniaturized by using nano LEDs. Those have less power than the used HP LEDs. However, when being excited with the optimum wavelength the power of nano LEDs could suffice. This would also decrease the temperature increase in samples caused by illumination. Another alternative for miniaturization could be the use of lasers. For example lasers could be used in an digital light processing (DLP) array. Here a laser beam is split and offers high spatial illumination control. A standard biological format to use for this setup could be a 384 well microtiter plate. Moreover, the sample volume required for such an assay could be considerably lowered down to a few microlitres.

As many photochemical applications require irradiation in the UV region, a high power LED array as developed in this thesis could be used for a wide range of other applications apart from the one presented in this work. It could be used for chemical, biochemical, as well as biological applications in a miniaturized scale offering stable illumination

conditions and parallel assays.

An application using photoacids apart from controlling enzymatic activity could be to control pH dependent structures that do not involve the use of enzymes. Examples for such controllable systems, that do not require a buffering environment or an enzyme, are click chemistry, polymerising systems or self-assembling proteins, such as prion assemblies.

Photoacids offer a local control of pH, making them extremely attractive for miniaturizable, non-invasive and time-resolved control of pH dependent reactions applications in biochemistry. From the findings in this work a "lab on a chip" or a portable device can be developed as well. The possible applications of photoacids in the biological field are large: While the efforts presented in thesis focus on controlling enzyme activity, possible applications based on photoacids are versatile. Hence, photoacids in biochemistry or biology can be considered a novel area of research and display a great potential for future development.

Results of this work clearly demonstrate that it is possible to control pH dependent biochemical reactions with light using a photoacid. These findings could greatly influence future approaches of how to control those processes non-invasively and on a much shorter time scale than in classical approaches using temperature variations.

Bibliography

[1] Stefanie Kohse, Antje Neubauer, Alexandra Pazidis, Stefan Lochbrunner, and Udo Kragl. Photoswitching of enzyme activity by laser-induced ph-jump. *Journal of the American Chemical Society*, 135 (25):pp 9407–9411, 05 2013. DOI:10.1021/ja400700x.

[2] Yang Luo, Chaoming Wang, Ping Peng, Mainul Hossain, Tianlun Jiang, Weiling Fu, Yi Liao, and Ming Su. Visible light mediated killing of multidrug - resistant bacteria using photoacids. *J. Mater. Chem. B*, 1:997–1001, 2013. [doi:10.1039/C2TB00317A].

[3] Tran-Thi, Gustavsson, Prayer, Pommeret, and Hynes. Primary ultrafast events preceding the photoinduced proton transfer from pyranine to water. *Chemical Physics Letters*, 329(56):421 – 430, 2000.

[4] Doug Spry, Alexei Goun, and Michael D Fayer. Deprotonation dynamics and stokes shift of pyranine (hpts). *The Journal of Physical Chemistry A*, 111(2):230–237, 2007. [doi:10.1021/jp066041k].

[5] Nadav Amdursky, Ron Simkovitch, and Dan Huppert. Excited-state proton transfer of photoacids adsorbed on biomaterials. *The Journal of Physical Chemistry B*, 118(48): 13859–13869, 2014. PMID: 25380297.

[6] Yi Liao. Design and applications of metastable-state photoacids. *Accounts of Chemical Research*, 50(8):1956–1964, 2017.

[7] Laren M. Tolbert and Kyril M. Solntsev. Excited-state proton transfer: From constrained systems to super photoacids to superfast proton transfer. *Accounts of Chemical Research*, 35(1):19–27, 2002.

[8] Monica Barroso, Luis G. Arnaut, and Sebastiao J. Formosinho. Intersecting-state model calculations on fast and ultrafst excited-state proton transfers in naphthols and subsitiuted naphthols. *Journal of Photochemistry and Photobiology*, 154 (1):13–21, 2002. DOI:10.1016/S1010-6030(02)00261-7.

[9] Luis G. Arnaut and Sebastiao J. Formosinho. Excited-state proton transfer reations i. fundamentals and intermolecular reactions. *Journal of Photochemistry and Photobiology A: Chemistry*, 75 (1):1–20, 1993. DOI:10.1016/1010-6030(93)80157-5.

[10] Matteo Rini. *Femtosecond mid-Infrared spectroscopy of elementary photoinduced reactions*. PhD thesis, Humboldt-Universität zu Berlin, Mathematisch-Naturwissenschaftliche Fakultät I, 2003.

[11] Menachem Gutman, Dan Huppert, and Ehud Pines. The ph jump: a rapid modulation of ph of aqueous solutions by a laser pulse. *Journal of the American Chemical Society*, 103(13):3709–3713, 1981.

[12] Arieh Warshel. Picosecond studies of excited-state protonation and deprotonation kinetics. the laser ph jump. *Journal of the American Chemical Society*, 101 (3):746–748, 1979. DOI:10.1007/978-3-642-67099-2-61.

[13] Menachem Gutman, Esther Nachliel, Eli Gershon, Rina Giniger, and Ehud Pines. ph jump: Kinetic analysis and determination of the difussion-controlled rate constants. *Journal of the Americal Chemical Society*, 105 (8):2210–2216, 1983. DOI:10.1002/kin.550050503.

[14] Heike Kagel, Hannes Jacobs, Jörn Glökler, and Marcus Frohme. A novel microtiter plate format high power open source led array. *Photonics*, 6 (1):17, 2019. DOI:https://doi.org/10.3390/photonics6010017.

[15] Mirabelle Premont-Schwarz. *Elementary solute-solvent interactions and the photophysical properties of photoacids*. PhD thesis, Humboldt-Universität zu Berlin, Mathematisch-Naturwissenschaftliche Fakultät I, 2013.

[16] Ehud Pines Noam Agmon and Dan Huppert. Geminate recombination in proton transfer reactions. ii. comparison of diffusional and kinetic schemes. *The Journal of Chemical Physics*, 88(9):5631–5638, 1988.

[17] 19th March) Author Index available at https://onlinelibrary.wiley.com/doi/10.1002/0470857277.indau (Accessed on 2019. *The chemistry of phenols*. John Wiley and Sons, 2003. DOI:10.1002/0470857277.

[18] Hatfield and Maciel. *Book, Macromolecules*. 1987.

[19] Chun Yang, Thaaer Khalil, and Yi Liao. Photocontrolled proton transfer in solution and polymers using a novel photoacid with strong c-h acidity. *RSC Adv.*, 6:85420–85426, 2016.

[20] Christian Anger. *Photosäure induzierte Polymerisation von Oxasilacyclen zum Aufbau neuer Polysiloxan Architekturen*. PhD thesis, Technische Universität München, 2013.

[21] Valentine K. Johns, Parth K. Patel, Shelly Hassett, Percy Calvo-Marzal, Yu Qin, and Karin Y. Chumbimuni-Torres. Visible light activated ion sensing using a photoacid polymer for calcium detection. *Analytical Chemistry*, 86(13):6184–6187, 2014. PMID: 24893213.

[22] Desuo Yang, Zongxiao Li, Yubo Allan Diwu, Hanzhuo Fu, Jinfang Liao, Chunmei Wei, and Zhenjun Diwu. A novel fluorogenic coumarin substrate for monitoring acid phosphatase activity at low ph environment. *Current chemical genomics*, 2:48–50, 2008. [doi:10.2174/1875397300802010048].

[23] Shima Haghighat, Sarah Ostresh, and Jahan M. Dawlaty. Controlling proton conductivity with light: A scheme based on photoacid doping of materials. *The Journal of Physical Chemistry B*, 120(5):1002–1007, 2016. PMID: 26771862.

[24] Bożena Bukowska and Sylwia Adamczyk. The presence and toxicity of phenol derivatives – their effect on human erythrocytes. *Current Topics in Biophysics*, 27: 43–51, 01 2003.

[25] Farrah Dahalan. Phenol and its toxicity. *Journal of Enviromental Microbiology and Toxicology*, 2:11–24, 06 2014.

[26] Juan YH, Wu Z, and Chen L. Study of determination of phenol derivatives based on ultraviolet absorption spectra. *Spectroscopy and Spectral Analysis*, 29 (8):2232–2235, 2009. [doi: doi.org/10.3964/j.issn.1000-0593(2009)08-2232-04, PMID: 19839345].

[27] Csanyi and Carolyn. How does uv light damage the dna strand?, https://sciencing.com/uv-light-damage-dna-strand-12687.html. *Sciencing*, 2017. [Accessed 18th March 2019].

[28] Z. Kuluncsics, D. Perdiz, E. Brulay, B. Muel, and E. Sage. Wavelength dependence of ultraviolet-induced dna damage distribution: Involvement of direct or indirect mechanisms and possible artefacts. *Journal of Photochemistry and Photobiology B: Biology*, 49(1):71 – 80, 1999. [doi:10.1016/S1011-1344(99)00034-2].

[29] Otto S. Wolfbeis, Eva Fürlinger, Herbert Kroneis, and Hermann Marsoner. Fluorimetric analysis. *Fresenius' Zeitschrift für analytische Chemie*, 314(2):119–124, 1983.

[30] Haley R. Kermis, Yordan Kostov, Peter Harms, and Govind Rao. Dual excitation ratiometric fluorescent ph sensor for noninvasive bioprocess monitoring: Development and application. *Biotechnology Progress*, 18(5):1047–1053, 2002. [doi:10.1021/bp0255560].

[31] James Hynes, Thu hoa Tran-thi, and Giovanni Granucci. Intermolecular photochemical proton transfer in solution: New insights and perspectives. *Journal of Photochemistry and Photobiology A Chemistry*, 2002. [doi:10.1016/S1010-6030(02)00304-0].

[32] Ritesh Tripathi and Kumar Dubey. A study of thermal denaturation /renaturatoin in dna using laser light scattering: A new approach. *Indian J Biochem Biophys.*, 42: 301–307, 2005.

[33] E. A. Slyusareva and M. A. Gerasimova. ph-dependence of the absorption and fluorescent properties of fluorone dyes in aqueous solutions. *Russian Physics Journal*, 56(12):1370–1377, Apr 2014.

[34] D. W. Piper and B. H. Fenton. ph stability and activity curves of pepsin with special reference to their clinical importance. *Gut.*, 6:506–8, Oct 1965. [PMC1552331].

[35] Hagit Peretz-Soroka, Alexander Pevzner, Guy Davidi, Vladimir Naddaka, Moria Kwiat, Dan Huppert, and Fernando Patolsky. Manipulating and monitoring on-surface biological reactions by light-triggered local ph alterations. *Nano Letters*, 15 (7):4758–4768, 2015.

[36] K.J. Kaufmann, D. Huppert, and M. Gutman. Picosecond proton ejection: An ultrafast ph jump. *Chemical Physics Letters*, 64:522–527, 1979. [doi:10.1016/0009-2614(79)80237-7].

[37] Nadav Amdursky, M. Harunur Rashid, Molly M. Stevens, and Irene Yarovsky. Exploring the binding sites and proton diffusion on insulin amyloid fibril surfaces

by naphthol-based photoacid fluorescence and molecular simulations. *Scientific Reports*, 7(1):6245, July 2017. DOI:https://doi.org/10.1038/s41598-017-06030-4.

[38] Fabrizio Chiti and Christopher M. Dobson. Protein misfolding, functional amyloid, and human disease. *Annual Review of Biochemistry*, 75(1):333–366, 2006. PMID: 16756495.

[39] Jean-Christophe Rochet and Peter T Lansbury. Amyloid fibrillogenesis: themes and variations. *Current Opinion in Structural Biology*, 10(1):60 – 68, 2000.

[40] Mark A. Findeis and Susan M. Molineaux. *Design and testing of inhibitors of fibril formation*, volume 309 of *Methods in Enzymology*. Academic Press, 1999. 476 - 488 pp.

[41] M. Bouchard, J. Zurdo, E. J. Nettleton, C. M. Dobson, and C. V. Robinson. Formation of insulin amyloid fibrils followed by ftir simultaneously with cd and electron microscopy. *Protein Science : A Publication of the Protein Society*, 9:1960–7, Oct 2000.

[42] James Merrington, Mark James, and Mark Bradley. Supported diazonium salts—convenient reagents for the combinatorial synthesis of azo dye. *Chemical Communications*, 21(2):140–1, 2002. [doi: 10.1039/B109799G].

[43] Wenjian Shi, Shuwei Chen, Fei Chang, Yue Han, and Yuanzhang Zhang. Studies on the adsorption of sulfo-group-containing aromatics by chitosan-β-cyclodextrin. *Water science and technology : a journal of the International Association on Water Pollution Research*, 65:802–7, 02 2012. [doi:10.2166/wst.2012.474].

[44] Bhim Chandra Mondal, Debasis Das, and Arabinda K Das. Synthesis and characterization of a new resin functionalized with 2-naphthol-3,6-disulfonic acid and its application for the speciation of chromium in natural water. *Talanta*, 56:145–52, 02 2002. [doi:10.1016/S0039-9140(01)00558-6].

[45] Akira Yamaguchi, Manato Namekawa, Toshio Kamijo, Tetsuji Itoh, and Norio Teramae. Acid-base equilibria inside amine-functionalized mesoporous silica. *Analytical Chemistry*, 83(8):2939–2946, 2011. [doi: 10.1021/ac102935q ,PMID: 21417214].

[46] Lj.M Vračar and D.M Dražić. Adsorption and corrosion inhibitive properties of some organic molecules on iron electrode in sulfuric acid. *Corrosion Science*, 44(8): 1669 – 1680, 2002. [doi:10.1016/S0010-938X(01)00166-4].

[47] Sigma Aldrich Biochemie GmbH. *Anonymus, Safety Sheet 6-Cyano-2-Naphthol,*. `https://www.sigmaaldrich.com/catalog/product/aldrich/530263?lang=de&region=DE&gclid=CjwKCAiAqOriBRAfEiwAEb9oXfF2a68a9HHOPxsSQ8OoQWZCIPAH2_PcYhvSGfExjYMvBJMsyDaPcRoCkmIQAvD_BwE`,Accessed on 2019, 19th March.

[48] Yong-Hong Liang, Qiu-Qin He, Zhao-Sen Zeng, Zhi-Qian Liu, Xiao-Qing Feng, Fen-Er Chen, Jan Balzarini, Christophe Pannecouque, and Erik De Clercq. Synthesis and anti-hiv activity of 2-naphthyl substituted dapy analogues as non-nucleoside reverse transcriptase inhibitors. *Bioorganic & Medicinal Chemistry*, 18(13):4601 – 4605, 2010. [doi:10.1016/j.bmc.2010.05.036].

[49] Richard Knochenmuss, Kyril M. Solntsev, and Laren M. Tolbert. Molecular beam

studies of the "super" photoacid 5-cyano-2-naphthol in solvent clusters. *The Journal of Physical Chemistry*, 105 (26):6393–6401, 2001.

[50] Toyoo Nakayama, Seizo Taira, Masato Ikeda, Hiroshi Ashizawa, Minoru Oda, Arakawa Katsumasa, and Setsuro Fujii. Synthesis and structure-activity study of protease inhibitors. v. chemical modification of 6-amidino-2-naphthyl 4-guanidinobenzoate. *Chemical & pharmaceutical bulletin*, 41:117–25, 02 1993. [doi:.

[51] Irina V. Gopich, Kyril Solntsev, and Noam Agmon. Excited-state reversible geminate reaction. i. two different lifetimes. *The Journal of Chemical Physics*, 110:2164–2174, 01 1999. [doi:10.1063/1.477827].

[52] Kyril Solntsev, D Huppert, and Noam Agmon. Photochemistry of "super"-photoacids. solvent effects. *Journal of Physical Chemistry A*, 103:6984–6997, 09 1999. DOI: 10.1021/jp9902295.

[53] Sigma Aldrich Biochemie GmbH. *Anonymus, Safety Information 3-Amino-2-naphthol,*. `https://www.sigmaaldrich.com/catalog/product/aldrich/164267?lang=de&region=DE&gclid=EAIaIQobChMI_aSGj7yf3wIVl-F3Ch39IgBwEAAYASAAEgLeI_D_BwE`, [Accessed on 2019, 19th March].

[54] Malcolm S. Groves, Kacie J. Nelson, Ryan C. Nelsona, and Kana Takematsu. ph switch for oh-photoacidity in 5-amino-2-naphthol and 8-amino-2-naphthol. *Physical Chemisty, Chemical Physics*, 20(33):21325–21333, 2018. [doi: 10.1039/c8cp03984d.].

[55] *Hiroji Fukui and Shunsuke and KondoKoji Arimitsu, 2007, Patent, US8536242B2, Photocurable composition*, 2007.

[56] Paige Brown, editor. *Proton Transfer in 3-amino-2-naphthol, https://www.bowdoin.edu/student-fellowships/recent-winners/bowdoin-funded/Brown,-Paige.pdf*, 2018.

[57] Sigma Aldrich Biochemie GmbH. *Anonymus, Safety Information 3-Bromo-2-Naphthol*. `https://www.sigmaaldrich.com/catalog/product/aldrich/690120?lang=de&region=DE`, Accessed on 2019, 19th March.

[58] Jerome L. Rosenberg and Ira Brinn. Excited state dissociation rate constants in naphthols. *The Journal of Physical Chemistry*, 76(24):3558–3562, 1972. [doi:10.1021/j100668a008].

[59] Y. Liao. Photoacid compositions having extended lifetime of proton dissociation state, September 1 2016. US Patent App. 15/057,856.

[60] Julien Vallet, Jean Claude Micheau, and Christophe Coudret. Switching a ph indicator by a reversible photoacid: A quantitative analysis of a new two-component photochromic system. *Dyes and Pigments*, 125:179–184, 2015. [doi:10.1016/j.dyepig.2015.10.025].

[61] Yi Liao Hongbin Chen. Photochromism based on reversible proton transfer. *Journal of Photochemistry and Photobiology A: Chemistry*, 300:22–26, 2015. [10.1016/j.jphotochem.2014.12.008].

[62] Valentine K. Johns, Zhuozhi Wang, Xinxue Li, and Yi Liao. Physicochemical study of a metastable-state photoacid. *The Journal of Physical Chemistry A*, 117(49):13101–13104, 2013. PMID: 24266331.

[63] Nawodi Abeyrathna and Yi Liao. A reversible photoacid functioning in pbs buffer under visible light. *Journal of the American Chemical Society*, 137 (35),:11282–11284, 2015.

[64] Kyeong Sik Jin, Su Ryon Shin, Byungcheol Ahn, Yecheol Rho, Seon Jeong Kim, and Moonhor Ree. ph-dependent structures of an i-motif dna in solution. *J. Phys. Chem. B*, 113(7):1852–1856, February 2009.

[65] Liu Huajie, Xu Yun, Li Fengyu, Yang Yang, Wang Wenxing, Song Yanlin, and Liu Dongsheng. Light-driven conformational switch of i-motif dna. *Angewandte Chemie (International ed. in English)*, 46(14):2515 – 2517, 2007.

[66] Ipsita Roy and Munishwar Nath Gupta. Smart polymeric materials: Emerging biochemical applications. *Chemistry & Biology*, 10(12):1161 – 1171, 2003.

[67] *Anonymus, Biological Applications of pH, https://groups.chem.ubc.ca/courseware/pH/section19/index.html*. [Accessed on 2019, 18th March].

[68] O. Vesterberg. Physicochemical properties of the carrier ampholytes and some biochemical applications*. *Annals of the New York Academy of Sciences*, 209(1):23–33, 1973. [doi:10.1111/j.1749-6632.1973.tb47516.x].

[69] Ashok Katyal and Robert D. Morrison. Chapter 11 - forensic applications of contaminant transport models in the subsurface. In Brian L. Murphy and Robert D. Morrison, editors, *Introduction to Environmental Forensics (Second Edition)*, pages 513 – 575. Academic Press, Burlington, second edition edition, 2007. ISBN 978-0-12-369522-2. [doi:10.1016/B978-012369522-2/50012-9].

[70] Tran Quoc Khanh, Peter Bodrogi, Trinh Quang Vinh, and Holger Winkler. *LED Lighting: Technology and Perception*. Wiley VCH Verlag GmbH & Co. KGaA, Weinheim, Germany, 2014. DOI: 10.1002/9783527670147.

[71] Nadarajah Narendran, Lei Deng, Richard M. Pysar, Yimin Gu, and Hua Yu. Performance characteristics of high-power light-emitting diodes. *Analytical Biochemistry*, 5187:267–275, 01 2004. [doi 10.1117/12.515647].

[72] Shuji Nakamura. Nobel lecture: Background story of the invention of efficient blue ingan light emitting diodes. *Nobel Lecture, December 8, 2014*, 87:1139–1151, 10 2015. [doi:10.1103/RevModPhys.87.1139].

[73] Daisuke Morita, Masahiko Sano, Masashi Yamamoto, Takashi Murayama, Shinichi Nagahama, and Takashi Mukai. High output power 365 nm ultraviolet light emitting diode of gan-free structure. *Japanese Journal of Applied Physics*, 41:1434, 11 2002. [doi:10.1143/JJAP.41.L1434].

[74] Asif Khan, Krishnan Balakrishnan, and Tom Katona. Ultraviolet light-emitting

diodes based on group three nitrides. *Nature Photonics*, 2:77, February 2008. [doi:10.1038/nphoton.2007.293].

[75] K. Hoelz, J. Lietard, and M. M. Somoza. High-power 365 nm uv led mercury arc lamp replacement for photochemistry and chemical photolithography. *ACS Sustainable Chemistry & Engineering*, 5(1):828–34, Jan 2017. [doi: 10.1021/acssuschemeng.6b02175].

[76] Galina Matafonova and Valeriy Batoev. Recent advances in application of uv light-emitting diodes for degrading organic pollutants in water through advanced oxidation processes: A review. *Water Research*, 132, 01 2018. [doi:10.1016/j.watres.2017.12.079].

[77] Kendric C. Smith. Dose dependent decrease in extractability of dna from bacteria following irradiation with ultraviolet light or with visible light plus dye. *Biochemical and Biophysical Research Communications*, 8(3):157 – 163, 1962.

[78] Sangeet Singh-Gasson, Roland D. Green, Yongjian Yue, Clark Nelson, Fred Blattner, Michael R. Sussman, and Franco Cerrina. Maskless fabrication of light-directed oligonucleotide microarrays using a digital micromirror array. *Nature Biotechnology*, 17:974, October 1999. [doi:10.1038/13664].

[79] Lajla Bruntse Hansen, Soren Buus, and Claus Schafer-Nielsen. Identification and mapping of linear antibody epitopes in human serum albumin using high-density peptide arrays. *PLOS ONE*, 8(7):1–10, 07 2013. [https://doi.org/10.1371/journal.pone.0068902].

[80] Björn Forsström, Barbara Bisławska Axnäs, Klaus-Peter Stengele, Jochen Bühler, Thomas J. Albert, Todd A. Richmond, Francis Jingxin Hu, Peter Nilsson, Elton P. Hudson, Johan Rockberg, and Mathias Uhlen. Proteome-wide epitope mapping of antibodies using ultra-dense peptide arrays. *Molecular & cellular proteomics : MCP*, 13:1585–97, Jun 2014. [doi:10.1074/mcp.M113.033308].

[81] Kazuhiko Takeda, Katsunari Fujisawa, Hitoshi Nojima, Ryota Kato, Ryuta Ueki, and Hiroshi Sakugawa. Hydroxyl radical generation with a high power ultraviolet light emitting diode (uv-led) and application for determination of hydroxyl radical reaction rate constants. *Journal of Photochemistry and Photobiology A: Chemistry*, 340, 02 2017. [doi:10.1016/j.jphotochem.2017.02.020].

[82] Marzieh Khademalrasool, Mansoor Farbod, and Mohammad Davoud Talebzadeh. The improvement of photocatalytic processes: Design of a photoreactor using high-power leds. *Journal of Science: Advanced Materials and Devices*, 1(3):382 – 387, 2016. [https://doi.org/10.1016/j.jsamd.2016.06.012].

[83] Christian G. Bochet. Photolabile protecting groups and linkers. *J. Chem. Soc., Perkin Trans. 1*, 1:125–142, 2013.

[84] CETONI GmbH, Korbussen, Germany. *Anolymus, CELED 96 Hardware Manual, https://www.cetoni.com/products/led-array-celed-96/, Accessed on 2019, 19th March*, March 2016.

[85] Anonymus. Four section led array, leda4-x, amuza inc. https://amuzainc.com/shop/optogenetics/led-array-multiwell-plates, Accessed on 2019, 19th March, 2018.

[86] Teleopt. *Anonymus, BIO RESEARCH CENTER CO. LTD., 2019, LED Array System Teleopt, http://www.teleopto.com/teleopto/led-array-system, Accessed on 2019, 19th March*.

[87] sansuido. *Anonymus, SANSUIDO LIMITED, 2014: 96 well LED array, http://sansuidojp.com/ledarray.html, Accessed on 2019, 19th March*.

[88] *Axion BioSystems, LUMOS WITH MAESTRO, https : //www.axionbiosystems.com/products/lumos , 2016*. Atlanta, Georgia.

[89] Prizmatix Ltd. *Anonymus, Prizmatix Ltd., 2019, Microplate and Petri Dish Illumination by Ultra High Power LEDs, https://www.prizmatix.com/UHP/UHP-LED-for-96-wells-Microplate-illumination.htm, Accessed on 2019, 19th March*. Prizmatix Ltd., Holon, Israel, 2019.

[90] John Bullough. Led lighting systems. Technical report, Lightning Research Center, Troy, NY, USA, 2003.

[91] Cypress Semiconductor Corp., San Jose, CA 95134 USA. *Anonymus, Understanding Temperature Specifications: An Introduction*, April 2017. `http://www.cypress.com/file/38656/download`, Accessed on 2019, 19th March.

[92] James S. Lowe and Peter G. Anderson. Chapter 11 - alimentary tract. In James S. Lowe and Peter G. Anderson, editors, *Stevens & Lowe's Human Histology (Fourth Edition) (Fourth Edition)*, pages 186 – 224. Mosby, Philadelphia, fourth edition edition, 2015. ISBN 978-0-7234-3502-0. [doi:10.1016/B978-0-7234-3502-0.00011-5].

[93] J. Bigby. Harrisons principles of internal medicine. *Archives of Dermatology*, 124(2): 287–287, February 1988. [doi:10.1001/archderm.1988.01670020093028].

[94] Roboklon GmbH. *Ananymus, S1 Nuclease*, 2017.

[95] Lee, Kitamoto, Yamada, and Kumagai. Cloning, characterization and overproduction of nuclease s1 gene (nucs) from aspergillus oryzae. *Applied Microbiology Biotechnology*, 44(3-4):425–31, 1995.

[96] Vogt V. M. Purification and further properties of single-strand-specific nuclease from aspergillus oryzae. *European journal of biochemistry*, 33:192–200, Feb 1973. [PMID:4691356].

[97] Asha Anand and Pramod Kumar Srivastava. A molecular description of acid phosphatase. *Applied biochemistry and biotechnology*, 167:2174–97, 06 2012.

[98] H. N. Fernley and P. G. Walker. Studies on alkaline phosphatase. inhibition by phosphate derivatives and the substrate specificity. *The Biochemical Journal*, 104: 1011–8, 1967. DOI: 10.1042/bj1041011.

[99] K. S. Gellatly, G. B. G. Moorhead, S. M. G. Duff, D. D. Lefebvre, and W. C. Plaxton.

Purification and characterization of a potato tuber acid phosphatase having significant phosphotyrosine phosphatase activity. *Plant physiology*, 106:223–232, Sep 1994. [PMCID: PMC159520 PMID: 12232323].

[100] Parvin P. Waymack and Robert L. Van Etten. Isolation and characterization of a homogeneous isoenzyme of wheat germ acid phosphatase. *Archives of Biochemistry and Biophysics*, 288(2):621 – 633, 1991.

[101] Kruzel M. and Morawiecka B. Acid phosphatase of potato tubers (solanum tuberosum l). purification, properties, sugar and amino acid composition. *Acta Biochimica Polnica*, 29(3-4), 1982. [PMID: 7158177].

[102] *Anonymus, Abcam plc., Acid Phosphatase Assay Kit, 2015,. https://www.abcam.com/ps/products/83/ab83367/documents/ab83367*, Accessed on 2019, 19th March.

[103] Sciencell Research Laboratories. *Anonymus, pNPP Phosphatase Assay*. Primarycell. `https://www.primarycell.com/pdf/8108.pdf`, Accessed on 2019, 19th March.

[104] Heike Kagel, Frank Bier, and Marcus Frohme amd Jörn Glökler. Reversibly controlling enzymatic activity using a photoacid. 2019. [Manuscript unpublished].

[105] SERVA Electrophoresis GmbH. *Anonymus, SERVA Electrophoresis GmbH, Manual: SERVA DNA Stain Clear G, https://www.serva.de/enDE/ProductDetails/4503$_3$9804$_S$ERVA$_D$NA$_S$tain$_C$lear$_G$.html, Accessed on 2019, 19th March*.

[106] Zheng Shi, Ping Peng, Daniel Strohecker, and Yi Liao. Long-lived photoacid based upon a photochromic reaction. *Journal of the American Chemical Society*, 133(37): 14699–14703, 2011. PMID: 21823603.

[107] Ota Fekonja, Majda Zorec-Karlovšek, Manale El Kharbili, Didier Fournier, and Jure Stojan. Inhibition and protection of cholinesterases by methanol and ethanol. *Journal of Enzyme Inhibition and Medicinal Chemistry*, 22(4):407–415, 2007. [10.1080/14756360601143857].

[108] Rajesh P. Rastogi, Richa, Ashok Kumar, Madhu B. Tyagi, and Rajeshwar P. Sinha. Molecular mechanisms of ultraviolet radiation-induced dna damage and repair. *Journal of Nucleic Acids*, 2010:592980, 2010. [10.4061/2010/592980.].

[109] Worthington Biochemical Corp. *Anonymus, Worthington Biochemical Corp., Introduction to Enzymes, 2019, http://www.worthington-biochem.com/introbiochem/Enzymes.pdf, Accessed on 2019, 19th March*.

[110] Worthington Biochemical Corporation.; Worthington Diagnostics. *Book: Manual of clinical enzyme measurements.* Worthington Diagnostics, 1972.

[111] Roy M. Daniel and Michael J. Danson. Temperature and the catalytic activity of enzymes: A fresh understanding. *FEBS Letters*, 587(17):2738 – 2743, 2013. A century of Michaelis - Menten kinetics.

[112] Hans Bisswanger. Enzyme assays. *Perspectives in Science*, 1(1):41 – 55, 2014. Reporting Enzymology Data – STRENDA Recommendations and Beyond.

[113] Frank H. Johnson, Henry Eyring, and R. W. Williams. The nature of enzyme inhibitions in bacterial luminescence: Sulfanilamide, urethane, temperature and pressure. *Journal of Cellular Physiology*, 1942. [doi.org/10.1002/jcp.1030200302].

[114] Almudena Hernández and M. Pilar Cano. High pressure and temperature effects on enzyme inactivation in strawberry and orange products. *Journal of Food Science*, 46 (1):266–270, 1997. [doi:10.1111/j.1365-2621.1997.tb04373.x].

[115] westlab. *Anonymus, Westlab Group. Ltd., 2017, How Does Temperature Affect pH, https://www.westlab.com/blog/2017/11/15/how-does-temperature-affect-ph, accessed on 2019, 19th March*.

[116] Indika Perera, Yi-wei Liu, and Nadarajah Narendran. Accurate measurement of led lens surface temperature. *Proceedings of SPIE - The International Society for Optical Engineering*, 8835, 09 2013. [https://doi.org/10.1117/12.2023091].

[117] Davide Priante, Rami T. Elafandy, Aditya Prabaswara, Bilal Janjua, Chao Zhao, Mohd Sharizal Alias, Malleswararao Tangi, Yazeed Alaskar, Abdulrahman M. Albadri, Ahmed Y. Alyamani, Tien Khee Ng, and Boon S. Ooi. Diode junction temperature in ultraviolet algan quantum-disks-in-nanowires. *Journal of Applied Physics*, 124(1):015702, 2018. [doi:10.1063/1.5026650].

[118] Inc Cree. *Anonymus, Application Note: Thermal Management of Cree® XLamp® LEDs, Accessed on 2019, 19th March*. Cree, Inc, Durham, USA, 2004.

[119] Thermo Fisher Scientific GmbH. *Anonymus, Thermo Fisher Scientific GmbH, 2019, Coumarin and Coumarin Derivatives, https://www.thermofisher.com/de/de/home/life-science/cell-analysis/fluorophores/coumarin.htm, Accessed on 2019, 19th March*.

[120] Thermo Fisher Scientific GmbH. *Anonymus, Thermo Fisher Scientific GmbH, 2019, Manual: SNARF ® pH Indicators, https://assets.thermofisher.com/TFS-Assets/LSG/manuals/mp01270.pdf, Accessed on 2019, 19th March*.

[121] Jan Boyke Schönborn. *Dynamics of photoinduced switching processes*. PhD thesis, Faculty of Mathematics and Natural Sciences at Kiel University, 2012.

[122] A.I. Dragan, J.R. Casas-Finet, Casas-Finet, E.S. Bishop, R.J. Strouse, M.A. Schenerman, and C.D. Geddes. Characterization of picogreen interaction with dsdna and the origin of its fluorescence enhancement upon binding. *Biophys J*, 3;99(9):3010–9, 2010. [doi: 10.1016/j.bpj.2010.09.012].

[123] Gerard A.Lutty. The acute intravenous toxicity of biological stains, dyes, and other fluorescent substances. *Toxicol Appl Pharmacol.*, 44(2):225–49, 1978. [PMID: 79242].

[124] Abdullah, Gibriel, and Adel. Advances in ligase chain reaction and ligation-based amplifications for genotyping assays: detection and applications. *Mutation Research and Reviews in Mutation Research*, 773:66–90, 2017. [doi:10.1016/j.mrrev.2017.05.001].

[125] Noam Agmon, Dan Huppert, Asnat Masad, and Ehud Pines. Excited-state proton transfer to methanol-water mixtures. *The Journal of Physical Chemistry*, 95(25):10407–10413, 1991.

[126] Vincent Bouvet, Melinda Wuest, and Frank Wuest. Copper-free click chemistry with the short-lived positron emitter fluorine-18. *Organic & Biomolecular Chemistry*, 9,: 7393–7399, 2011. [doi:10.1039/C1OB06034A].

[127] Cheng Zhi Huanga, Qie Gen Liaob, Li Hua Ganb, Feng Ling Guob, and Yuan Fang Lib. Telomere dna conformation change induced aggregation of gold nanoparticles as detected by plasmon resonance light scattering technique. *Analytical Chimica Acta*, 604(165-169), 2007. [10.1016/j.aca.2007.10.016].

[128] Nathon Kaplan Sidney Colowick. *Book; Methods in Enzymology - Volume 221, Membrane Fusion Techniques, Part B*, volume 221. Sidney Colowick , Nathon Kaplan, 1 edition, 1993. [eBook ISBN: 9780080883342].

[129] Heather F. Crouse, Alex Doudt, Cassie Zerbe, and Swarna Basu. Detection of quadruplex dna by gold nanoparticles. *Journal of Analytical Methods in Chemistry*, 2012:7, 2012. [10.1155/2012/327603].

[130] Joan Pedley Crowther and A.E.R. Westman. The hydrolysis of the condensed phosphates. *Journal of the American Chemical Society*, 74 (19):4977–4978, 1953. [doi:10.1021/ja01139a534].

[131] Feng Li, Hongquan Zhang, Brittany Dever, Xing-Fang Li, and X. Chris Le. Thermal stability of dna functinalized gold nanoparticles. *Bioconjugate Chemistry*, 24 (11): 1790–1797, 2013. [DOI: 10.1021/bc300687z].

[132] Theodor Foerster. *Book: Fluoreszenz organischer Verbindungen*, volume 1. Vandenhoeck and Ruprecht, 312 edition, 1982. [https://doi.org/10.1002/ange.19540660521].

[133] Patrice Francois, Manuela Tangomo, Jonathan Hibbs, Eve-Julie Bonetti, Catharina C. Boehme, Tsugunori Notomi, Mark D. Perkins, and Jacques Schrenze. Robustness of a loop-mediated isothermal amplification reaction for diagnostic applications. *FEMS Immunology & Medical Microbiology*, 62(1):41–8, 2010. [doi:10.1111/j.1574-695X.2011.00785.x].

[134] Liat Genosar, Boiko Cohen, and Dan Huppert. Ultrafast direct photoacid base reaction. *The Journal of Physical Chemistry A*, 104(29):6689–6698, 2000.

[135] Pampa M. Guha, Hoa Phan, Jared S. Kinyon, Wendy S. Brotherton, Kesavapillai Sreenath, J. Tyler Simmons, Zhenxing Wang, Ronald J. Clark, Naresh S. Dalal, Michael Shatruk, and Lei Zhu. Structurally diverse copper(ii) complexes of polyaza ligands containing 1,2,3-triazoles: Site selectivity and magnetic properties. *Inorganic Chemistry*, 51 (6):3465–3477, 2012. [doi:10.1021/ic2021319].

[136] Menachem Gutman. The ph jump: Probing of macromolecules and solutions by a laser-induced, ultrashort proton pulse-theory and applications in biochemistry. *Methods of Biochemical Analysis*, 30:1–103, 1984. [doi:10.1002/9780470110515.ch1].

[137] Britta Hesseler. *pH-Schaltbare Rotaxane für den lichtgetriebenen Protonentransport*. PhD thesis, Christian-Albrechts-Universität zu Kiel, 2014.

[138] invitrogen. *Anonymus, Molecular Probes Handbook - A Guide to Fluorescent Probes and Labeling Technologies, thermofisher.com/handbook, Accessed on 2019, 19th March*. thermofisher, 11th edition edition, 2010.

[139] C. Rogers J. Coppeta. Dual emission laser induced fluorescence for direct planar scalar behavior measurements. *Experiments in Fluids*, 25 (1):1–15, 1998. [doi:https://doi.org/10.1007/s003480050202].

[140] P.A.H. Wyatt J. F. Ireland. Acid-base properties of electronically excited states of organic molecules. *Advances in Physical Organic Chemistry*, 12:131–221, 1976. [doi:10.1016/S0065-3160(08)60331-7].

[141] Jens Fischbach, Qiuting Loh, Frank F. Bier, Theam Soon Lim, Marcus Frohme, and Jörn Glökler. Alizarin red s for online pyrophosphate detection identified by a rapid screening method. *Scientific Reports*, 7:Article number: 45085, 2017. [doi:10.1038/srep45085].

[142] Valentine K. Johns, Ping Peng, Joseph DeJesus, Zhuozhi Wang, and Yi Lia. Visible-light-responsive reversible photoacid based on a metastable carbanion. *Chemistry - A European Journal*, 20(3):689–92, 2013. [doi:10.1002/chem.201304226].

[143] Daiki Kato and Motoi Oishi. Ultrasensitive detection of dna and rna based on enzyme-free click chemical ligation chain reaction on dispersed gold nanoparticles. *ACS Nano*, 8:9988–97, 2014. [doi:10.1021/nn503150w].

[144] Jaroslav Kypr, Iva Kejnovská, Daniel, and Michaela Vorlíčková. Circular dichroism and conformational polymorphism of dna. *Nucleic Acids Research*, 37(6):1713–1725, January 2009.

[145] Joerg Lahann. *Click Chemistry for Biotechnology and Materials Science*. John Wiley & Sons, Ltd, 2009. [DOI:10.1002/9780470748862].

[146] Mercedes López, Pastorac Ana Domínguez, Vidalab María José Ayora, and Cañadab Bernhard Lendla Miguel Valcárcelc. Enzyme kinetics assay in ionic liquid-based reaction media by means of raman spectroscopy and multivariate curve resolution. *Microchemical Journal*, 87(2):93–98, 2007. [doi:10.1016/j.microc.2007.05.010].

[147] Rui M. D. Nunes, Marta Pineiro, and Luis G. Arnaut. Photoacid for extremely long-lived and reversible ph - jumps. *Journal of the American Chemical Society*, 131 (26):9456–9462, 2009. PMID: 19518094.

[148] Ehud Pines and Daniel Huppert. ph jump: A relaxational approach. *The Journal of Physical Chemistry*, 87(22):4471–4478, 1983. [doi:10.1021/j100245a029].

[149] Dina Pines and Ehud Pines. Solvent assisted photoacidity. *in Book: Hydrogen-Transfer Reactions*, 2006. [doi:10.1002/9783527611546.ch12].

[150] Mirabelle Prémont-Schwarz, Tamar Barak, Dina Pines, Erik T. J. Nibbering, and

Ehud Pines. Ultrafast excited-state proton-transfer reaction of 1-naphthol-3,6-disulfonate and several 5-substituted 1-naphthol derivatives. *J. Phys. Chem. B*, 117(16):4594–4603, April 2013.

[151] Robert Carles, Bayle, Patrizio Benzo, Benassayag, Caroline Bonafos, Giuseppe Cacciato, and Vittorio Privitera. Plasmon-resonant raman spectroscopy in metallic nanoparticles: Surface-enhanced scattering by electronic excitations. *Physical Review*, 92 (17):174302 – 174302, 2015. [DOI : 10.1103/PhysRevB.92.174302].

[152] Doug Spry, Alexei Goun, C. B. Bell, and Michael D Fayer. Identification and properties of the l a 1 and l b 1 states of pyranine. *THE JOURNAL OF CHEMICAL PHYSICS*, 125:144514, 2006. [doi:10.1063/1.2358685].

[153] Nathan A. Tanner, Yinhua Zhang, and Thomas C. Evans Jr. Visual detection of isothermal nucleic acid amplification using ph-sensitive dyes. *Biotechniques*, 58(2): 59–68, 2015. [doi:10.2144/000114253].

[154] Tobias Tellkamp. *Synthese neuer Photoschalter zur Funktionalisierung von Triazatriangulenen auf Goldoberflächen*. PhD thesis, Mathematisch-Naturwissenschaftlichen Fakultät der Christian-Albrechts-Universität zu Kiel, 2014.

[155] Nguyen T. B. Thuy, Ryoko Yokogawa, Yoshinaga Yoshimura, Kenzo Fujimoto, Mikio Koyano, and Shinya Maenosono. Surface-enhanced raman spectroscopy for facile dna detection using gold nanoparticle aggregates formed via photoligation. *Analyst*, 135:595–602, 2010.

[156] Otto S. Wolfbeis, Eva Ffirlinger, Herbert Kroneis, and Hermann Marsoner. Fluorimetric analysis. *Analytical Chemistry*, 314:119–124, 1983. [doi:10.1021/ac60237a009].

[157] Xiaohua Huanga and Mostafa El-Sayed. Gold nanoparticles: Optical properties and implementations in cancer diagnosis and photothermal therapy. *Journal of Advanced Research*, 1:13–28, 2010. [doi: 10.1016/j.jare.2010.02.002].

[158] Xu Li-Jia, Lei Zhi-Chao, Li Jiuxing, Zong Cheng, Yang Chaoyong James, and Ren Bin. Label-free surface-enhanced raman spectroscopy detection of dna with single-base sensitivity. *Journal of the American Chemical Society*, 137(15):5149–5154, 2015.

[159] Irie Masahiro. Light-induced reversible ph change. *Journal of American Chemical Society*, 105 (7):2078–2079, 1983. [DOI: 10.1021/ja00345a075].

[160] Nicolas Klikovits, Patrick Knaack, Daniel Bomze, Ingo Krossing, and Robert Liska. Novel photoacid generators for cationic photopolymerization. *Polym. Chem.*, 8: 4414–4421, 2017.

[161] Ramakrishnan Ayothi, Yi, Heidi B. Cao, Wang Yueh, Steve Putna, and Christopher K. Ober. Arylonium photoacid generators containing environmentally compatible aryloxyperfluoroalkanesulfonate groups. *Chemistry of Materials*, 19(6):1434–1444, 2007.

[162] A. Walkty, M. DeCorby, K. Nichol, J. A. Karlowsky, D. J. Hoban, and G. G. Zhanel. In vitro activity of colistin (polymyxin e) against 3,480 isolates of gram-negative

bacilli obtained from patients in canadian hospitals in the canward study, 2007-2008, Nov 2009.

[163] Stephanie J. Wallace, Jian Li, Roger L. Nation, Craig R. Rayner, David Taylor, Deborah Middleton, Robert W. Milne, Kingsley Coulthard, and John D. Turnidge. Subacute toxicity of colistin methanesulfonate in rats: comparison of various intravenous dosage regimens. *Antimicrobial agents and chemotherapy*, 52:1159–61, Mar 2008.

[164] Weller A. Fast reactions of excited molecules. *Prog. React. Kinet. Mech.*, 1:189–214, 1961.

[165] Jose Luiz F. Barbosa, Dan Simon, and Wesley P. Calixto. Design Optimization of a High Power LED Matrix Luminaire. *Energies*, 10(5):1–18, May 2017. [doi:10.3390/en10050639].

[166] Yole Developement Anonymus. Uv leds - technology, manufacturing and application trends 2018. Technical report, Yole Developement, Milpitas, CA, USA, 2018.

[167] Petr Klàn, Tomáš Šolomek, Christian G. Bochet, Aurélien Blanc, Richard Givens, Marina Rubina, Vladimir Popik, Alexey Kostikov, and Jakob Wirz. Photoremovable protecting groups in chemistry and biology: Reaction mechanisms and efficacy. *Chemical Reviews*, 113(1):119–191, 2013.

[168] Brian S. Jasenak. How to design with leds: Concurrent engineering yields fully optimized lighting systems. *LED Professional, Dornbirn, Austria*, 2016. `https://www.led-professional.com/resources-1/articles/how-to-design-with-leds-concurrent-engineering-yields-fully-optimized-lighting-syste` accessed on 2019, 19th March.

[169] Azmi Naqvi and Pradip Nahar. Photochemical immobilization of proteins on microwave - synthesized photoreactive polymers. *Analytical Biochemistry*, 327(1):68 – 73, 2004. [doi: 10.1016/j.ab.2003.11.026].

[170] M.R. Haddon and T.J. Smith. The chemistry and applications of uv-cured adhesives. *International Journal of Adhesion and Adhesives*, 11(3):183 – 186, 1991. [doi:10.1016/0143-7496(91)90021-9].

[171] R. G. W. NORRISH and G. PORTER. Chemical reactions produced by very high light intensities. *Nature*, 164:658, October 1949. [doi:10.1038/164658a0].

[172] Adriana Hegedus, Victor Berca, Bogdan Druga, and Cosmin Sicora. The effect of different light intensities on photochemical activity in microcystis aeruginoa aicb702 strain (cyanphyta). *Studia UBB Biologia*, 1:71–81, 2013.

[173] Iqbal A Shahnavi, Q Fasihullah, and Faiyaz H.M. Vaid. Effect of light intensity and wavelengths on photodegradation reactions of riboflavin in aqueous solution. *jorunal of photochemistry and photobiology*, 82(1):21–7, 2005. [doi:10.1016/j.jphotobiol.2005.08.004].

[174] Adriana Hegedus, V Bercea, and Cosmin Sicora. The study of the photochemical activity of psii photosystem based on the chlorophyll fluorescence in cylindrosper-

mum alatosporum aicb 39 (nostocales). *Annals of the Romanian Society for Cell Biology*, 17:26–36, 01 2012.

[175] *Anonymus, Sigma Aldrich Biochemie GmbH, Enzymatic Assay of Acid Phosphatase, 2019, https : //www.sigmaaldrich.com/technical − documents/protocols/biology/enzymatic − assay − of − acid − phosphatase.htm, Accessed on 2019, 19th March.*

[176] Oren Gajst, Luis Pinto da Silva, Joaquim C. G. Esteves da Silva, and Dan Huppert. Excited-state proton transfer from the photoacid 2-naphthol-8-sulfonate to acetonitrile/water mixtures. *The Journal of Physical Chemistry A*, 122(30):6166–6175, 2018.

[177] Katrin Adamczyk, Jens Dreyer, Dina Pines, Ehud Pines, and Erik T. J. Nibbering. Ultrafast protonation of cyanate anion in aqueous solution. *Israel Journal of Chemistry*, 49(2):217 – 225, 2010. [doi: 10.1560/IJC.49.2.217].

[178] L. Song, E. J. Hennink, I. T. Young, and H. J. Tanke. Photobleaching kinetics of fluorescein in quantitative fluorescence microscopy. *Biophysical journal*, 68:2588–600, Jun 1995. DOI:10.1016/S0006-3495(95)80442-X.

[179] Ghauharali and Brakenhoff. Fluorescence photobleaching based image standardization for fluorescence microscopy. *Journal of Microscopy*, 198:88–100, 2001. DOI: 10.1046/j.1365-2818.2000.00683.

[180] Andrew J. Berglund. Nonexponential statistics of fluorescence photobleaching. *The Journal of Chemical Physics*, 121(7):2899–903, 2004. DOI: doi.org/10.1063/1.1773162.

[181] John M. Denu, DANIEL L. Lohse, J. Vijayalaksmi, Mark A. Saper, and Jack E. Dixon. Visualization of intermediate and transition-state structures in protein-tyrosine phosphatase catalysis. *Proceedings of the National Academy of Sciences*, 93(6):2493–8, 1996. DOI:10.1073/pnas.93.6.2493.

[182] Mark C. Williams, Jay R. Wenner, Ioulia Rouzina, and Victor A. Bloomfield. Effect of ph on the overstretching transition of double-stranded dna: Evidence of force-induced dna melting. *Biophysical Journal*, 80(2):874 – 881, 2001. [doi:10.1016/S0006-3495(01)76066-3].

[183] Heike Kagel, Jörn Glökler, and Marcus Frohme. Photoacids in biochemical applications. *Journal of Cellular Biotechnology*, 4(no. 1-2):23–30, 2018. DOI: 10.3233/JCB-189004.

[184] BRAND GMBH + CO KG. *Anonymus, BRAND GMBH + CO KG, 2013, 96-Well Plate Dimensions [Standard Microplate], https://www.wellplate.com/96-well-plate-dimensions/, Accessed on 2019, 19th March.* BRAND GMBH + CO KG, Wertheim, Germany, 2013.

[185] Ekaterina Schütt. *Ekaterina Schütt, Arcada University of Applied Sciences - Helsinki, Degree Thesis: Thermal management and design optimization for a high power LED work light.* `https://www.theseus.fi/bitstream/handle/10024/80460/Schutt_Ekaterina.pdf?sequence=1`, Accessed on 2019, 19th March.

[186] Yonghai Feng, Lei Liu, Jie Zhang, Hüsnü Aslan, and Mingdong Dong. Photoactive antimicrobial nanomaterials. *J. Mater. Chem. B*, 5:8631–8652, 2017. [Doi: 10.1039/C7TB01860F].

[187] J.F. ARTIOLA. 13 - environmental chemical properties and processes. In Janick F. Artiola, Ian L. Pepper, and Mark L. Brusseau, editors, *Environmental Monitoring and Characterization*, pages 241 – 261. Academic Press, Burlington, 2004. ISBN 978-0-12-064477-3.

[188] James W. Hindley, Yuval Elani, Catriona M. McGilvery, Simak Ali, Charlotte L. Bevan, Robert V. Law, and Oscar Ces. Light-triggered enzymatic reactions in nested vesicle reactors. *Nature Communications*, 9(1):1093, March 2018. DOI: https://doi.org/10.1038/s41467-018-03491-7.

[189] Nicholas Turner. Enzymes team up with light-activated catalysts. *Nature*, 560: 310–311, 08 2018.

[190] Maite Cueto, Mauricio Piedrahita, Carlos Caro, Bruno Martínez-Haya, Mikel Sanz, Mohamed Oujja, and Marta Castillejo. Platinum nanoparticles as photoactive substrates for mass spectrometry and spectroscopy sensors. *The Journal of Physical Chemistry C*, 118(21):11432–11439, 2014.

[191] Madanodaya Sundhoro, Hui Wang, Scott T. Boiko, Xuan Chen, H. Surangi N. Jayawardena, JaeHyeung Park, and Mingdi Yan. Fabrication of carbohydrate microarrays on a poly(2-hydroxyethyl methacrylate)-based photoactive substrate. *Org. Biomol. Chem.*, 14:1124–1130, 2016.

[192] H.U. Bergmeyer, K. Gawehn, and M Grassl. *Methods of Enzymatic Analysis*. 1974. DOI: https://doi.org/10.1016/B978-0-12-091302-2.X5001-4.

[193] Antoni Bautista-Barrufet, Fernando López-Gallego, Víctor Rojas-Cervellera, Carme Rovira, Miquel A. Pericàs, José M. Guisán, and Pau Gorostiza. Optical control of enzyme enantioselectivity in solid phase. *ACS Catalysis*, 4(3):1004–1009, 2014.

[194] Xin X. Zhou, Hokyung K. Chung, Amy J. Lam, and Michael Z. Lin. Optical control of protein activity by fluorescent protein domains. *Science*, 338(6108):810–814, 2012.

[195] Ulrich Krauss, Thomas Drepper, and Karl-Erich Jaeger. Enlightened enzymes: Strategies to create novel photoresponsive proteins. *Chem. Eur. J.*, 17(9):2552–2560, May 2019.

[196] Bernd Reisinger, Natascha Kuzmanovic, Patrick Löffler, Rainer Merkl, Burkhard König, and Reinhard Sterner. Exploiting protein symmetry to design light-controllable enzyme inhibitors. *Angew. Chem. Int. Ed.*, 53(2):595–598, May 2019.

[197] John B. Lloyd and Robert W. Mason. *Biology of the Lysosome*, volume 416 pp. Plenum Press, 1996.

[198] Noam Agmon. Elementary steps in excited-state proton transfer. *The journal of physical chemistry. A*, 109:13–35, 02 2005. [doi:10.1021/jp047465m].

Declaration of Authorship

I hereby declar that the thesis with the title

LipH- cycle - a noninvasive method to control biochemical reactions

I am submitting is entirely my own original work except where otherwise indicated.

I am aware of the University Potsdam regulations concerning plagiarism, including those regulations concerning disciplinary actions that may result from plagiarism.

Any use of the works of any other author, in any form, is properly acknowledged at their point of use.

Potsdam, August 25, 2019 Heike Kagel

List of Figures

List of Tables

Appendix

LED control with a microcontroller

Schematic plan

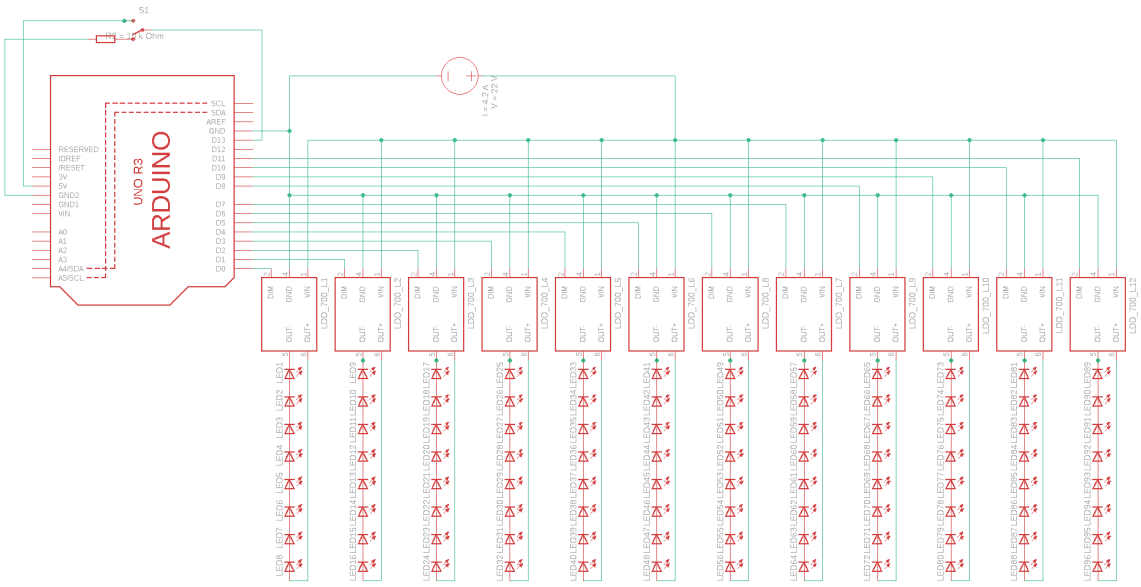

Figure 8.1: Schematic control of LEDs using an Arduino Uno

Example code

The following code is written in the Arduino IDE Software (5.1.8) and shall serve as an example of how the LED illumination is controlled by the micro controller Example code to control LED rows

The program can be copied directly into the free of charge Arduino software, which is available online. LED control can also be programmed as an array, however this does not allow individual frequency control of each LED row.

Start of code:

```
// This is an example code to control 12 rows of LED with an Arduino UNO microcontroller - program is started with a 5 seconds delay after pressing a simple push button

#define LED1 2 //initializing LED rows
#define LED2 3
#define LED3 4
#define LED4 5
#define LED5 6
#define LED6 7
#define LED7 8
#define LED8 9
#define LED9 10
#define LED10 11
#define LED11 12
#define LED12 13
#define BUTTON 14
#define FREQUENCY1_ON 300000L // Defining an abritrary amount of different Frequencies in which row should be pulsed FREQUENCY1_ON being the on time, FREQUENCY1_OFF being the off time
#define FREQUENCY1_OFF 300000L // time is defined in milliseconds, minimum time is 1 ms when using described setup
#define FREQUENCY2_ON 3000L
#define FREQUENCY2_OFF 0L
#define FREQUENCY3_ON 3000L
#define FREQUENCY3_OFF 444L
#define DELAY 30000L // Define Delay between each LED row
#define RUNTIME1 60000L //Overall runtime per LED row in Millisecs 1 min= 60000 ms 2 min 120000, 3 min 180000, 4 min 240000, 5 min 300000, 6 min 360000, 7 min 420000 etc..
#define RUNTIME2 120000L
#define RUNTIME3 180000L
#define RUNTIME4 240000L
#define RUNTIME5 300000L
#define RUNTIME6 0L
#define ON 1
#define OFF 0

long int timestamp1 = 0;                  //define a timestamp for each LED row, so each row can be started at a certain time. Here rows are started 30 seconds after preceding row
long int timestamp2 = timestamp1 + DELAY;
long int timestamp3 = timestamp2 + DELAY;
long int timestamp4 = timestamp3 + DELAY;
long int timestamp5 = timestamp4 + DELAY;
long int timestamp6 = timestamp5 + DELAY;
long int timestamp7 = timestamp6 + DELAY;
long int timestamp8 = timestamp7 + DELAY;
long int timestamp9 = timestamp8 + DELAY;
long int timestamp10 = timestamp9 + DELAY;
long long int timestamp11 = timestamp10 + DELAY;
long long int timestamp12 = timestamp11 + DELAY;
long int button_start = 0;

long long int zeit = 0;   //define variables for LED states (defines if LED is on or off)
int ledstate1 = OFF;
int ledstate2 = OFF;
int ledstate3 = OFF;
int ledstate4 = OFF;
int ledstate5 = OFF;
```

End of Code